Doctoral Thesis

Hamiltonian Formalism of Generalized Magnetohydrodynamics — Structures Created on Casimir Leaves

（一般化磁気流体力学のハミルトニアン形式
―― カシミール葉層に形成される構造）

ハムディ　モハメド　アブデルハミド　ハッサン
Hamdi　Mohamed　Abdelhamid　Hassan

Hamiltonian Formalism of Generalized Magnetohydrodynamics — Structures Created on Casimir Leaves

Hamdi Mohamed Abdelhamid Hassan

A Thesis
Submitted to the University of Tokyo
in Partial Fulfillment of the Requirements for
The Degree of Doctor of Philosophy

Supervisor
Professor Zensho Yoshida

Department of Advanced Energy
Graduate School of Frontier Sciences
The University of Tokyo
Japan

March 2017

"To the memory of my dear parents,"

Acknowledgments

First and above all, praise be to my Lord, ***Allah***, the Almighty, who provided me this opportunity and granted me the capability to proceed successfully. This dissertation appears in its present form due to the assistance and guidance of several people. Therefore, I would like to offer my sincere thanks and gratitude to all of them.

Firstly, I would like to express my deep appreciation and sincerest thanks to my advisor Professor Zensho Yoshida for many enlightening discussions and for giving me complete freedom to choose my research topics. I am also deeply thankful for his supervision, immense knowledge, and encouragement during the accomplishment of this work.

Besides my advisor, I would like to thank the rest of my dissertation committee members, Professor Tohru Ozawa (Waseda University), Professor Yuichi Ogawa, Professor Kojiro Suzuki, and Associate Professor Masaki Nishiura, for their great support and invaluable advice. My profound gratitude is expressed to Professor Tohru Ozawa for agreeing to serve on my dissertation committee. It is a great honor for me. I would like to express my sincere thanks to Professor Yuichi Ogawa for his encouragement, kindness, and continuous support. I am also grateful to Professor Kojiro Suzuki for valuable suggestions and comments during the oral defense. I would like to give very special thanks to Associate Professor Masaki Nishiura for his elegant plasma physics course, and for his ongoing encouragement and

support.

I also would like to thank the Egyptian Ministry of Higher Education for the financial support provided during my PhD course of study.

I wish to thank Dr. Haruhiko Saito, Dr. Yoshihisa Yano, and Dr. Francesco Volponi for encouragement, support and for making my first days in The University of Tokyo easier. I am also grateful to Dr. Yohei Kawazura for fruitful discussions and for being one of my research collaborators.

I want to thank my colleagues Mr. Naoki Sato, and Mr. Yuji Ohno for their ever cordial and valuable discussions about different topics in mathematics and physics, from which I greatly benefited. I am also grateful to Mr. Wakabayashi Tomoaki for his kindness and for being my counselor in the first six months in Japan. I thank and appreciate Ms. Kitayama Kyoko for her kindness, and for handling of all the needed administrative work.

My appreciation and gratefulness extend to Professor Philip J. Morrison (University of Texas) for stimulating and helpful discussions, encouragement, and support, to Dr. Emanuele Tassi, Dr. Cristel Chandre (CPT Marseille) for the hospitality during my visit to the Centre de Physique Théorique, Marseille, France, to Dr. Stuart R. Hudson (PPPL) for his kindness and for the hospitality during my visit to PPPL, Princeton, NJ, USA.

My special thanks to Professor Swadesh M. Mahajan (University of Texas) for his encouragement and support and for being my research collaborator. My special thanks and gratitude to my friend and research collaborator Dr. Manasvi Lingam (Harvard University) for his continuous

encouragement and support. I am highly appreciative of our almost weekly Skype conversation regarding all aspects of physics and life.

Thanks have to be given to Professor Elsayed A. Elwakil, Professor Essam M. Abulwafa, Professor Emad K. Elshewy (Mansoura University), and Professor Abuozeid M. Shalaby (Qatar University) for their continuous encouragement and invaluable advice. I am also grateful to all members of Physics Department, Faculty of Science, Mansoura University.

Thanks are due to my friends and colleagues at Mansoura University Ayman Sobhy, Ahmed Habib, Mohamed Raslan, Emam Zakaria, Walid Abdelghani, Mohamed Al-Zaibani, Dr. Elkenany Brens, Musa Mahfouz, Ashraf Tawfik, Mahmoud Refaat, Mohamed Elhenawy, Shaaban Mohamed, Ehab Elrefae, Ehab Saleh, Ibrahim Elkamash, Mohamed Mustafa, Attia Kassem, Dr. Moniem Elshobky, Dr. Reda Felfel and Mohamed Abdelghany for making my life full of joy and happiness. Also my deep gratitude to my colleagues and friends at the University of Tokyo, Dr. Ahmed Haroun, Mohamed Samara, Dr. Mahmoud Khalil, Dr. Natheer Alabsi, Dr. Hossam Nabil, Hamdi Sahloul, Dr. Alaa Eldin Hamid, and all of the Muslims community in Kashiwa campus for maintaining our faith and for removing the sense of homesickness.

Last but not least, I would like to express my love and gratitude to my big family to my brothers Kassem and Fathy to my sisters Amal, SoSo, Hanan, and Seham and to my father-in-law Police Maj. Gen. Mohamed Abdelaal, and mother-in-law Salwa Hamza, for their great support and continuous prayers for my family and me.

Finally, I want to express my love and gratitude for the person that moved with me to Japan and awarded me the most precious gift in my life my sons Ziad and Muaz; My lovely wife, Dear Sara, without your continuous support and encouragement, I could not have finished this work, it was you who kept the fundamental of our family, and I understand it was difficult for you, therefore, I can just say thanks for everything and may ***Allah*** reward you all the best in return.

Abstract

One of the most important aspects of plasma physics is the existence of a scale hierarchy. The scale hierarchy encapsulates the complexity of plasmas, which is reflected in the richness of plasma behavior in laboratory as well as in astrophysical and space plasmas. Such plasma phenomena require a nonlinear interaction between distinct scales. A typical example of a plasma fluid model endowed with scale hierarchy is extended magnetohydrodynamics (MHD). Extended MHD is the generalization of ideal MHD, and it is endowed with two primary two-fluid effects, i.e., Hall drift and electron inertia effects. These effects constitute the scale hierarchy in the extended MHD model—three disparate scales; one of them is the large scale defining the macroscopic structures, while the other two arise because of the ion and electron skin depths. By invoking the framework of Hamiltonian mechanics, the role of small scales in the creation of nonlinear structures in plasma can be thoroughly delineated.

Hence, in this dissertation, we present a rigorous and complete mathematical formulation of the noncanonical Hamiltonian structure of the extended MHD model for the first time. The underlying Poisson structure of the basic dynamical equations is obtained using a novel Lie algebra (generating bracket). This generating bracket satisfies an extended permutation law, which gives a unified framework for proving the important Jacobi's identity for hydrodynamical and magnetohydrodynamical models. The for-

mulated Poisson algebra is shown to possess a nontrivial center, i.e., the Hamiltonian system is noncanonical in nature. Hence, this property gives rise to the Casimir invariants (generalized helicities). These Casimir invariants for extended MHD and the subsumed models are calculated, i.e., for Hall, inertial, and ideal MHD. Moreover, the necessary boundary conditions for extended MHD are investigated.

The extended MHD model is applied to derive nonlinear Alfvén, helicon, and TG waves, as well as for studying turbulence in the solar wind. The Casimir invariants of the system, which are features of the noncanonical nature of the Hamiltonian of the system, are the key to studying such plasma processes. Since the dynamics of plasma are restricted to stay on the surfaces of constant Casimir, thus all of these nonlinear phenomena appear as structures embodied on Casimir leaves.

Firstly, using the Casimir invariants in determining the equilibrium of the system by extremizing the energy-Casimir functional, the exact nonlinear Alfvén wave solutions of the fully nonlinear extended MHD system are derived for the first time. The solutions consist of two Beltrami eigenfunctions, which incorporate different length scales. A remarkable feature of the inclusion of these small-scale effects is that the wave patterns are no longer arbitrary; the large-scale component of the wave cannot be independent of the small-scale component, and the coexistence of them forbids the large-scale component to have a free wave form. This is in marked contrast to the ideal MHD picture where the Alfvén wave propagating on a uniform ambient magnetic field keeps its arbitrary shape constant.

Second, we originate a rigorous nonlinear theory for helicon and Trivelpiece-Gould (TG) waves that delineates the multi-scale structure of electromagnetic waves in extended MHD. The derived analytical solutions, which satisfy the set of nonlinear equations of extended MHD, manifest the intrinsic coupling of the large scale and the electron skin depth small scale; the former is realized as a helicon mode and the latter as a TG mode. In the regime of relatively low frequency or high density, however, the combination is shown to be comprised of the TG mode and an ion cyclotron wave (slow wave). The energy partition between these modes is determined by the helicities carried by the wave fields.

Finally, we use the nonlinear Alfvénic wave solutions to derive the kinetic and magnetic spectra by resorting to a Kolmogorov-like hypothesis based on the assumption of constant cascading rates of the energy and generalized helicities of extended MHD. The magnetic and kinetic spectra are derived in the ideal, Hall, and electron inertia regimes. The resultant spectra are compared against the observational evidence and shown to be in good agreement.

Thus, by tackling these set of problems, the utility and elegance of the Hamiltonian formalism in understanding the scale hierarchy of plasma fluid models has been demonstrated.

Table of Contents

List of Figures

Chapter 1

Introduction

1.1 Scale hierarchy

The complexity in plasma physics arises from the existence of the scale hierarchy brought about by small-scale effects such as Hall drift and electron inertia. The scale hierarchy is one of the key issues in plasma physics. Magnetic reconnection, turbulence, flares and accretion discs are few examples of the processes created by the interactions of different scales [15, 17, 18, 123, 124]. These interactions of the disparate scales are derived from the nonlinearity of the system. Therefore, it is physically true to state that the microscopic processes strongly affect the evolution of structures at macroscopic scales even if they are not expressed in the final macroscopic event. In the macroscopic level, ideal fluid equations are sufficient (with a fair degree of accuracy) to govern the overall dynamics of these systems. However, it is these idealized laws that prevent certain processes from occurring. The singular perturbation that represents the physics controlling microscopic scale on the macroscopic equations of motion, is the means of breaking these idealizations and allowing the creation of such patterns at new characteristic scales. This singular perturbation appears in the macroscopic equations of motion as a higher order derivatives term multiplied by a small parameter. The identification and understanding of the changes

caused by the singular perturbation is the measure of our success in understanding the evolution of the system.

1.2 From ideal to extended magnetohydrodynamics

Ideal magnetohydrodynamics (MHD) can be considered as the most basic single-fluid model for describing the dynamics of electrically conducting fluids, such as plasmas, in a strong magnetic field. It represents the simplest and widely applied theory for describing the macroscopic equilibrium and stability properties of plasma in the laboratory as well as space and astrophysical plasmas [51, 89, 143]. Ideal MHD has simply generalized the hydrodynamic theory of fluids by coupling the latter with the classical electrodynamics theory (Maxwell's equations). In standard plasma physics texts, ideal MHD is often derived as a limiting case of the two-fluid model, the latter of which is obtained by taking moments of the Boltzmann equation [30, 51, 81]. In spite of all these approximations, the ideal MHD model still possesses a conservation of mass, momentum and energy. Another non-trivial conserved quantity in ideal MHD is the conservation of magnetic topology (frozen-in condition) [81]. The frozen-in condition means that the fluid and magnetic field are frozen in each other, i.e., there is no vertical motion. In other words, the propagation of a plasma element is restricted to a magnetic field line, which is initially connected. One other very important property of ideal MHD is the conservation of the magnetic and cross helicities. Because of the importance of these helicities as topological quantities [16, 113, 114], they are essential for the theory of self-organization

and relaxation of plasmas [161, 162, 174].

However, despite its considerable simplicity and elegance, ideal MHD model often falls short of describing interesting phenomena in plasmas originating from different scale hierarchies which are scaled by ion and electron inertial lengths. For example, as noted above, the electric field in the direction of the magnetic field must vanish in the ideal MHD model, by which the topology of magnetic field lines (such as the linking numbers or writhe) are invariant [16,113,114,182]. In a high-temperature (collisionless) plasma, topological change of magnetic field lines can occur at a small scale on which the electron inertia produces a finite parallel electric field, which, however, is ignored in the ideal MHD model.

We can elucidate the most striking effects of the scale hierarchy in MHD models from the perspective of linear theory. For instance, ideal MHD can be considered dispersionless since all waves, e.g., sound waves, and compressible and shear Alfvén waves, have the same dispersion relations of the form $\omega^2 \sim k^2$, which mean that waves with different wavelengths propagate with the same phase velocity. However, moving beyond the ideal MHD regime by including small-scale effects such as Hall drift, which is referred to as Hall MHD, the ideal single waves branch bifurcates and new wave modes (dispersive waves) introduced. Hall MHD is distinguished from the ideal MHD by additional term (Hall current) in the induction equation (Ohm's law). Hall term can be mathematically considered as a singular perturbation of ideal MHD since it is expressed in terms of a high spatial derivative term multiplied by a small factor [177, 181]. This small factor

introduces a short length scale (ion skin depth) to the scale-free ideal MHD. Hall term also causes the decoupling of the ion fluid and the magnetic field; however, the electron fluid still tied to the magnetic field lines. Also, because of the high nonlinearity of the Hall term, waves with short wavelength are allowed to propagate with different phase velocity ($\omega^2 \sim k^4$); these waves are called whistler waves. Including electron inertia into the Hall MHD, arrive at the vicinity of extended MHD. Extended MHD is endowed with two small length scales, the electron, and ion skin depths. As in the case of the Hall MHD, the inclusion of the electron inertia effect change the profiles of the waves propagated in plasma, in which a further bifurcation of the waves branches occurred and new modes appeared such as kinetic and inertial Alfvén waves. Roughly speaking, we can see that the scale hierarchy in MHD models is built by the electron and ion skin depths, in which ideal MHD is scaleless, and then comes Hall MHD with one intrinsic physical scale (ion skin depth), and at the end is extended MHD that brings two intrinsic physical scales (electron and ion skin depths). Hall MHD has been successfully employed in space and laboratory plasmas [32, 76], especially in the regimes which the Hall current effect becomes significant such as magnetic reconnection [17], turbulence [54, 71, 82, 87, 90, 108], and dynamo [91, 99, 109, 111] as well as in neutron stars [45] and protoplanetary discs [171]. However, in the regimes when the electron inertia effect becomes effective, Hall MHD suffers some crucial limitations, such as in fast magnetic reconnection [20, 149] and small scale turbulence [72].

As we showed above, in the linear level of the analysis, the scale hierarchy in plasma is very clear, and the role of the small scale effects

can be explicitly written down. However, if the phenomena are nonlinear, the analysis becomes drastically complicated. This complexity comes from the coupling between the small scale effects. Hence, the scale hierarchy in the context of nonlinear physics requires a more general mathematical framework for analyzing these effects. Our strategy is to use the Hamiltonian structure, in which the role of this scale hierarchy could be clearly elaborated.

1.3 Geometrical theory

Mathematical models in plasma physics are rather complex, due to the existence of many variables described by a large number of highly nonlinear equations. This complexity is often indicative of the richness of plasma behavior in the laboratory as well as in astrophysical and space plasmas. However, this is true only when such models do not violate any of the fundamental laws of physics, e.g., the physical conservation laws. To ensure that, these models has to be formulated in terms of Lagrangian or Hamiltonian mechanics.

Besides that the Hamiltonian formalism guarantees the preservation of the energy of a dynamical system for closed boundary conditions, and it is also an elegant framework to study dynamics in geometrical perspective. Since the plasma fluid models are noncanonical Hamiltonian systems [117], hence, geometrical invariants arose due to the *topological defect* (kernel) of the Poisson bracket; these invariants are called *Casimir invariants*. Casimir invariants play a crucial role in determining the equilibria and analyzing

stability of a dynamical system, which guarantees non-trivial equilibrium states of the system. This is done by constructing the so-called *energy-Casimir* functional [13, 67, 83]. We refer the reader to Chapter 2, in which a detailed discussion of this issue is provided. Moreover, Hamiltonian formulation of plasma models also shows promising results in studying phenomena such as magnetic reconnection [33, 68, 125], dynamos [91, 110], and turbulence [119, 183, 184].

The Hamiltonian formalism of the ideal magnetohydrodynamics (MHD) system was given for the first time by Morrison and Green [117]; see [63] for recent studies on the noncanonical properties of the Poisson bracket. Many different attempts have been made to generalize the model to include small-scale effects, and formulate them as Hamiltonian systems; see [69, 133, 178] for different Hamiltonian forms of Hall MHD, [77] for the Casimir invariants of noncanonical Hall MHD, [178] for the canonized Hamiltonian formalism of Hall MHD and its action principle delineating the limiting path to the ideal MHD system. Another important effect is due to the electron inertia, which brings about a finite parallel electric field, allowing magnetic field lines reconnect. In this direction, two-dimensional models have been intensively studied; see [33, 62, 142, 159, 160] as well as [94] for recent developments.

1.4 Objective and outline of the thesis

This thesis is devoted to exploring the theory of extended MHD in the framework of Hamiltonian mechanics. The merit of extended MHD

lies in its capability of describing of the scale hierarchy of plasma systems, i.e., it can explain the underlying small-scale physics both in the ion skin depth and electron skin depth regimes. From the perspective of Hamiltonian mechanics, the multi-scale effect on three phenomena in plasma physics will be elucidated by deriving fully-nonlinear exact solutions.

The thesis outline is described below.

- In Chapter 2, we shall present a brief review of noncanonical Hamiltonian mechanics and some of its features.

- In Chapter 3, the derivation of the extended MHD model starting from the two-fluid model and its Hamiltonian structure is presented. A basic theorem on Lie algebras is unearthed for proving the Jacobi's identity. This Lie algebra is used to generate the noncanonical Poisson bracket for the Hall, inertial and Hall MHD systems. Boundary conditions and Casimir invariants are also investigated.

- In Chapter 4, we start by constructing the linear theory of the extended MHD model and studying several limits of the dispersion relation. Based on the results obtained in Chapter 2, we shall investigate the nonlinear Alfvén wave in extended MHD. The Casimir invariants of the system serve as the root for studying these nonlinear structures. Via constructing equilibrium solutions (so-called Beltrami equilibrium) on Casimir leaves, we derive nonlinear wave solutions. The dispersion relation is exactly that of the linear theory, while the wave amplitude may be arbitrarily large.

- In Chapter 5, a complete nonlinear theory for helicon and TG waves is constructed. We start with the linear theory for helicon waves. Subsequently, the exact solutions of the double curl Beltrami equation are derived in the cylindrical geometry. To construct the nonlinear theory we follow the same approach used in Chapter 4. Detailed discussions of the dispersion relations for different boundary conditions, energy deposition and the partition of the waves energy are presented.

- In Chapter 6, extended MHD is used to derive the kinetic and magnetic spectra by resorting to a Kolmogorov-like hypothesis based on the constant cascading rates of the energy and Casimir invariants of this model. The magnetic and kinetic spectra are derived in the ideal, Hall, and electron inertia regimes. The resultant spectra are compared against the observational evidence, and shown to be in good agreement.

- In Chapter 7, the main conclusions arising from the work accomplished in this thesis are presented.

Chapter 2

Noncanonical Hamiltonian mechanics: A review

2.1 Canonical Hamiltonian mechanics

The description of a dynamical system in a Hamiltonian form requires the specification of a Hamiltonian and the formulation of a Poisson bracket; the Hamiltonian is physically the energy of the dynamical system, whilst the Poisson bracket mathematically characterizes the geometry. In other words, the Hamiltonian mechanics formulates the energy of the dynamical system as a function on a phase space X (Hamiltonian) and characterizes the geometry of the phase space using a Poisson bracket (Poisson manifold). Before going further, we would like to note that all discussions in this chapter are based on the following references [12,13,85,95,115,116,138].

Let us consider a dynamical system that described by

$$\frac{dq^i}{dt} = \frac{\partial}{\partial p_i}\mathscr{H}(\boldsymbol{q},\boldsymbol{p}), \tag{2.1}$$

$$\frac{dp_i}{dt} = -\frac{\partial}{\partial q^i}\mathscr{H}(\boldsymbol{q},\boldsymbol{p}), \tag{2.2}$$

where $\boldsymbol{q} = \sum_{i=1}^{N} q^i(t)$ are the N position coordinates, $\boldsymbol{p} = \sum_{i=1}^{N} p_i(t)$ are the N conjugate momenta and N is the number of the degree of freedom of the system. Here $\mathscr{H}$ is a function denoting the Hamiltonian of the system.

The above system of equations (2.1) and (2.2) are known as Hamilton's canonical equations.

The above canonical equations can be rewritten in a more general form as follows:

$$\frac{d\boldsymbol{z}}{dt} = \mathcal{J}_c \frac{\partial}{\partial \boldsymbol{z}} \mathscr{H}(\boldsymbol{z}), \tag{2.3}$$

where the state vector $\boldsymbol{z} = (\boldsymbol{q}, \boldsymbol{p}) = \sum_{i=1}^{2N} z^i$, is a point in an affine space $X = \mathbb{R}^{2N}$, $\mathscr{H}(\boldsymbol{z})$ is a Hamiltonian (a smooth function on X), and $\mathcal{J}_c$ is a canonical (symplectic) Poisson operator, which is an antisymmetric $2N \times 2N$ matrix with the form

$$\mathcal{J} = \begin{pmatrix} 0_N & I_N \\ -I_N & 0_N \end{pmatrix}. \tag{2.4}$$

Here, I_N and 0_N represent $N \times N$ identity and null matrices, respectively.

We define a bilinear form

$$\begin{aligned} \{F, G\} &= \left(\frac{\partial F}{\partial \boldsymbol{z}}, \mathcal{J}_c \frac{\partial G}{\partial \boldsymbol{z}} \right), \\ &= \sum_{i,j}^{N} \frac{\partial F}{\partial z_i} \mathcal{J}_c^{ij} \frac{\partial G}{\partial z_j}, \\ &= \sum_{i}^{N} \left(\frac{\partial F}{\partial q^i} \frac{\partial G}{\partial p_i} - \frac{\partial F}{\partial p_i} \frac{\partial G}{\partial q^i} \right), \end{aligned} \tag{2.5}$$

where F and G are any arbitrary scalar smooth functions (observables) of the dynamical variables ($\boldsymbol{q}$,$\boldsymbol{p}$) on the affine space X. The bracket $\{\ ,\ \}$ defined by (2.5) denotes a Poisson bracket, wherein it is a bilinear derivative map to a scalar function. In other words, it is a map that maps two smooth scalars functions F and G to produce a new smooth scalar functional (the left-hand side of (2.5)), defined over the affine space X.

Now, we can construct an adjoint representation of Hamilton's equations (2.3) as

$$\begin{aligned}\frac{d}{dt}F &= \{F, \mathscr{H}\}, \\ &= \sum_i^N \left(\frac{\partial F}{\partial q^i}\frac{\partial \mathscr{H}}{\partial p_i} - \frac{\partial F}{\partial p_i}\frac{\partial \mathscr{H}}{\partial q^i}\right). \end{aligned} \tag{2.6}$$

Thus, we can write the Hamilton's canonical equations (2.1) and (2.2) in terms of the Poisson bracket (2.5) as follows:

$$\frac{dq^i}{dt} = \left\{q^i, \mathscr{H}\right\}, \tag{2.7}$$

$$\frac{dp_i}{dt} = \left\{p_i, \mathscr{H}\right\}. \tag{2.8}$$

For any given bracket to be a Poisson bracket, it must satisfy the following postulates. In the case of canonical system defined above it easy to derive those axioms using its definition (2.5).

Let E, F and G be any arbitrary functions of the dynamical variables. The Poisson bracket properties are:

I. Antisymmetry: If we interchange the two functions in the bracket slots, the bracket sign has to change,

$$\{F, G\} = -\{G, F\} \quad \forall F, G \in C^\infty(X), \tag{2.9}$$

Proof.

$$\begin{aligned}\{F, G\} &= \sum_i^N \left(\frac{\partial F}{\partial q^i}\frac{\partial G}{\partial p_i} - \frac{\partial F}{\partial p_i}\frac{\partial G}{\partial q^i}\right), \\ &= -\sum_i^N \left(\frac{\partial G}{\partial q^i}\frac{\partial F}{\partial p_i} - \frac{\partial G}{\partial p_i}\frac{\partial F}{\partial q^i}\right), \\ &= -\{G, F\}. \quad \#\end{aligned}$$

Also, it follows from the anti-symmetry property of the Poisson bracket that Hamiltonian systems conserve energy,

$$\frac{d\mathscr{H}}{dt} = \{\mathscr{H}, \mathscr{H}\} = 0. \tag{2.10}$$

II. Bilinearity:

$$\{E, \alpha F + \beta G\} = \alpha \{E, F\} + \beta \{E, G\} \quad \forall E, F, G \in C^{\infty}(X), \tag{2.11}$$

where α and β are real numbers.

Proof.

$$\begin{aligned}
\{E, \alpha F + \beta G\} &= \sum_{i}^{N} \left(\frac{\partial E}{\partial q^i} \frac{\partial (\alpha F + \beta G)}{\partial p_i} - \frac{\partial E}{\partial p_i} \frac{\partial (\alpha F + \beta G)}{\partial q^i} \right), \\
&= \sum_{i}^{N} \left[\alpha \left(\frac{\partial E}{\partial q^i} \frac{\partial F}{\partial p_i} - \frac{\partial E}{\partial p_i} \frac{\partial F}{\partial q^i} \right) + \beta \left(\frac{\partial E}{\partial q^i} \frac{\partial G}{\partial p_i} - \frac{\partial E}{\partial p_i} \frac{\partial G}{\partial q^i} \right) \right], \\
&= \alpha \{E, F\} + \beta \{E, G\}.
\end{aligned}$$

This proves that the bracket is linear, using the antisymmetry (2.9) together with (2.11), it is straightforward to show that the linearity propriety holds on both sides of the Poisson bracket. #

III. Leibniz rule:

$$\{E\,F, G\} = E \{F, G\} + \{E, G\} F \quad \forall E, F, G \in C^{\infty}(X), \tag{2.12}$$

Proof.

$$\begin{aligned}
\{E\,F, G\} &= \sum_{i}^{N} \left(\frac{\partial (E\,F)}{\partial q^i} \frac{\partial G}{\partial p_i} - \frac{\partial (E\,F)}{\partial p_i} \frac{\partial G}{\partial q^i} \right), \\
&= \sum_{i}^{N} \left[E \left(\frac{\partial F}{\partial q^i} \frac{\partial G}{\partial p_i} - \frac{\partial F}{\partial p_i} \frac{\partial G}{\partial q^i} \right) + \left(\frac{\partial E}{\partial q^i} \frac{\partial G}{\partial p_i} - \frac{\partial E}{\partial p_i} \frac{\partial G}{\partial q^i} \right) F \right], \\
&= E \{F, G\} + \{E, G\} F. \quad \#
\end{aligned}$$

IV. Constant function C: If one of the observables is constant, the Poisson bracket is equal to zero,

$$\{F, C\} = 0 \quad \forall F \in C^{\infty}(X), \tag{2.13}$$

The proof can be directly obtained from the definition of the Poisson bracket (2.5).

V. Jacobi's identity:

$$\{E, \{F, G\}\} + \{G, \{E, F\}\} + \{F, \{G, E\}\} = 0 \quad \forall E, F, G \in C^{\infty}(X), \tag{2.14}$$

which holds for the Poisson brackets formed from any three functions. In other words, the summation of the brackets formed by cyclic permutations of any three functions must be equal zero.

Proof.

The proof of the Jacobi's identity is rather difficult since it contains second order derivatives of the functions E, F and G. At first, we shall collect all the terms that contain a second order derivative of one of the functions, e.g., F. The first and second brackets of (2.14) are the only terms contained a second order derivative of F, since the third bracket involves only the first derivative of F . Now, we will write the sum of the first and second brackets of (2.14) in terms of linear differential operators defined by

$$\{E, F\} = \frac{\partial E}{\partial q^i}\frac{\partial F}{\partial p_i} - \frac{\partial E}{\partial p_i}\frac{\partial F}{\partial q^i} = \mathscr{L}_e F,$$

and similarly,

$$\{G, F\} \;=\; \mathscr{L}_g F.$$

Then the sum can be written as

$$\{E, \{F, G\}\} + \{G, \{E, F\}\} = \left(\mathscr{L}_g \mathscr{L}_e - \mathscr{L}_e \mathscr{L}_g\right) F.$$

It is very clear in the above equation that this combination of the linear operators $\mathscr{L}_e$ and $\mathscr{L}_g$ does not involve a second order derivative of F. To show that, let us define the linear operators in more general form

$$\begin{aligned} \mathscr{L}_e &= \sum_{l}^{N} e_l \frac{\partial}{\partial z_l}, \\ \mathscr{L}_g &= \sum_{l}^{N} g_l \frac{\partial}{\partial z_l}, \end{aligned}$$

where e_l and g_l are arbitrary functions of the variables z_l, $l = 1, ..., N$. Then

$$\begin{aligned} \mathscr{L}_e \mathscr{L}_g &= \sum_{l,m}^{N} e_l g_m \frac{\partial^2}{\partial z_l \partial z_m} + \sum_{l,m=1}^{N} e_l \frac{\partial g_m}{\partial z_l} \frac{\partial}{\partial z_m}, \\ \mathscr{L}_g \mathscr{L}_e &= \sum_{l,m}^{N} g_l e_m \frac{\partial^2}{\partial z_l \partial z_m} + \sum_{l,m=1}^{N} g_l \frac{\partial e_m}{\partial z_l} \frac{\partial}{\partial z_m}. \end{aligned}$$

The subtraction of the above equations yields

$$\mathscr{L}_e \mathscr{L}_g - \mathscr{L}_g \mathscr{L}_e \;=\; \sum_{l,m}^{N} \left(e_l \frac{\partial g_m}{\partial z_l} - g_l \frac{\partial e_m}{\partial z_l} \right) \frac{\partial}{\partial z_m},$$

which is an operator including only single differentiations. Therefore, all the second order derivatives of F on the left-hand side of (2.14)

cancel out. It is easy to show that the same applies for the other functions E and G, and so the left-hand side of (2.14) is identically zero, which proves the Jacobi's identity.

Now, we can generalize the space $X = \mathbb{R}^{2N}$ to a general cotangent bundle T^*M of a smooth manifold M of dimension N, which represents the phase space of the system. Therefore, we can define a symplectic 2-form in terms of the local coordinates $(\boldsymbol{q}, \boldsymbol{p})$ as

$$\omega = d\boldsymbol{q} \wedge d\boldsymbol{p} = \sum_{i}^{N} dq^i \wedge dp_i, \tag{2.15}$$

where we have used the symbol d to denote the exterior derivative and the symbol $\wedge$ to denote the exterior product. The merit of defining a 2-form is to allow us to define a Hamiltonian vector field $X_{\mathscr{H}}$, such that $i_{X_{\mathscr{H}}}\omega = d\mathscr{H}$, where the definition of the Left-hand side is provided below.

Let

$$X_{\mathscr{H}} = \sum_{i}^{N} \left(\frac{\partial \mathscr{H}}{\partial p_i} \frac{\partial}{\partial q^i} - \frac{\partial \mathscr{H}}{\partial q^i} \frac{\partial}{\partial p_i} \right),$$

then

$$i_{X_{\mathscr{H}}}\omega = \sum_{i}^{N} dq^i \wedge dp_i \sum_{j}^{N} \left(\frac{\partial \mathscr{H}}{\partial p_j} \frac{\partial}{\partial q^j} - \frac{\partial \mathscr{H}}{\partial q^j} \frac{\partial}{\partial p_j} \right),$$

since, $dq^i \frac{\partial}{\partial q^j} = \delta_{ij}$, $dp_i \frac{\partial}{\partial p_j} = \delta_{ij}$, $dq^i \frac{\partial}{\partial p_j} = 0$, $dp_i \frac{\partial}{\partial q^j} = 0$, and $dq^i \wedge dp_i = -dp_i \wedge dq^i$, we have

$$\begin{aligned} i_{X_{\mathscr{H}}}\omega &= \sum_{i}^{N} dq^i \wedge dp_i \left(\frac{\partial \mathscr{H}}{\partial p_i} \frac{\partial}{\partial q^i} - \frac{\partial \mathscr{H}}{\partial q^i} \frac{\partial}{\partial p_i} \right) \\ &= \sum_{i}^{N} \left(\frac{\partial \mathscr{H}}{\partial p_i} dp_i + \frac{\partial \mathscr{H}}{\partial q^i} dq^i \right) \\ &= d\mathscr{H} \end{aligned}$$

The Poisson bracket (2.5) can be written in terms of the symplectic 2-form ω as

$$\{F, G\} \;=\; \omega\left(X_F, X_G\right), \tag{2.16}$$

where X_F and X_G are the gradient (or Hamiltonian) vector fields of the F and G. Then, we have

$$\begin{aligned}
\{F, G\} &= \omega\left(X_F, X_G\right), \\
&= \sum_i^N dq^i \wedge dp_i \sum_j^N \left(\frac{\partial F}{\partial p_j}\frac{\partial}{\partial q^j} - \frac{\partial F}{\partial q^j}\frac{\partial}{\partial p_j}\right) \sum_k^N \left(\frac{\partial G}{\partial p_k}\frac{\partial}{\partial q^k} - \frac{\partial G}{\partial q^k}\frac{\partial}{\partial p_k}\right) \\
&= \sum_i^N \left(\frac{\partial F}{\partial p_i}dp_i + \frac{\partial \mathscr{H}}{\partial q^i}dq^i\right) \sum_k^N \left(\frac{\partial G}{\partial p_k}\frac{\partial}{\partial q^k} - \frac{\partial G}{\partial q^k}\frac{\partial}{\partial p_k}\right) \\
&= \sum_i^N \left(\frac{\partial F}{\partial q^i}\frac{\partial G}{\partial p_i} - \frac{\partial F}{\partial p_i}\frac{\partial G}{\partial q^i}\right),
\end{aligned}$$

In the generalized coordinates $\boldsymbol{z} = (\boldsymbol{q}, \boldsymbol{p})$, we may write the above relation as

$$\{F, G\} = \omega\left(X_F, X_G\right) = \sum_{i,j}^N \frac{\partial F}{\partial z_i}\mathcal{J}_c^{ij}\frac{\partial G}{\partial z_j}, \tag{2.17}$$

where $\mathcal{J}_c = \mathcal{J}_c^{-1}$.

2.2 Noncanonical Hamiltonian mechanics

In reality, most of the physical systems are described by noncanonical (physical) variables (coordinates). Noncanonical Hamiltonian systems are common in classical field theories, e.g., fluid and plasma systems. In this section, we shall explore the notion of noncanonical Hamiltonian mechanics. We still restrict ourselves to systems with finite degrees of freedom.

The noncanonical Hamiltonian system is a generalization of the canonical Hamiltonian system to a phase space, in which the Poisson operator is a function of the state vector. The system still has to preserve the energy (2.10).

As in the previous section, let us consider a physical system described by a state vector $\boldsymbol{z}$ of dimension N. Here, N is an arbitrary finite number, which is not necessary even. This system is said to be Hamiltonian, if and only if it satisfy the Hamilton's equation of motion

$$\frac{d\boldsymbol{z}}{dt} = \{\boldsymbol{z}, \mathscr{H}\}, \tag{2.18}$$

where $\{\ ,\ \}$ here denote the noncanonical Poisson bracket. This bracket still has to satisfy the conditions of antisymmetry, bilnearity, Leibniz rule and the Jacobi's identities, mentioned in Sec. 2.1. Introducing the noncanonical Poisson operator $\mathcal{J}(\boldsymbol{z})$, that is now a function of the state vector $\boldsymbol{z}$, the general Hamilton's equation of motion (2.18) can be written as

$$\frac{d\boldsymbol{z}}{dt} = \mathcal{J}(\boldsymbol{z}) \frac{\partial}{\partial \boldsymbol{z}} \mathscr{H}(\boldsymbol{z}). \tag{2.19}$$

The Poisson operator $\mathcal{J}(\boldsymbol{z})$ is said to be singular, if the condition $\det\mathcal{J} = 0$ holds true. This singularity in the Poisson operator gives rise to some scalar functions $C(\boldsymbol{z})$. Those functions $C(\boldsymbol{z})$ satisfy

$$\{F(\boldsymbol{z}), C(\boldsymbol{z})\} = 0, \tag{2.20}$$

for any function F. These functions are usually referred to as *Casimir element*.

In this case, there exists a theory known as the Lie-Darboux theorem [95], in which enables us to separate the canonical part of the noncanonical Poisson operator under a limited condition. The theory stated that if the $Rank(\mathcal{J}) = 2m < N$ (m is constant) and the $\det\mathcal{J} = 0$, then, there exist a k independent Casimir elements $(C_1, ..., C_k)$, such that $N = 2m + k$. In that case, the Poisson operator $\mathcal{J}$ can be transformed to the following standard form

$$\mathcal{J}^{\star} = \left(\begin{array}{cc:c} 0_m & I_m & \\ -I_m & 0_m & \\ \hdashline & & 0_k \end{array}\right). \tag{2.21}$$

We can note that the new operator $\mathcal{J}^{\star}$ subsumed a canonical part of $\text{rank}(\mathcal{J}^{\star}) = 2m$ and a degenerate part with k's extraneous coordinates. This means that there are k null eigenfunctions of the $\mathcal{J}^{\star}$ represented by the Casimir elements given by the solution of the following differential equation,

$$\mathcal{J}^{ij}\frac{\partial C^l}{\partial z^j} = 0, \quad l = 1, 2...k. \tag{2.22}$$

Before moving further, it is worth remarking here that, the Lie-Darboux theorem applies only for finite-dimensional systems and does not give any method to identify the new coordinates, i.e., we can not obtain the equations of motions in terms of the new coordinates.

2.3 Casimir invariant

The Casimir invariants are one of the most interesting features of the noncanonical Poisson brackets, which is a consequence of the topological defect (kernel) of the Poisson operator. A Casimir function need to satisfy

the following identity:

$$\{F(\boldsymbol{z}), C(\boldsymbol{z})\} = 0, \tag{2.23}$$

This implies that the gradient of $C(\boldsymbol{z})$ is

$$\mathcal{J}(\boldsymbol{z}) \frac{\partial C(\boldsymbol{z})}{\partial \boldsymbol{z}} = 0. \tag{2.24}$$

Moreover, we can easy see that the Casimir is an invariant of the dynamical system. Due to the antisymmetry of the Poisson operator, we can obtain

$$\frac{d}{dt} C(\boldsymbol{z}) = \{C(\boldsymbol{z}), \mathscr{H}(\boldsymbol{z})\} = 0. \tag{2.25}$$

We can observe from the above relations that even when the Hamiltonian is one of the system invariants, the Poisson bracket of it does not vanish. This implies that the Casimir is a feature of the kinematics or in another word a geometrical constant of motion in the phase space. Thus, the properties of the Casimir invariant are determined by the degenerate structure of the Poisson operator, not the Hamiltonian.The Casimir invariant as a constant of motion constrains the dynamics to the surface of constant Casimir invariants. Such a constant Casimir is called leaf, and the phase space is foliated by such leaves.

2.4 Energy-Casimir functional

The existence of Casimir invariants has some interesting consequences. One of the most promising consequences of the existence of a Casimir invariant is that the physical Hamiltonian of the system is not unique. To

clarify the last sentence, let us replace the physical Hamiltonian ($\mathscr{H}(\boldsymbol{z})$) by ($\mathscr{H}_{\mu}(\boldsymbol{z})$), defined by

$$\mathscr{H}_{\mu}(\boldsymbol{z}) = \mathscr{H}(\boldsymbol{z}) - \mu C(\boldsymbol{z}), \tag{2.26}$$

where μ is constant. Substituting (2.26) into the equations of motion (2.18), gives

$$\begin{aligned} \frac{d\boldsymbol{z}}{dt} &= \{\boldsymbol{z}, \mathscr{H}_{\mu}(\boldsymbol{z})\}, \\ &= \{\boldsymbol{z}, \mathscr{H}(\boldsymbol{z})\} - \mu\{\boldsymbol{z}, C(\boldsymbol{z})\}, \\ &= \{\boldsymbol{z}, \mathscr{H}\}, \end{aligned} \tag{2.27}$$

where the antisymmetry (2.9) and bilinearity (2.11) properties of the Poisson bracket are used and equation (2.24) is invoked. From (2.27), we can observe that substituting the perturbed Hamiltonian (2.26) into the equations of motion (2.18), does not change the dynamics. However, the equilibrium of the system may change under the substitution of (2.26). Let us discuss the latter sentence in more detail.

Let z_0 be an equilibrium point that satisfies the equation of motion

$$\frac{dz}{dt}|_{z_0} = \mathcal{J}(z_0)\frac{\partial}{\partial z}\mathscr{H}(z)|_{z_0} = 0. \tag{2.28}$$

If the Poisson operator is non-singular (canonical), i.e., $det(\mathcal{J}) \neq 0$, this means that the equilibria of the system are the extremal points of the Hamiltonian only, i.e., $\partial_{\boldsymbol{z}}\mathscr{H} = 0$. So, in canonical Hamiltonian mechanics, the equilibria of the dynamical system can only be described by the structure of the Hamiltonian. If we moved to the noncanonical case, the situation is completely different. Now, the Poisson operator is singular,

i.e., $det(\mathcal{J}) = 0$, thus, the noncanonical system can have a richer set of equilibrium points, because of the existence of the null-space of the Poisson operator. This null-space is spanned by the Casimir invariants of the system. As already mentioned, the dynamics are restricted to surfaces of constant Casimir invariants, therefore, the equilibrium points can be characterized as fixed points on the Casimir leaves. Consequently, the equilibria of the noncanonical system can be obtained as critical points on the Casimir leaves by

$$\frac{\partial}{\partial \boldsymbol{z}} \mathscr{H}_{\mu}(\boldsymbol{z}) = 0, \tag{2.29}$$

where $\mathscr{H}_{\mu}$ defined by (2.26) is known as the energy-Casimir function [13, 67, 83].

2.5 Infinite-dimensional noncanonical systems

The finite-dimensional Hamiltonian formulation discussed above used usually to describe discrete systems such as particles, whilst the infinite-dimensions are critical for describing field theories such as hydrodynamics and magnetohydrodynamics. Moving to the infinite-dimensional systems (or continuous systems), we have to use the functionals instead of functions, and the functional derivative instead of partial derivative. We prepare general notations to formulate infinite-dimensional noncanonical Hamiltonian systems.

Analogous to the finite-dimensional case, a general Hamiltonian equation can be written as

$$\frac{\partial u}{\partial t} = \mathcal{J}(u) \frac{\partial}{\partial u} \mathscr{H}(u), \tag{2.30}$$

where the state vector u is a point in a phase space (Hilbert space) X, $\mathscr{H}(u)$ is a Hamiltonian (a smooth functional on X), $\partial_u \mathscr{H}$ is the gradient of $\mathscr{H}$ in X, and $\mathcal{J}(u)$ is a Poisson operator (co-symplectic 2-covector). In the latter discussions, the state vector u is a vector-valued function on a base space $\Omega \subset R^3$. The inner product of the phase space X is defined by $\langle u, v \rangle = \int_\Omega u \cdot v d^3x$.

The Poisson bracket that is still mandated to satisfy the formal properties, e.g., antisymmetry, Leibniz property, and Jacobi's identity, can be defined as

$$\{F, G\} = \left\langle \frac{\partial}{\partial u} F, \mathcal{J} \frac{\partial}{\partial u} G \right\rangle, \tag{2.31}$$

where F and G are scalar smooth functionals on the phase space X. The adjoint representation of Hamilton's equation (2.30) reads, for an arbitrary observable $F \in C^\infty_{\{\,,\,\}}(X)$.

$$\frac{d}{dt} F = \{F, \mathscr{H}\}. \tag{2.32}$$

Before going further, it is worth remarking that, all the above discussions about the Casimir invariants and the energy-Casimir method can be defined here analogously to the finite-dimensional case.

Next, we shall give example of the infinite-dimensional noncanonical Hamiltonian system, ideal fluid.

2.5.1 The ideal fluid

Consider a $3+1$ barotropic ideal fluid in Eulerian coordinates (denoted by $\boldsymbol{x} := (x, y, z)$ and t). The equations of motion comprise of the

mass conservation

$$\frac{\partial \rho}{\partial t} = -\nabla \cdot (\rho \boldsymbol{V}), \tag{2.33}$$

the dynamical equation for velocity,

$$\frac{\partial \boldsymbol{V}}{\partial t} = -(\nabla \times \boldsymbol{V}) \times \boldsymbol{V} - \nabla \left(h + \frac{V^2}{2} \right), \tag{2.34}$$

where ρ is mass density, $\boldsymbol{V}$ fluid velocity and $h(\rho)$ is the enthalpy (the relation between the fluid scalar pressure p and the enthalpy is $\nabla h = \rho^{-1} \nabla p$.

The Hamiltonian (energy) of the ideal fluid is given by

$$\mathscr{H} = \int_\Omega \rho \left\{ \frac{V^2}{2} + U(\rho) \right\} d^3x, \tag{2.35}$$

where U is the internal energy of the system, which is connected to the enthalpy by $\frac{\partial \rho U(\rho)}{\partial \rho} = h(\rho)$.

The noncanonical Poisson operator is

$$\mathcal{J} = \begin{pmatrix} 0 & -\nabla \cdot \\ -\nabla & -\rho^{-1} (\nabla \times \boldsymbol{V}) \times \circ \end{pmatrix}, \tag{2.36}$$

and the corresponding noncanonical Poisson bracket of the barotropic compressible fluid is given by

$$\begin{aligned} \{F, G\} \;=\; & \int_\Omega \Big[\rho^{-1} (\nabla \times \boldsymbol{V}) \cdot (\partial_{\boldsymbol{V}} F \times \partial_{\boldsymbol{V}} G) \\ & - \Big(\partial_\rho F \, (\nabla \cdot \partial_{\boldsymbol{V}} G) - (\nabla \cdot \partial_{\boldsymbol{V}} F) \, \partial_\rho G \Big) \Big] d^3x, \end{aligned} \tag{2.37}$$

where the state vector is $u = (\rho, \boldsymbol{V})^t$, and ∂_u the functional derivative of the arbitrary scalar functionals F and G with respect to the dynamical variables of the system u.

Now, we can easily show that the bracket (2.37) satisfies the antisymmetry and Leibniz properties by using a standard vector calculus identity. However the proof of the Jacobi's identity is not that easy to obtain. A complete proof of the Jacobi's identity is given in Chapter. 3, see lemma 1.

Using the above Hamiltonian structure, we can derive the equations of motion (2.33) and (2.34) from the Poisson bracket (2.37) using Hamilton's equations,

$$\frac{\partial u}{\partial t} = \{u, \mathscr{H}\}\,. \tag{2.38}$$

At first, we will calculate the gradient of the Hamiltonian, which is

$$\partial_u \mathscr{H} = \begin{pmatrix} \partial_\rho \mathscr{H} \\ \\ \partial_{\boldsymbol{V}} \mathscr{H} \end{pmatrix} = \begin{pmatrix} \frac{V^2}{2} + h \\ \\ \rho \boldsymbol{V} \end{pmatrix}. \tag{2.39}$$

To drive the equation of mass conservation, one need to introduce the following functional

$$\frac{\partial u}{\partial t} = \int_\Omega \rho\delta\left(\boldsymbol{x} - \boldsymbol{x}_0\right) d^3x, \tag{2.40}$$

to remove the integrals from (2.38), where δ is the delta function. Then, using (2.39) and (2.40) in (2.38), we have

$$\frac{\partial \rho}{\partial t} = -\nabla \cdot (\rho \boldsymbol{V})\,,$$

The derivation of the velocity equation of motion can be done through a similar procedure. It is seen from (2.38) that two terms involving the functional derivative of $\boldsymbol{V}$ are manifested, the first and third terms, which after simple manipulation lead to

$$\frac{\partial \boldsymbol{V}}{\partial t} = -\left(\nabla \times \boldsymbol{V}\right) \times \boldsymbol{V} - \nabla\left(h + \frac{V^2}{2}\right),$$

Now to find the Casimir invariants of the ideal fluid, we have to satisfy the condition $\{F, C\}$ for all F. Using Poisson bracket (2.37), the Casimir condition imply

$$\rho^{-1}\left(\nabla \times \boldsymbol{V}\right) \times \partial_{\boldsymbol{V}} C + \nabla \partial_{\rho} C \;\; = \;\; 0,$$

$$\nabla \cdot \partial_{\boldsymbol{V}} C \;\; = \;\; 0.$$

The solution of this system of equations yields

total mass

$$C_1 = \int_{\Omega} \rho d^3 x, \tag{2.41}$$

fluid helicity

$$C_2 = \int_{\Omega} \boldsymbol{V} \cdot \nabla \times \boldsymbol{V} d^3 x. \tag{2.42}$$

Applying the energy-Casimir functional (2.26), which now reads

$$\mathscr{H}_{\mu} = \mathscr{H} - \mu_1 C_1 - \mu_2 C_2,$$

then the equilibrium points are given by setting $\partial \mathscr{H}_{\mu} = 0$, which gives

$$\rho \boldsymbol{V} \;\; = \;\; \mu_2 \nabla \times \boldsymbol{V}, \tag{2.43}$$

$$\frac{V^2}{2} + h \;\; = \;\; \mu_1. \tag{2.44}$$

2.5.1.1 Beltrami fields

Beltrami fields are eigenfunctions of the curl operator ($\nabla \times$) when the flow field and its associated vorticity are aligned. Considering the incompressible fluid limit that ($\nabla \cdot \boldsymbol{V} = 0$), which yields a constant density ($\rho = 1$), the equilibrium equation (2.43) gives the Beltrami flow equation

$$\nabla \times \boldsymbol{V} \;\; = \;\; \frac{1}{\mu_2}\boldsymbol{V}, \tag{2.45}$$

The general solution of equation (2.45) can be given as

$$\boldsymbol{V} = a\boldsymbol{G}, \tag{2.46}$$

where a is a constant, and $\boldsymbol{G}$ is the eigenfunction of the single Beltrami condition ($\nabla \times \boldsymbol{G} = \lambda \boldsymbol{G}$) with $\lambda = \frac{1}{\mu_2}$. In the rectangular coordinates (x, y, z), the eigenfunctions of the Beltrami equation possess the form of a sinusoidal function given in a form of a circularly polarized wave, as

$$\boldsymbol{G}_1 = \begin{pmatrix} \sin(\lambda z) \\ \cos(\lambda z) \\ 0 \end{pmatrix}.$$

Chapter 3

Hamiltonian formalism of extended magnetohydrodynamics

3.1 Extended MHD model

3.1.1 Two-fluid system

Consider a collisionless plasma consisting of electrons with charge $(-e)$ and one kind of ions with charge(Ze), where Z is charge number. The set of the dissipativeless two-fluid equations is

$$\frac{\partial n_e}{\partial t} = -\nabla \cdot (n_e \boldsymbol{V}_e)\,, \tag{3.1}$$

$$\frac{\partial n_i}{\partial t} = -\nabla \cdot (n_i \boldsymbol{V}_e)\,. \tag{3.2}$$

$$n_e m_e \left(\frac{\partial \boldsymbol{V}_e}{\partial t} + (\boldsymbol{V}_e \cdot \nabla)\, \boldsymbol{V}_e\right) = -\nabla p_e - e n_e \left(\boldsymbol{E} + \boldsymbol{V}_e \times \boldsymbol{B}\right), \tag{3.3}$$

$$n_i m_i \left(\frac{\partial \boldsymbol{V}_i}{\partial t} + (\boldsymbol{V}_i \cdot \nabla)\, \boldsymbol{V}_i\right) = -\nabla p_i + Z e n_i \left(\boldsymbol{E} + \boldsymbol{V}_i \times \boldsymbol{B}\right), \tag{3.4}$$

where the two-fluid variables n_e, $\boldsymbol{V}_e$, n_i and $\boldsymbol{V}_i$ are the electron density, the electron velocity, the ion density and the ion velocity respectively. p_e and p_i denote the electron and ion pressures, whilst $\boldsymbol{E}$ and $\boldsymbol{B}$ are the electric and magnetic fields, and m_e and m_i are the electron and ion masses. The two-fluid system of equations (3.1)-(3.4) are closed by the Maxwell's equations,

$$\nabla \times \boldsymbol{E} \;\; = \;\; -\frac{\partial \boldsymbol{B}}{\partial t}, \tag{3.5}$$

$$\nabla \times \boldsymbol{B} = \mu_0 \boldsymbol{J} + \frac{1}{c^2}\frac{\partial \boldsymbol{E}}{\partial t}, \tag{3.6}$$

$$\nabla \cdot \boldsymbol{E} = \frac{\tau}{\epsilon_0}, \tag{3.7}$$

$$\nabla \cdot \boldsymbol{B} = 0, \tag{3.8}$$

with the current and charge density,

$$\boldsymbol{J} \equiv e\left(Zn_i\boldsymbol{V}_i - n_e\boldsymbol{V}_e\right), \qquad \tau \equiv e\left(Zn_i - n_e\right), \tag{3.9}$$

acting as sources. Here, $c = 1/\sqrt{\epsilon_0\mu_0}$ is the speed of light, whilst ϵ_0 and μ_0 are the permittivity and permeability of vacuum space.

3.1.2 One-fluid system

We are now in a position to derive the one-fluid MHD model from the two-fluid equations (3.1)-(3.4). Imposing the quasineutrality condition ($\tau \cong 0$), which is one of the most fundamental properties that plasmas have to maintain, we obtain a system of equations governing the total mass density ρ, the center of mass velocity $\boldsymbol{V}$, and the current density $\boldsymbol{J}$. By adding of the electron and ion continuity equations((3.1) and (3.2)), we obtain the mass conservation law

$$\frac{\partial \rho}{\partial t} = -\nabla \cdot (\rho \boldsymbol{V}). \tag{3.10}$$

where $\rho = (m_i n_i + m_e n_e) = (1+\delta)\, m_i n$ ($\delta = m_e/m_i$ is a small parameter; by charge neutrality, we put $n_i = n_e = n$). Notice that, without loss of generality, for simplicity, we put $Z = 1$. The formulae of the electron velocity $\boldsymbol{V}_e$ and the ion velocity $\boldsymbol{V}_i$ in terms of the plasma flow velocity $\boldsymbol{V}$ and the plasma current density $\boldsymbol{J}$ are

$$\boldsymbol{V}_e = \boldsymbol{V} - \frac{\boldsymbol{J}}{en\,(1+\delta)} \qquad \text{and} \qquad \boldsymbol{V}_i = \boldsymbol{V} + \delta\frac{\boldsymbol{J}}{en\,(1+\delta)}. \tag{3.11}$$

Summing the equations of motion (3.3) amd (3.4) yields the momentum equation

$$\rho\left(\frac{\partial \boldsymbol{V}}{\partial t}+(\boldsymbol{V}\cdot\nabla)\,\boldsymbol{V}\right)=-\nabla p+\boldsymbol{J}\times\boldsymbol{B}-\frac{m_e}{e}\,(\boldsymbol{J}\cdot\nabla)\,\frac{\boldsymbol{J}}{en}, \tag{3.12}$$

where $p = p_i + p_e$ is the total pressure. Notice that, the last term on the right-hand side of equation (3.12) is of $O(\delta)$, which plays an essential role in conservation of energy [79]. To make (3.12) exact up to $O(\delta^2)$, we should replace m_e by $m_e' = m_e/(1+\delta)$. The other equation determines the evolution of electron fluid momentum. Instead of using $\boldsymbol{V}_e$, we write the electron inertia in terms of $\boldsymbol{J}/en$:

$$\begin{aligned}\frac{m_e}{e^2}\left[\frac{\partial}{\partial t}\left(\frac{\boldsymbol{J}}{n}\right)+(\boldsymbol{V}\cdot\nabla)\frac{\boldsymbol{J}}{n}+\left(\frac{\boldsymbol{J}}{n}\cdot\nabla\right)\boldsymbol{V}-\left(\frac{\boldsymbol{J}}{n}\cdot\nabla\right)\frac{\boldsymbol{J}}{en}\right]\\ =\boldsymbol{E}+\boldsymbol{V}\times\boldsymbol{B}-\frac{1}{en}\Big(\boldsymbol{J}\times\boldsymbol{B}-\nabla p_e\Big),\end{aligned} \tag{3.13}$$

where $\boldsymbol{E}$ is the electric field. On the left-hand side of equation (3.13), we have neglected

$$\frac{m_e}{e}\frac{d\boldsymbol{V}}{dt}\equiv\frac{m_e}{e}\left(\frac{\partial \boldsymbol{V}}{\partial t}+(\boldsymbol{V}\cdot\nabla)\,\boldsymbol{V}\right),$$

assuming

$$\left|\frac{d\boldsymbol{V}}{dt}\right|<<\left|\frac{d}{dt}\left(\frac{\boldsymbol{J}}{en}\right)\right|.$$

This approximation may not be appropriate in discussions of some phenomena in which the momentum balance between electrons and ions plays an essential role; for example see the studies on whistler oscillitons [49, 106, 139, 172]. The merit of replacing $\boldsymbol{V}_e$ by $\boldsymbol{J}/en$ and writing the electron fluid equation as (3.13) is, by combining with pre-Maxwell relation $\nabla\times\boldsymbol{B}=\boldsymbol{J}$,

the dimensions of dynamical variables are substantially reduced; see (3.18). Summarizing the equations and normalizing variables in the standard Alfvén units, we obtain a system of governing equations

$$\frac{\partial \rho}{\partial t} = -\nabla \cdot (\rho \boldsymbol{V}), \tag{3.14}$$

$$\rho \left(\frac{\partial \boldsymbol{V}}{\partial t} + (\boldsymbol{V}.\nabla)\, \boldsymbol{V} \right) = -\nabla p + \boldsymbol{J} \times \boldsymbol{B} - d_e^2 (\boldsymbol{J} \cdot \nabla) \frac{\boldsymbol{J}}{\rho}, \tag{3.15}$$

$$\begin{aligned} \boldsymbol{E} + \boldsymbol{V} \times \boldsymbol{B} \;=\; & -\frac{d_i}{\rho} \nabla p_e + d_i \frac{\boldsymbol{J}}{\rho} \times \boldsymbol{B} \\ & + d_e^2 \left[\frac{\partial}{\partial t} \left(\frac{\boldsymbol{J}}{\rho} \right) + (\boldsymbol{V} \cdot \nabla) \frac{\boldsymbol{J}}{\rho} + \left(\frac{\boldsymbol{J}}{\rho} \cdot \nabla \right) \boldsymbol{V} \right] \\ & - d_i d_e^2 \left(\frac{\boldsymbol{J}}{\rho} \cdot \nabla \right) \frac{\boldsymbol{J}}{\rho}, \end{aligned} \tag{3.16}$$

where $d_e = c/(\omega_{pe} L)$ is the normalized electron skin depth, $d_i = c/(\omega_{pi} L)$ is the normalized ion skin depth, whilst ω_{pe} and ω_{pi} are the electron and ion plasma frequencies, and L is the system size.

The above equations are coupled with the pre-Maxwell equations

$$\nabla \times \boldsymbol{E} = -\frac{\partial \boldsymbol{B}}{\partial t}, \tag{3.17}$$

and

$$\nabla \times \boldsymbol{B} = \boldsymbol{J}. \tag{3.18}$$

We omit Maxwell displacement current to make the field equations consistent with the above fluid equations. There are some phenomena, however, in which charge neutrality may be broken (see [169]), then one needs to consider independent electron and ion densities.

3.2 Noncanonical Hamiltonian structure of extended MHD

3.2.1 Poisson algebra of extended MHD

Operating $\nabla\times$ on both side of (3.16), assuming barotropic pressures ($\rho^{-1}\nabla p = \nabla h(\rho)$, $\rho^{-1}\nabla p_e = \nabla h_e(\rho)$, where $h(\rho)$ is the total enthalpy and $h_e(\rho)$ is the electron enthalpy) and using (3.18), we obtain a system of evolution equations

$$\frac{\partial \rho}{\partial t} = -\nabla\cdot(\rho \boldsymbol{V}), \tag{3.19}$$

$$\begin{aligned}\frac{\partial \boldsymbol{V}}{\partial t} &= -(\nabla\times\boldsymbol{V})\times\boldsymbol{V} + \rho^{-1}(\nabla\times\boldsymbol{B})\times\boldsymbol{B}^* \\ &\quad -\nabla\left(h + \frac{V^2}{2} + d_e^2\frac{(\nabla\times\boldsymbol{B})^2}{2\rho^2}\right),\end{aligned} \tag{3.20}$$

$$\begin{aligned}\frac{\partial \boldsymbol{B}^*}{\partial t} &= \nabla\times(\boldsymbol{V}\times\boldsymbol{B}^*) - d_i\nabla\times\left(\rho^{-1}(\nabla\times\boldsymbol{B})\times\boldsymbol{B}^*\right) \\ &\quad +d_e^2\nabla\times\left(\rho^{-1}(\nabla\times\boldsymbol{B})\times(\nabla\times\boldsymbol{V})\right),\end{aligned} \tag{3.21}$$

where

$$\boldsymbol{B}^* = \boldsymbol{B} + d_e^2\nabla\times\rho^{-1}(\nabla\times\boldsymbol{B}). \tag{3.22}$$

For the simplicity, we consider a domain S_3 with periodic boundary conditions.

The conservation of energy of the extended MHD was studied by [78, 79]; the total energy is given as

$$\mathscr{H} := \int_\Omega \left\{\rho\left(\frac{V^2}{2} + U(\rho)\right) + \frac{B^2}{2} + d_e^2\frac{(\nabla\times\boldsymbol{B})^2}{2\rho}\right\} d^3x. \tag{3.23}$$

This $\mathscr{H}$ is the natural candidate for the Hamiltonian.

To formulate the Hamiltonian system, we consider a *phase space* spanned by the variables $\rho, \boldsymbol{V}$, and $\boldsymbol{B}^*$; we denote the state vector by $u = (\rho, \boldsymbol{V}, \boldsymbol{B}^*)^t$. Then, $\boldsymbol{B}$ in $\mathscr{H}$ must be evaluated as a function of $\boldsymbol{B}^*$ and ρ by (3.22). The gradient of the Hamiltonian $\mathscr{H}$ is

$$\partial_u \mathscr{H} = \begin{pmatrix} \partial_\rho \mathscr{H} \\ \partial_{\boldsymbol{V}} \mathscr{H} \\ \partial_{\boldsymbol{B}^*} \mathscr{H} \end{pmatrix} = \begin{pmatrix} \frac{V^2}{2} + h + d_e^2 \left(\frac{(\nabla \times \boldsymbol{B})^2}{2\rho^2} \right) \\ \rho \boldsymbol{V} \\ \boldsymbol{B} \end{pmatrix}. \tag{3.24}$$

Now, we propose a Poisson operator for the extended MHD equations:

$$\mathcal{J} = \begin{pmatrix} 0 & -\nabla\cdot & 0 \\ -\nabla & -\frac{(\nabla\times\boldsymbol{V})\times\circ}{\rho} & \frac{(\nabla\times\circ)\times\boldsymbol{B}^*}{\rho} \\ 0 & \nabla\times\frac{(\circ\times\boldsymbol{B}^*)}{\rho} & \left[-\nabla\times\left(\frac{(\nabla\times\circ)\times\boldsymbol{B}^*}{\rho}\right) \right. \\ & & \left. +d_e^2\nabla\times\left(\frac{(\nabla\times\circ)\times(\nabla\times\boldsymbol{V})}{\rho}\right) \right] \end{pmatrix}, \tag{3.25}$$

With the Poisson operator (3.25) and the Hamiltonian (3.23), Hamilton's equation (2.30) reproduces the extended MHD equations (3.19), (3.20), and (3.21).

Using the periodic boundary conditions, we can easily demonstrate the antisymmetry of $\mathcal{J}$. Hence the Poisson bracket defined by this $\mathcal{J}$ satisfies antisymmetry. However, the proof of Jacobi's identity is rather elaborate. Leaving it for the next section, we end this section by stating the main assertion:

Theorem 1 (Poisson algebra of extended MHD)**.** *We define a bilinear form*

$$\{F, G\} = \langle \partial_u F, \mathcal{J} \partial_u G \rangle.$$

Then, $\{\ ,\ \}$ *is a Poisson bracket, and* $C^\infty_{\{\ ,\ \}}(X)$ *is a Poisson algebra. Providing it with a Hamiltonian* $\mathscr{H}$ *of (3.23), we obtain the extended MHD system.*

Before concluding this section we want to mention that, if we construct a bracket by a semidirect product of sub Lie algebras, we can prove that the bracket satisfies Jacobi's identity [102–104]. Examples of ideal fluid, MHD and multifluid plasmas [70, 152], as well as Hall-MHD [69], were studied by this method. However, the present model of generalized MHD is not an example of such systems.

3.3 Jacobi's identity

3.3.1 Basic algebra

We have yet to prove Jacobi's identity for the Poisson bracket. Apparently, it is not of a Lie-Poisson type. Complexity is caused by the factor ρ^{-1}, as well as differential operator $\nabla\times$ appearing in many places of $\mathcal{J}$. However, there is a basic, common permutation relation that generates the total Poisson system. We prove the following lemma:

Lemma 1. *On* $C^\infty(X)$*, we define a bracket (bilinear form)*

$$\begin{aligned}[F, G]^{\boldsymbol{p}}_{\boldsymbol{q},\boldsymbol{r}} \quad = \quad & \int_\Omega \Big[\rho^{-1} \left(\nabla \times \boldsymbol{p}\right) \cdot \left(\partial_{\boldsymbol{q}} F \times \partial_{\boldsymbol{r}} G\right) \\ & - \partial_\rho F \left(\nabla \cdot \partial_{\boldsymbol{r}} G\right) - \partial_{\boldsymbol{q}} F \cdot \nabla \partial_\rho G \Big] d^3x, \end{aligned} \tag{3.26}$$

where $\boldsymbol{p}, \boldsymbol{q}$, *and* $\boldsymbol{r}$ *are vector fields arbitrarily chosen from* $\boldsymbol{V}$ *or* $\boldsymbol{A}^*$ *(where* $\boldsymbol{A}^*$*is the vector potential and is related to* $\boldsymbol{B}^*$ *by the relation* $\boldsymbol{B}^* = \nabla \times \boldsymbol{A}^*$*). This bracket satisfies an antisymmetry relation*

$$[F, G]^{\boldsymbol{p}}_{\boldsymbol{q},\boldsymbol{r}} = -[G, F]^{\boldsymbol{p}}_{\boldsymbol{r},\boldsymbol{q}},$$

as well as a permutation law

$$\left[E, [F, G]^{\boldsymbol{p}}_{\boldsymbol{q},\boldsymbol{r}}\right]^{\boldsymbol{p}}_{\boldsymbol{s},\boldsymbol{p}} + \left[G, [E, F]^{\boldsymbol{p}}_{\boldsymbol{s},\boldsymbol{q}}\right]^{\boldsymbol{p}}_{\boldsymbol{r},\boldsymbol{p}} + \left[F, [G, E]^{\boldsymbol{p}}_{\boldsymbol{r},\boldsymbol{s}}\right]^{\boldsymbol{p}}_{\boldsymbol{q},\boldsymbol{p}} = O(\partial^2), \quad (3.27)$$

where $O(\partial^2)$ *denotes terms including second-order derivatives. Hence, the sum over the permutation vanishes on the modulo operation by* ∂^2*.*

The combination of the functionals E, F, G and the corresponding state variables $\boldsymbol{q}$, $\boldsymbol{r}$, $\boldsymbol{s}$ is a unique aspect of this bracket. Notice that the permutation law (3.27) resembles Jacobi's identity. In fact, the algebraic relation delineated by this Lemma 1 is the root cause of Jacobi's identity satisfied by the Poisson bracket.

Proof of Lemma 1

The antisymmetry is evident. To prove Jacobi's identity, we have to calculate the functional derivative of the bracket. Because of the inhomogeneous factor $\rho^{-1}(\nabla \times \boldsymbol{p})$ included in the bracket, the derivatives such as $\partial_\rho [F, G]^{\boldsymbol{p}}_{\boldsymbol{q},\boldsymbol{r}}$ and $\partial_{\boldsymbol{p}} [F, G]^{\boldsymbol{p}}_{\boldsymbol{q},\boldsymbol{r}}$ are sums of the terms that consist of only first derivatives of F and G, as well as the terms including second-order derivatives (the second-order terms are modulo-outed in (3.27)). The former ones are such that

$$\partial_\rho [F, G]^{\boldsymbol{p}}_{\boldsymbol{q},\boldsymbol{r}} = -\rho^{-2}(\nabla \times \boldsymbol{p}) \cdot (\partial_{\boldsymbol{q}} F \times \partial_{\boldsymbol{r}} G) + O(\partial^2),$$

$$\partial_{\boldsymbol{p}}\,[F,G]^{\boldsymbol{p}}_{\boldsymbol{q},\boldsymbol{r}} = \nabla\times\rho^{-1}\,(\partial_{\boldsymbol{q}}F\times\partial_{\boldsymbol{r}}G)+O(\partial^2).$$

The permutation law is given as

$$\begin{aligned}\Big[E,[F,G]^{\boldsymbol{p}}_{\boldsymbol{q},\boldsymbol{r}}\Big]^{\boldsymbol{p}}_{\boldsymbol{s},\boldsymbol{p}} \;+\; &\Big[G,[E,F]^{\boldsymbol{p}}_{\boldsymbol{s},\boldsymbol{q}}\Big]^{\boldsymbol{p}}_{\boldsymbol{r},\boldsymbol{p}}+\Big[F,[G,E]^{\boldsymbol{p}}_{\boldsymbol{r},\boldsymbol{s}}\Big]^{\boldsymbol{p}}_{\boldsymbol{q},\boldsymbol{p}} = \\ &\int_\Omega\Big\{\,(\nabla\times\boldsymbol{p})\cdot[\rho^{-1}\partial_{\boldsymbol{s}}E\times[\nabla\times(\partial_{\boldsymbol{q}}F\times\rho^{-1}\partial_{\boldsymbol{r}}G)]] \\ &+\partial_{\boldsymbol{s}}E\cdot\nabla[\,(\nabla\times\boldsymbol{p})\cdot\big(\rho^{-1}\partial_{\boldsymbol{q}}F\times\rho^{-1}\partial_{\boldsymbol{r}}G\big)\,] \\ &+(\nabla\times\boldsymbol{p})\cdot[\rho^{-1}\partial_{\boldsymbol{r}}G\times[\nabla\times(\partial_{\boldsymbol{s}}E\times\rho^{-1}\partial_{\boldsymbol{q}}F)]] \\ &+\partial_{\boldsymbol{r}}G\cdot\nabla[\,(\nabla\times\boldsymbol{p})\cdot\big(\rho^{-1}\partial_{\boldsymbol{s}}E\times\rho^{-1}\partial_{\boldsymbol{q}}F\big)\,] \\ &+(\nabla\times\boldsymbol{p})\cdot[\rho^{-1}\partial_{\boldsymbol{q}}F\times[\nabla\times(\partial_{\boldsymbol{r}}G\times\rho^{-1}\partial_{\boldsymbol{s}}E)]] \\ &+\partial_{\boldsymbol{q}}F\cdot\nabla[\,(\nabla\times\boldsymbol{p})\cdot\big(\rho^{-1}\partial_{\boldsymbol{r}}G\times\rho^{-1}\partial_{\boldsymbol{s}}E\big)\,]\Big\}d^3x \\ &+O(\partial^2). \end{aligned}\tag{3.28}$$

Denoting $\mathbf{e}:=\partial_{\mathbf{S}}E$, etc., equation (3.28) reads

$$\begin{aligned}\Big[E,[F,G]^{\boldsymbol{p}}_{\boldsymbol{q},\boldsymbol{r}}\Big]^{\boldsymbol{p}}_{\boldsymbol{s},\boldsymbol{p}} \;+\; &\Big[G,[E,F]^{\boldsymbol{p}}_{\boldsymbol{s},\boldsymbol{q}}\Big]^{\boldsymbol{p}}_{\boldsymbol{r},\boldsymbol{p}}+\Big[F,[G,E]^{\boldsymbol{p}}_{\boldsymbol{r},\boldsymbol{s}}\Big]^{\boldsymbol{p}}_{\boldsymbol{q},\boldsymbol{p}} = \\ &\int_\Omega\{\,(\nabla\times\boldsymbol{p})\cdot[\rho^{-1}\boldsymbol{e}\times[\nabla\times(\boldsymbol{f}\times\rho^{-1}\boldsymbol{g})]] \\ &+\boldsymbol{e}\cdot\nabla[\,(\nabla\times\boldsymbol{p})\cdot\big(\rho^{-1}\boldsymbol{f}\times\rho^{-1}\boldsymbol{g}\big)\,]+\circlearrowleft\}d^3x \\ &+O(\partial^2) \end{aligned}\tag{3.29}$$

where $\circlearrowleft$ denotes the summation over cyclic permutation of the vectors $\boldsymbol{e}$, $\boldsymbol{f}$, and $\boldsymbol{g}$. After integrating by parts, the integrand of $\Big[E,[F,G]^{\boldsymbol{p}}_{\boldsymbol{q},\boldsymbol{r}}\Big]^{\boldsymbol{p}}_{\boldsymbol{s},\boldsymbol{p}}$ can be written as

$$(\nabla\times\boldsymbol{p})\cdot\{\rho^{-1}\boldsymbol{e}\times\big[\nabla\times\big(\boldsymbol{f}\times\rho^{-1}\boldsymbol{g}\big)\big]-\big(\rho^{-1}\boldsymbol{f}\times\rho^{-1}\boldsymbol{g}\big)\,\nabla\cdot\boldsymbol{e}\}.\tag{3.30}$$

The term bracketed by { } can be rewritten by vector identities as

$$\rho^{-1}\boldsymbol{e}\times[\boldsymbol{f}\,\big(\nabla\cdot\rho^{-1}\boldsymbol{g}\big)-\rho^{-1}\boldsymbol{g}\,(\nabla\cdot\boldsymbol{f})+\big(\rho^{-1}\boldsymbol{g}\cdot\nabla\big)\,\boldsymbol{f}-(\boldsymbol{f}\cdot\nabla)\,\rho^{-1}\boldsymbol{g}]$$

$$- \left(\rho^{-1}\boldsymbol{f} \times \rho^{-1}\boldsymbol{g}\right) \nabla \cdot \boldsymbol{e}$$

The second term and the last term cancel by summation over permutations. To deal with the residual terms in (3.30), we use the symmetry of the curl operator

$$\boldsymbol{p} \cdot \nabla \times \Big\{ \rho^{-1}\boldsymbol{e} \times [\boldsymbol{f}\left(\nabla \cdot \rho^{-1}\boldsymbol{g}\right) + \left(\rho^{-1}\boldsymbol{g} \cdot \nabla\right)\boldsymbol{f} - \left(\boldsymbol{f} \cdot \nabla\right)\rho^{-1}\boldsymbol{g}] \Big\}.$$

Invoking Levi-Civita symbol, we may write

$$\begin{aligned} \epsilon_{ijk}\partial_j \Big\{ \epsilon_{klm}\rho^{-1} \quad & e_l \quad [f_m \partial_n \left(\rho^{-1} g_n\right) + \rho^{-1} g_n \partial_n f_m - f_n \partial_n \left(\rho^{-1} g_m\right)] \Big\} \\ & = \partial_j \Big\{ \rho^{-1} e_i [\partial_n \left(\rho^{-1} g_n f_j\right) - f_n \partial_n \left(\rho^{-1} g_j\right)] \\ & \quad -\rho^{-1} e_j [\partial_n \left(\rho^{-1} g_n f_i\right) - f_n \partial_n \left(\rho^{-1} g_i\right)] \Big\}. \end{aligned} \tag{3.31}$$

The last two terms are manipulated as

$$-\partial_n \left(\rho^{-2} g_n f_i e_j\right) + \rho^{-1} g_n f_i \partial_n \left(\rho^{-1} e_j\right) + \partial_n \left(\rho^{-2} g_i f_n e_j\right) - \rho^{-1} g_i \partial_n \left(\rho^{-1} f_n e_j\right).$$

Now (3.31) is summarized as

$$\begin{aligned} \partial_j \partial_n \left[\rho^{-2} \left(g_i f_n e_j - g_n f_i e_j\right)\right] \quad + \quad & \partial_j \left[\rho^{-1} e_i \partial_n \left(\rho^{-1} g_n f_j\right) - \rho^{-1} g_i \partial_n \left(\rho^{-1} f_n e_j\right)\right] \\ & + \partial_j \left[\rho^{-1} g_n f_i \partial_n \left(\rho^{-1} e_j\right) - \rho^{-1} f_n e_i \partial_n \left(\rho^{-1} g_j\right)\right]. \end{aligned}$$

each term of which cancels out by summation over the permutation. (QED)

Remark 1. *If we choose* $\boldsymbol{p} = \boldsymbol{q} = \boldsymbol{r} = \boldsymbol{V}$*, the bracket (3.26) is the Poisson bracket of the barotropic compressible fluid:*

$$\begin{aligned} \{F, G\} \quad = \quad & \int_\Omega \Big[\rho^{-1} \left(\nabla \times \boldsymbol{V}\right) \cdot \left(\partial_{\boldsymbol{V}} F \times \partial_{\boldsymbol{V}} G\right) \\ & -\partial_\rho F \left(\nabla \cdot \partial_{\boldsymbol{V}} G\right) - \partial_{\boldsymbol{V}} F \cdot \nabla \partial_\rho G \Big] d^3x, \end{aligned} \tag{3.32}$$

where the state vector is $u = (\rho, \boldsymbol{V})^t$. *The Poisson operator corresponding to Poisson bracket (3.32) is*

$$\mathcal{J} = \begin{pmatrix} 0 & -\nabla\cdot \\ -\nabla & -\rho^{-1}\left(\nabla \times \boldsymbol{V}\right) \times \circ \end{pmatrix}. \tag{3.33}$$

Giving a Hamiltonian

$$\mathscr{H} := \int_\Omega \rho \left(\frac{V^2}{2} + U\left(\rho\right) \right) d^3x, \tag{3.34}$$

Hamilton's equations read

$$\frac{\partial \rho}{\partial t} = -\nabla \cdot \left(\rho \boldsymbol{V}\right), \tag{3.35}$$

$$\frac{\partial \boldsymbol{V}}{\partial t} = -\left(\nabla \times \boldsymbol{V}\right) \times \boldsymbol{V} - \nabla \left(h + \frac{V^2}{2} \right). \tag{3.36}$$

3.3.2 Jacobi's identity for the Poisson bracket of extended MHD

Now we complete the proof of Theorem (1) by verifying Jacobi's identity for the Poisson bracket

$$\begin{aligned} \{F, G\} \;=\; & -\int_\Omega \Big\{ \left[F_\rho \nabla \cdot G_{\boldsymbol{V}} + F_{\boldsymbol{V}} \cdot \nabla G_\rho\right] - \left[\rho^{-1}\left(\nabla \times \boldsymbol{V}\right) \cdot \left(F_{\boldsymbol{V}} \times G_{\boldsymbol{V}}\right)\right] \\ & - \left[\boldsymbol{B}^* \cdot \rho^{-1}(F_{\boldsymbol{V}} \times (\nabla \times G_{\boldsymbol{B}^*})) + \boldsymbol{B}^* \cdot \rho^{-1}((\nabla \times F_{\boldsymbol{B}^*}) \times G_{\boldsymbol{V}})\right] \\ & + d_i \left[\boldsymbol{B}^* \cdot \rho^{-1}((\nabla \times F_{\boldsymbol{B}^*}) \times (\nabla \times G_{\boldsymbol{B}^*}))\right] \\ & - d_e^2 \left[(\nabla \times \boldsymbol{V}) \cdot \rho^{-1}((\nabla \times F_{\boldsymbol{B}^*}) \times (\nabla \times G_{\boldsymbol{B}^*}))\right] \Big\} d^3x, \end{aligned} \tag{3.37}$$

where the subscripts indicate functional derivative of the functional F, G with respect to the state variables $\rho, \boldsymbol{V}, \boldsymbol{B}^*$, i.e $F_\rho = \partial_\rho F$.

To examine Jacobi's identity, we have to study the derivatives of the bracket by the state variables, which consists of two groups of terms;

group (A) is the collection of terms that include second-order derivatives (such as $F_{\boldsymbol{B}^*,\boldsymbol{V}}$). Formally, group (A) is generated by pretending that the coefficients in the Poisson operator $\mathcal{J}$ are independent to (or, different from) the state vector u. The terms of group (A) cancel out when summed up in $\{E,\{F,G\}\}+\circlearrowleft$. Group (B) summarizes the remaining terms that are due to the derivatives of $\mathcal{J}$ by u; explicitly, we have

$$\begin{aligned}\{F,G\}_{\rho} \bmod \partial^2 \;=\;& -\rho^{-2}\,(\nabla\times\boldsymbol{V})\cdot(F_{\boldsymbol{V}}\times G_{\boldsymbol{V}})\\ & -\rho^{-2}\boldsymbol{B}^*\cdot[F_{\boldsymbol{V}}\times(\nabla\times G_{\boldsymbol{B}^*})]\\ & -\rho^{-2}\boldsymbol{B}^*\cdot[(\nabla\times F_{\boldsymbol{B}^*})\times G_{\boldsymbol{V}}]\\ & +d_i\Big[\rho^{-2}\boldsymbol{B}^*\cdot[(\nabla\times F_{\boldsymbol{B}^*})\times(\nabla\times G_{\boldsymbol{B}^*})]\Big]\\ & -d_e^2\Big[\rho^{-2}\,(\nabla\times\boldsymbol{V})\cdot[(\nabla\times F_{\boldsymbol{B}^*})\times(\nabla\times G_{\boldsymbol{B}^*})]\Big],\end{aligned} \tag{3.38}$$

$$\begin{aligned}\{F,G\}_{\boldsymbol{V}} \bmod \partial^2 \;=\;& \nabla\times\rho^{-1}\,(F_{\boldsymbol{V}}\times G_{\boldsymbol{V}})\\ & +d_e^2\Big[\nabla\times\rho^{-1}(\,(\nabla\times F_{\boldsymbol{B}^*})\times(\nabla\times G_{\boldsymbol{B}^*})\,)\Big],\end{aligned} \tag{3.39}$$

$$\begin{aligned}\{F,G\}_{\boldsymbol{B}^*} \bmod \partial^2 \;=\;& \rho^{-1}(F_{\boldsymbol{V}}\times(\nabla\times G_{\boldsymbol{B}^*})\,)\\ & +\rho^{-1}(\,(\nabla\times F_{\boldsymbol{B}^*})\times G_{\boldsymbol{V}})\\ & -d_i\Big[\rho^{-1}(\,(\nabla\times F_{\boldsymbol{B}^*})\times(\nabla\times G_{\boldsymbol{B}^*})\,)\Big].\end{aligned} \tag{3.40}$$

In what follows, we show that the remaining group (B) terms cancel out. By (3.38), (3.39), and (3.40), we obtain

$$\begin{aligned}&\{E,\{F,G\}\}+\circlearrowleft=\\ &\int_\Omega E_{\boldsymbol{V}}\cdot\Big[\nabla\Big(\rho^{-2}\,(\nabla\times\boldsymbol{V})\cdot(F_{\boldsymbol{V}}\times G_{\boldsymbol{V}})\Big)\end{aligned}$$

$$
\begin{aligned}
&-\rho^{-1}\left(\nabla\times\boldsymbol{V}\right)\times\left[\nabla\times\rho^{-1}\left(F_{\boldsymbol{V}}\times G_{\mathbf{V}}\right)\right]\Big]d^3x\\
&+\int_\Omega E_{\boldsymbol{V}}\cdot\Bigg[\nabla\Big(\rho^{-2}\boldsymbol{B}^*\cdot\left[F_{\boldsymbol{V}}\times\left(\nabla\times G_{\boldsymbol{B}^*}\right)\right]\Big)\\
&+\left[\nabla\times\left(\rho^{-1}F_{\boldsymbol{V}}\times\left(\nabla\times G_{\boldsymbol{B}^*}\right)\right)\right]\times\rho^{-1}\boldsymbol{B}^*\Bigg]d^3x\\
&+\int_\Omega E_{\boldsymbol{V}}\cdot\Bigg[\nabla\Big(\rho^{-2}\boldsymbol{B}^*\cdot\left[\left(\nabla\times F_{\boldsymbol{B}^*}\right)\times G_{\boldsymbol{V}}\right]\Big)\\
&+\left[\nabla\times\left(\rho^{-1}\left(\nabla\times F_{\boldsymbol{B}^*}\right)\times G_{\boldsymbol{V}}\right)\right]\times\rho^{-1}\boldsymbol{B}^*\Bigg]d^3x\\
&-d_i\int_\Omega E_{\boldsymbol{V}}\cdot\Bigg[\nabla\Big(\rho^{-2}\boldsymbol{B}^*\cdot\left[\left(\nabla\times F_{\boldsymbol{B}^*}\right)\times\left(\nabla\times G_{\boldsymbol{B}^*}\right)\right]\Big)\\
&+\left[\nabla\times\left(\rho^{-1}\left(\nabla\times F_{\boldsymbol{B}^*}\right)\times\left(\nabla\times G_{\boldsymbol{B}^*}\right)\right)\right]\times\rho^{-1}\boldsymbol{B}^*\Bigg]d^3x\\
&+d_e^2\int_\Omega E_{\boldsymbol{V}}\cdot\Bigg[\nabla\Big(\rho^{-2}\left(\nabla\times\boldsymbol{V}\right)\cdot\left[\left(\nabla\times F_{\boldsymbol{B}^*}\right)\times\left(\nabla\times G_{\boldsymbol{B}^*}\right)\right]\Big)\\
&-\rho^{-1}\left(\nabla\times\boldsymbol{V}\right)\times\left[\nabla\times\left(\rho^{-1}\left(\nabla\times F_{\boldsymbol{B}^*}\right)\times\left(\nabla\times G_{\boldsymbol{B}^*}\right)\right)\right]\Bigg]d^3x\\
&-d_i\int_\Omega E_{\boldsymbol{B}^*}\cdot\nabla\times\Bigg[\left[\nabla\times\left(\rho^{-1}F_{\boldsymbol{V}}\times\left(\nabla\times G_{\boldsymbol{B}^*}\right)\right)\right]\times\rho^{-1}\boldsymbol{B}^*\\
&+\left[\nabla\times\left(\rho^{-1}\left(\nabla\times F_{\boldsymbol{B}^*}\right)\times G_{\boldsymbol{V}}\right)\right]\times\rho^{-1}\boldsymbol{B}^*\Bigg]d^3x\\
&+d_e^2\int_\Omega E_{\boldsymbol{B}^*}\cdot\nabla\times\Bigg[\left[\nabla\times\left(\rho^{-1}F_{\boldsymbol{V}}\times\left(\nabla\times G_{\boldsymbol{B}^*}\right)\right)\right]\times\rho^{-1}\left(\nabla\times\boldsymbol{V}\right)\\
&+\left[\nabla\times\left(\rho^{-1}\left(\nabla\times F_{\boldsymbol{B}^*}\right)\times G_{\boldsymbol{V}}\right)\right]\times\rho^{-1}\left(\nabla\times\boldsymbol{V}\right)\Bigg]d^3x\\
&+\int_\Omega E_{\boldsymbol{B}^*}\cdot\nabla\times\Bigg[\left[\nabla\times\rho^{-1}\left(F_{\boldsymbol{V}}\times G_{\mathbf{V}}\right)\right]\times\rho^{-1}\boldsymbol{B}^*\Bigg]d^3x\\
&+d_e^2\int_\Omega E_{\boldsymbol{B}^*}\cdot\nabla\times\Bigg[\left[\nabla\times\left(\rho^{-1}\left(\nabla\times F_{\boldsymbol{B}^*}\right)\times\left(\nabla\times G_{\boldsymbol{B}^*}\right)\right)\right]\times\rho^{-1}\boldsymbol{B}^*\Bigg]d^3x\\
&+d_i^2\int_\Omega E_{\boldsymbol{B}^*}\cdot\nabla\times\Bigg[\left[\nabla\times\left(\rho^{-1}\left(\nabla\times F_{\boldsymbol{B}^*}\right)\times\left(\nabla\times G_{\boldsymbol{B}^*}\right)\right)\right]\times\rho^{-1}\boldsymbol{B}^*\Bigg]d^3x\\
&-d_id_e^2\int_\Omega E_{\boldsymbol{B}^*}\cdot\nabla\times\Bigg[\left[\nabla\times\rho^{-1}(\left(\nabla\times F_{\boldsymbol{B}^*}\right)\times\left(\nabla\times G_{\boldsymbol{B}^*}\right))\right]\times\rho^{-1}\left(\nabla\times\boldsymbol{V}\right)\Bigg]d^3x+\circlearrowleft\\
&\quad+O(\partial^2).
\end{aligned}
\tag{3.41}
$$

To prove Jacobi's identity, we collect terms that have the same combinations of functional derivatives such that $(E_{\boldsymbol{V}},F_{\boldsymbol{V}},G_{\boldsymbol{V}})$, $(E_{\boldsymbol{V}},F_{\boldsymbol{V}},G_{\boldsymbol{B}^*})$, ...,$(E_{\boldsymbol{B}^*},F_{\boldsymbol{B}^*},G_{\boldsymbol{B}^*})$.

Then,

$$
\begin{aligned}
&\{E,\{F,G\}\}+\circlearrowleft= \\
&\int_\Omega \Big\{ (\nabla\times \boldsymbol{V})\cdot[\rho^{-1}E_{\boldsymbol{V}}\times(\nabla\times\rho^{-1}\,(F_{\boldsymbol{V}}\times G_{\boldsymbol{V}})\,)] \\
&+E_{\boldsymbol{V}}\cdot[\nabla(\rho^{-2}\,(\nabla\times\boldsymbol{V})\cdot(F_{\boldsymbol{V}}\times G_{\boldsymbol{V}})\,)] \\
&+(\nabla\times\boldsymbol{V})\cdot[\rho^{-1}G_{\boldsymbol{V}}\times(\nabla\times\rho^{-1}\,(E_{\boldsymbol{V}}\times F_{\boldsymbol{V}})\,)] \\
&+G_{\boldsymbol{V}}\cdot[\nabla(\rho^{-2}\,(\nabla\times\boldsymbol{V})\cdot(E_{\boldsymbol{V}}\times F_{\boldsymbol{V}})\,)] \\
&+(\nabla\times\boldsymbol{V})\cdot[\rho^{-1}F_{\boldsymbol{V}}\times(\nabla\times\rho^{-1}\,(G_{\boldsymbol{V}}\times E_{\boldsymbol{V}})\,)] \\
&+F_{\boldsymbol{V}}\cdot[\nabla(\rho^{-2}\,(\nabla\times\boldsymbol{V})\cdot(G_{\boldsymbol{V}}\times E_{\boldsymbol{V}})\,)]\Big\}d^3x \\
&+\int_\Omega \Big\{ \boldsymbol{B}^*\cdot[\rho^{-1}\,(\nabla\times E_{\boldsymbol{B}^*})\times(\nabla\times\rho^{-1}\,[F_{\boldsymbol{V}}\times G_{\boldsymbol{V}}]\,)] \\
&+\boldsymbol{B}^*\cdot[\rho^{-1}G_{\boldsymbol{V}}\times(\nabla\times\rho^{-1}\,[(\nabla\times E_{\boldsymbol{B}^*})\times F_{\boldsymbol{V}}]\,)] \\
&+G_{\boldsymbol{V}}\cdot\nabla[\rho^{-2}\boldsymbol{B}^*\cdot(\,(\nabla\times E_{\boldsymbol{B}^*})\times F_{\boldsymbol{V}})] \\
&+\boldsymbol{B}^*\cdot[\rho^{-1}F_{\boldsymbol{V}}\times(\nabla\times\rho^{-1}\,[G_{\boldsymbol{V}}\times(\nabla\times E_{\boldsymbol{B}^*})]\,)] \\
&+F_{\boldsymbol{V}}\cdot\nabla[\rho^{-2}\boldsymbol{B}^*\cdot(G_{\boldsymbol{V}}\times(\nabla\times E_{\boldsymbol{B}^*})\,)]\Big\}d^3x \\
&+\int_\Omega \Big\{ \boldsymbol{B}^*\cdot[\rho^{-1}E_{\boldsymbol{V}}\times(\nabla\times\rho^{-1}\,[F_{\boldsymbol{V}}\times(\nabla\times G_{\boldsymbol{B}^*})]\,)] \\
&+E_{\boldsymbol{V}}\cdot\nabla[\rho^{-2}\boldsymbol{B}^*\cdot(F_{\boldsymbol{V}}\times(\nabla\times G_{\boldsymbol{B}^*})\,)] \\
&+\boldsymbol{B}^*\cdot[\rho^{-1}\,(\nabla\times G_{\boldsymbol{B}^*})\times(\nabla\times\rho^{-1}\,[E_{\boldsymbol{V}}\times F_{\boldsymbol{V}}]\,)] \\
&+\boldsymbol{B}^*\cdot[\rho^{-1}F_{\boldsymbol{V}}\times(\nabla\times\rho^{-1}\,[(\nabla\times G_{\boldsymbol{B}^*})\times E_{\boldsymbol{V}}]\,)] \\
&+F_{\boldsymbol{V}}\cdot\nabla[\rho^{-2}\boldsymbol{B}^*\cdot(\,(\nabla\times G_{\boldsymbol{B}^*})\times E_{\boldsymbol{V}})]\Big\}d^3x \\
&+\int_\Omega \Big\{ \boldsymbol{B}^*\cdot[\rho^{-1}E_{\boldsymbol{V}}\times(\nabla\times\rho^{-1}\,[(\nabla\times F_{\boldsymbol{B}^*})\times G_{\boldsymbol{V}}]\,)] \\
&+E_{\boldsymbol{V}}\cdot\nabla[\rho^{-2}\boldsymbol{B}^*\cdot(\,(\nabla\times F_{\boldsymbol{B}^*})\times G_{\boldsymbol{V}})] \\
&+\boldsymbol{B}^*\cdot[\rho^{-1}G_{\boldsymbol{V}}\times(\nabla\times\rho^{-1}\,[E_{\boldsymbol{V}}\times(\nabla\times F_{\boldsymbol{B}^*})]\,)] \\
&+G_{\boldsymbol{V}}\cdot\nabla[\rho^{-2}\boldsymbol{B}^*\cdot(E_{\boldsymbol{V}}\times(\nabla\times F_{\boldsymbol{B}^*})\,)] \\
&+\boldsymbol{B}^*\cdot[\rho^{-1}\,(\nabla\times F_{\boldsymbol{B}^*})\times(\nabla\times\rho^{-1}\,[G_{\boldsymbol{V}}\times E_{\boldsymbol{V}}]\,)]\Big\}d^3x \\
&-d_i\int_\Omega \Big\{ \boldsymbol{B}^*\cdot[\rho^{-1}E_{\boldsymbol{V}}\times(\nabla\times\rho^{-1}\,[(\nabla\times F_{\boldsymbol{B}^*})\times(\nabla\times G_{\boldsymbol{B}^*})]\,)] \\
&+E_{\boldsymbol{V}}\cdot\nabla[\rho^{-2}\boldsymbol{B}^*\cdot(\,(\nabla\times F_{\boldsymbol{B}^*})\times(\nabla\times G_{\boldsymbol{B}^*})\,)] \\
&+\boldsymbol{B}^*\cdot[\rho^{-1}\,(\nabla\times G_{\boldsymbol{B}^*})\times(\nabla\times\rho^{-1}\,[E_{\boldsymbol{V}}\times(\nabla\times F_{\boldsymbol{B}^*})]\,)]
\end{aligned}
$$

$$
\begin{aligned}
&+\boldsymbol{B}^* \cdot [\rho^{-1} (\nabla \times F_{\boldsymbol{B}^*}) \times (\nabla \times \rho^{-1} [(\nabla \times G_{\boldsymbol{B}^*}) \times E_{\boldsymbol{V}}])] \Big\} d^3x \\
&+d_e^2 \int_\Omega \Big\{ (\nabla \times \boldsymbol{V}) \cdot [\rho^{-1} E_{\boldsymbol{V}} \times (\nabla \times \rho^{-1} [(\nabla \times F_{\boldsymbol{B}^*}) \times (\nabla \times G_{\boldsymbol{B}^*})])] \\
&+E_{\boldsymbol{V}} \cdot \nabla [\rho^{-2} (\nabla \times \boldsymbol{V}) \cdot ((\nabla \times F_{\boldsymbol{B}^*}) \times (\nabla \times G_{\boldsymbol{B}^*}))] \\
&+(\nabla \times \boldsymbol{V}) \cdot [\rho^{-1} (\nabla \times G_{\boldsymbol{B}^*}) \times (\nabla \times \rho^{-1} [E_{\boldsymbol{V}} \times (\nabla \times F_{\boldsymbol{B}^*})])] \\
&+(\nabla \times \boldsymbol{V}) \cdot [\rho^{-1} (\nabla \times F_{\boldsymbol{B}^*}) \times (\nabla \times \rho^{-1} [(\nabla \times G_{\boldsymbol{B}^*}) \times E_{\boldsymbol{V}}])] \Big\} d^3x \\
&-d_i \int_\Omega \Big\{ \boldsymbol{B}^* \cdot [\rho^{-1} (\nabla \times E_{\boldsymbol{B}^*}) \times (\nabla \times \rho^{-1} [F_{\boldsymbol{V}} \times (\nabla \times G_{\boldsymbol{B}^*})])] \\
&+\boldsymbol{B}^* \cdot [\rho^{-1} (\nabla \times G_{\boldsymbol{B}^*}) \times (\nabla \times \rho^{-1} [(\nabla \times E_{\boldsymbol{B}^*}) \times F_{\boldsymbol{V}}])] \\
&+\boldsymbol{B}^* \cdot [\rho^{-1} F_{\boldsymbol{V}} \times (\nabla \times \rho^{-1} [(\nabla \times G_{\boldsymbol{B}^*}) \times (\nabla \times E_{\boldsymbol{B}^*})])] \\
&+F_{\boldsymbol{V}} \cdot \nabla [\rho^{-2} \boldsymbol{B}^* \cdot ((\nabla \times G_{\boldsymbol{B}^*}) \times (\nabla \times E_{\boldsymbol{B}^*}))] \Big\} d^3x \\
&+d_e^2 \int_\Omega \Big\{ (\nabla \times \boldsymbol{V}) \cdot [\rho^{-1} (\nabla \times E_{\boldsymbol{B}^*}) \times (\nabla \times \rho^{-1} [F_{\boldsymbol{V}} \times (\nabla \times G_{\boldsymbol{B}^*})])] \\
&+(\nabla \times \boldsymbol{V}) \cdot [\rho^{-1} (\nabla \times G_{\boldsymbol{B}^*}) \times (\nabla \times \rho^{-1} [(\nabla \times E_{\boldsymbol{B}^*}) \times F_{\boldsymbol{V}}])] \\
&+(\nabla \times \boldsymbol{V}) \cdot [\rho^{-1} F_{\boldsymbol{V}} \times (\nabla \times \rho^{-1} [(\nabla \times G_{\boldsymbol{B}^*}) \times (\nabla \times E_{\boldsymbol{B}^*})])] \\
&+F_{\boldsymbol{V}} \cdot \nabla [\rho^{-2} (\nabla \times \boldsymbol{V}) \cdot ((\nabla \times G_{\boldsymbol{B}^*}) \times (\nabla \times E_{\boldsymbol{B}^*}))] \Big\} d^3x \\
&-d_i \int_\Omega \Big\{ \boldsymbol{B}^* \cdot [\rho^{-1} (\nabla \times E_{\boldsymbol{B}^*}) \times (\nabla \times \rho^{-1} [(\nabla \times F_{\boldsymbol{B}^*}) \times G_{\boldsymbol{V}}])] \\
&+\boldsymbol{B}^* \cdot [\rho^{-1} G_{\boldsymbol{V}} \times (\nabla \times \rho^{-1} [(\nabla \times E_{\boldsymbol{B}^*}) \times (\nabla \times F_{\boldsymbol{B}^*})])] \\
&+G_{\boldsymbol{V}} \cdot \nabla [\rho^{-2} \boldsymbol{B}^* \cdot ((\nabla \times E_{\boldsymbol{B}^*}) \times (\nabla \times F_{\boldsymbol{B}^*}))] \\
&+\boldsymbol{B}^* \cdot [\rho^{-1} (\nabla \times F_{\boldsymbol{B}^*}) \times (\nabla \times \rho^{-1} [G_{\boldsymbol{V}} \times (\nabla \times E_{\boldsymbol{B}^*})])] \Big\} d^3x \\
&+d_e^2 \int_\Omega \Big\{ (\nabla \times \boldsymbol{V}) \cdot [\rho^{-1} (\nabla \times E_{\boldsymbol{B}^*}) \times (\nabla \times \rho^{-1} [(\nabla \times F_{\boldsymbol{B}^*}) \times G_{\boldsymbol{V}}])] \\
&+(\nabla \times \boldsymbol{V}) \cdot [\rho^{-1} G_{\boldsymbol{V}} \times (\nabla \times \rho^{-1} [(\nabla \times E_{\boldsymbol{B}^*}) \times (\nabla \times F_{\boldsymbol{B}^*})])] \\
&+G_{\boldsymbol{V}} \cdot \nabla [\rho^{-2} (\nabla \times \boldsymbol{V}) \cdot ((\nabla \times E_{\boldsymbol{B}^*}) \times (\nabla \times F_{\boldsymbol{B}^*}))] \\
&+(\nabla \times \boldsymbol{V}) \cdot [\rho^{-1} (\nabla \times F_{\boldsymbol{B}^*}) \times (\nabla \times \rho^{-1} [G_{\boldsymbol{V}} \times (\nabla \times E_{\boldsymbol{B}^*})])] \Big\} d^3x \\
&+d_i^2 \int_\Omega \Big\{ \boldsymbol{B}^* \cdot [\rho^{-1} (\nabla \times E_{\boldsymbol{B}^*}) \times (\nabla \times \rho^{-1} [(\nabla \times F_{\boldsymbol{B}^*}) \times (\nabla \times G_{\boldsymbol{B}^*})])] \\
&+\boldsymbol{B}^* \cdot [\rho^{-1} (\nabla \times G_{\boldsymbol{B}^*}) \times (\nabla \times \rho^{-1} [(\nabla \times E_{\boldsymbol{B}^*}) \times (\nabla \times F_{\boldsymbol{B}^*})])] \\
&+\boldsymbol{B}^* \cdot [\rho^{-1} (\nabla \times F_{\boldsymbol{B}^*}) \times (\nabla \times \rho^{-1} [(\nabla \times G_{\boldsymbol{B}^*}) \times (\nabla \times E_{\boldsymbol{B}^*})])] \Big\} d^3x
\end{aligned}
$$

$$
\begin{aligned}
&+d_e^2 \int_\Omega \Big\{ \boldsymbol{B}^* \cdot [\rho^{-1} (\nabla \times E_{\boldsymbol{B}^*}) \times (\nabla \times \rho^{-1} [(\nabla \times F_{\boldsymbol{B}^*}) \times (\nabla \times G_{\boldsymbol{B}^*})])] \\
&+ \boldsymbol{B}^* \cdot [\rho^{-1} (\nabla \times G_{\boldsymbol{B}^*}) \times (\nabla \times \rho^{-1} [(\nabla \times E_{\boldsymbol{B}^*}) \times (\nabla \times F_{\boldsymbol{B}^*})])] \\
&+ \boldsymbol{B}^* \cdot [\rho^{-1} (\nabla \times F_{\boldsymbol{B}^*}) \times (\nabla \times \rho^{-1} [(\nabla \times G_{\boldsymbol{B}^*}) \times (\nabla \times E_{\boldsymbol{B}^*})])] \Big\} d^3x \\
&-d_i d_e^2 \int_\Omega \Big\{ (\nabla \times \boldsymbol{V}) \cdot [\rho^{-1} (\nabla \times E_{\boldsymbol{B}^*}) \times (\nabla \times \rho^{-1} [(\nabla \times F_{\boldsymbol{B}^*}) \times (\nabla \times G_{\boldsymbol{B}^*})])] \\
&+ (\nabla \times \boldsymbol{V}) \cdot [\rho^{-1} (\nabla \times G_{\boldsymbol{B}^*}) \times (\nabla \times \rho^{-1} [(\nabla \times E_{\boldsymbol{B}^*}) \times (\nabla \times F_{\boldsymbol{B}^*})])] \\
&+ (\nabla \times \boldsymbol{V}) \cdot [\rho^{-1} (\nabla \times F_{\boldsymbol{B}^*}) \times (\nabla \times \rho^{-1} [(\nabla \times G_{\boldsymbol{B}^*}) \times (\nabla \times E_{\boldsymbol{B}^*})])] \Big\} d^3x \\
&\quad + O(\partial^2). \qquad (3.42)
\end{aligned}
$$

To apply Lemma1, we rewrite (3.42) in terms of the bilinear form (3.26):

$$
\begin{aligned}
&\{E, \{F, G\}\} + \circlearrowleft = \\
&\Big[E, [F, G]^{\boldsymbol{V}}_{\boldsymbol{V},\boldsymbol{V}}\Big]^{\boldsymbol{V}}_{\boldsymbol{V},\boldsymbol{V}} + \Big[G, [E, F]^{\boldsymbol{V}}_{\boldsymbol{V},\boldsymbol{V}}\Big]^{\boldsymbol{V}}_{\boldsymbol{V},\boldsymbol{V}} + \Big[F, [G, E]^{\boldsymbol{V}}_{\boldsymbol{V},\boldsymbol{V}}\Big]^{\boldsymbol{V}}_{\boldsymbol{V},\boldsymbol{V}} \\
&+ \Big[E, [F, G]^{\boldsymbol{A}^*}_{\boldsymbol{V},\boldsymbol{V}}\Big]^{\boldsymbol{A}^*}_{\boldsymbol{A}^*,\boldsymbol{A}^*} + \Big[G, [E, F]^{\boldsymbol{A}^*}_{\boldsymbol{A}^*,\boldsymbol{V}}\Big]^{\boldsymbol{A}^*}_{\boldsymbol{V},\boldsymbol{A}^*} + \Big[F, [G, E]^{\boldsymbol{A}^*}_{\boldsymbol{V},\boldsymbol{A}^*}\Big]^{\boldsymbol{A}^*}_{\boldsymbol{V},\boldsymbol{A}^*} \\
&+ \Big[E, [F, G]^{\boldsymbol{A}^*}_{\boldsymbol{V},\boldsymbol{A}^*}\Big]^{\boldsymbol{A}^*}_{\boldsymbol{V},\boldsymbol{A}^*} + \Big[G, [E, F]^{\boldsymbol{A}^*}_{\boldsymbol{V},\boldsymbol{V}}\Big]^{\boldsymbol{A}^*}_{\boldsymbol{A}^*,\boldsymbol{A}^*} + \Big[F, [G, E]^{\boldsymbol{A}^*}_{\boldsymbol{A}^*,\boldsymbol{V}}\Big]^{\boldsymbol{A}^*}_{\boldsymbol{V},\boldsymbol{A}^*} \\
&+ \Big[E, [F, G]^{\boldsymbol{A}^*}_{\boldsymbol{A}^*,\boldsymbol{V}}\Big]^{\boldsymbol{A}^*}_{\boldsymbol{V},\boldsymbol{A}^*} + \Big[G, [E, F]^{\boldsymbol{A}^*}_{\boldsymbol{V},\boldsymbol{A}^*}\Big]^{\boldsymbol{A}^*}_{\boldsymbol{V},\boldsymbol{A}^*} + \Big[F, [G, E]^{\boldsymbol{A}^*}_{\boldsymbol{V},\boldsymbol{V}}\Big]^{\boldsymbol{A}^*}_{\boldsymbol{A}^*,\boldsymbol{A}^*} \\
&-d_i \Big(\Big[E, [F, G]^{\boldsymbol{A}^*}_{\boldsymbol{A}^*,\boldsymbol{A}^*}\Big]^{\boldsymbol{A}^*}_{\boldsymbol{V},\mathbf{A}^*} + \Big[G, [E, F]^{\boldsymbol{A}^*}_{\boldsymbol{V},\boldsymbol{A}^*}\Big]^{\boldsymbol{A}^*}_{\boldsymbol{A}^*,\boldsymbol{A}^*} + \Big[F, [G, E]^{\boldsymbol{A}^*}_{\boldsymbol{A}^*,\boldsymbol{V}}\Big]^{\boldsymbol{A}^*}_{\boldsymbol{A}^*,\boldsymbol{A}^*} \Big) \\
&+d_e^2 \Big(\Big[E, [F, G]^{\boldsymbol{V}}_{\boldsymbol{A}^*,\boldsymbol{A}^*}\Big]^{\boldsymbol{V}}_{\boldsymbol{V},\boldsymbol{V}} + \Big[G, [E, F]^{\boldsymbol{V}}_{\boldsymbol{V},\boldsymbol{A}^*}\Big]^{\boldsymbol{V}}_{\boldsymbol{A}^*,\boldsymbol{V}} + \Big[F, [G, E]^{\boldsymbol{V}}_{\boldsymbol{A}^*,\boldsymbol{V}}\Big]^{\boldsymbol{V}}_{\boldsymbol{A}^*,\boldsymbol{V}} \Big) \\
&-d_i \Big(\Big[E, [F, G]^{\boldsymbol{A}^*}_{\boldsymbol{A}^*,\boldsymbol{V}}\Big]^{\boldsymbol{A}^*}_{\boldsymbol{A}^*,\boldsymbol{A}^*} + \Big[G, [E, F]^{\boldsymbol{A}^*}_{\boldsymbol{A}^*,\boldsymbol{A}^*}\Big]^{\boldsymbol{A}^*}_{\boldsymbol{V},\boldsymbol{A}^*} + \Big[F, [G, E]^{\boldsymbol{A}^*}_{\boldsymbol{V},\boldsymbol{A}^*}\Big]^{\boldsymbol{A}^*}_{\boldsymbol{A}^*,\boldsymbol{A}^*} \Big) \\
&+d_e^2 \Big(\Big[E, [F, G]^{\boldsymbol{V}}_{\boldsymbol{A}^*,\boldsymbol{V}}\Big]^{\boldsymbol{V}}_{\boldsymbol{A}^*,\boldsymbol{V}} + \Big[G, [E, F]^{\boldsymbol{V}}_{\boldsymbol{A}^*,\boldsymbol{A}^*}\Big]^{\boldsymbol{V}}_{\boldsymbol{V},\boldsymbol{V}} + \Big[F, [G, E]^{\boldsymbol{V}}_{\boldsymbol{V},\boldsymbol{A}^*}\Big]^{\boldsymbol{V}}_{\boldsymbol{A}^*,\boldsymbol{V}} \Big) \\
&-d_i \Big(\Big[E, [F, G]^{\boldsymbol{A}^*}_{\boldsymbol{V},\boldsymbol{A}^*}\Big]^{\boldsymbol{A}^*}_{\boldsymbol{A}^*,\boldsymbol{A}^*} + \Big[G, [E, F]^{\boldsymbol{A}^*}_{\boldsymbol{A}^*,\boldsymbol{V}}\Big]^{\boldsymbol{A}^*}_{\boldsymbol{A}^*,\boldsymbol{A}^*} + \Big[F, [G, E]^{\boldsymbol{A}^*}_{\boldsymbol{A}^*,\boldsymbol{A}^*}\Big]^{\boldsymbol{A}^*}_{\boldsymbol{V},\boldsymbol{A}^*} \Big) \\
&+d_e^2 \Big(\Big[E, [F, G]^{\boldsymbol{V}}_{\boldsymbol{V},\boldsymbol{A}^*}\Big]^{\boldsymbol{V}}_{\boldsymbol{A}^*,\boldsymbol{V}} + \Big[G, [E, F]^{\boldsymbol{V}}_{\boldsymbol{A}^*,\boldsymbol{V}}\Big]^{\boldsymbol{V}}_{\boldsymbol{A}^*,\boldsymbol{V}} + \Big[F, [G, E]^{\boldsymbol{V}}_{\boldsymbol{A}^*,\boldsymbol{A}^*}\Big]^{\boldsymbol{V}}_{\boldsymbol{V},\boldsymbol{V}} \Big) \\
&+d_i^2 \Big(\Big[E, [F, G]^{\boldsymbol{A}^*}_{\boldsymbol{A}^*,\boldsymbol{A}^*}\Big]^{\boldsymbol{A}^*}_{\boldsymbol{A}^*,\boldsymbol{A}^*} + \Big[G, [E, F]^{\boldsymbol{A}^*}_{\boldsymbol{A}^*,\boldsymbol{A}^*}\Big]^{\boldsymbol{A}^*}_{\boldsymbol{A}^*,\boldsymbol{A}^*} + \Big[F, [G, E]^{\boldsymbol{A}^*}_{\boldsymbol{A}^*,\boldsymbol{A}^*}\Big]^{\boldsymbol{A}^*}_{\boldsymbol{A}^*,\boldsymbol{A}^*} \Big) \\
&+d_e^2 \Big(\Big[E, [F, G]^{\boldsymbol{A}^*}_{\boldsymbol{A}^*,\boldsymbol{A}^*}\Big]^{\boldsymbol{A}^*}_{\boldsymbol{A}^*,\boldsymbol{A}^*} + \Big[G, [E, F]^{\boldsymbol{A}^*}_{\boldsymbol{A}^*,\boldsymbol{A}^*}\Big]^{\boldsymbol{A}^*}_{\boldsymbol{A}^*,\boldsymbol{A}^*} + \Big[F, [G, E]^{\boldsymbol{A}^*}_{\boldsymbol{A}^*,\boldsymbol{A}^*}\Big]^{\boldsymbol{A}^*}_{\boldsymbol{A}^*,\boldsymbol{A}^*} \Big)
\end{aligned}
$$

$$-d_i d_e^2 \Big(\Big[E, [F,G]^{\boldsymbol{V}}_{\boldsymbol{A}^*,\boldsymbol{A}^*}\Big]^{\boldsymbol{V}}_{\boldsymbol{A}^*,\boldsymbol{V}} + \Big[G, [E,F]^{\boldsymbol{V}}_{\boldsymbol{A}^*,\boldsymbol{A}^*}\Big]^{\boldsymbol{V}}_{\boldsymbol{A}^*,\boldsymbol{V}} + \Big[F, [G,E]^{\boldsymbol{V}}_{\boldsymbol{A}^*,\boldsymbol{A}^*}\Big]^{\boldsymbol{V}}_{\boldsymbol{A}^*,\boldsymbol{V}} \Big) + O(\partial^2). \tag{3.43}$$

By Lemma1, only $O(\partial^2)$ terms remain on the right-hand side and the rest of the terms vanish. As we have mentioned, on the other hand, $O(\partial^2)$ vanishes in $\{E,\{F,G\}\} + \circlearrowleft$. Hence, Jacobi's identity has been proved.

3.4 Extended MHD Casimir invariants

The Poisson bracket (3.37) posses three independent Casimir invariants, given as

- electron helicity at the one-fluid limit

$$C_1 = \frac{1}{2}\int_\Omega \left(\boldsymbol{A}^* - \frac{2d_e^2}{d_i}\boldsymbol{V}\right)\cdot \boldsymbol{B}^* d^3x, \tag{3.44}$$

- ion helicity at the one-fluid limit

$$C_2 = \frac{1}{2}\int_\Omega \left[(\boldsymbol{A}^* + d_i\boldsymbol{V})\cdot(\boldsymbol{B}^* + d_i\nabla\times\boldsymbol{V}) + d_e^2\boldsymbol{V}\cdot(\nabla\times\boldsymbol{V})\right] d^3x, \tag{3.45}$$

- total mass density

$$C_3 = \int_\Omega \rho\, d^3x, \tag{3.46}$$

whilst the following are dependent invariants, which are created as a special combinations of (3.44) and (3.45),

- combined modified magnetic and flow helicities

$$C_4 = \frac{1}{2}\int_\Omega \left[\boldsymbol{A}^*\cdot\boldsymbol{B}^* + d_e^2\boldsymbol{V}\cdot(\nabla\times\boldsymbol{V})\right] d^3x, \tag{3.47}$$

- combined modified cross and flow helicities

$$C_5 = \frac{1}{2}\int_\Omega \boldsymbol{V}\cdot[2\boldsymbol{B}^* + d_i\nabla\times\boldsymbol{V}]\,d^3x, \tag{3.48}$$

- generalized helicity

$$C_6 = \frac{1}{2}\int_\Omega \boldsymbol{P}^*_\pm\cdot\left(\nabla\times\boldsymbol{P}^*_\pm\right)d^3x, \tag{3.49}$$

where $\boldsymbol{P}^*_\pm = \boldsymbol{V} + \theta_\pm\boldsymbol{A}^*$ and $\theta_\pm = \left(d_i \pm \sqrt{d_i^2+4d_e^2}\right)/(2d_e^2)$.

It is also worth to mention here that, the extended MHD invariants (3.49), which endow two helicities akin to the magnetic or fluid helicity, is different from ideal MHD in this respect since the ideal MHD has only one [1,2,92,93]. This has to do with the fact that Hall MHD (and, in a similar manner, extended MHD as well) is a singular perturbation of ideal MHD [100,179].

3.5 Boundary conditions

Unlike the canonical Poisson bracket, if we deal with noncanonical Poisson bracket, the boundary condition will become critical. To prove the bracket properties, viz., antisymmetry, Leibniz property, Jacobi's identity, or to derive the equations of motion from the Poisson bracket, or to find Casimir invariants of the dynamical system, surface terms must be vanished using appropriate boundary conditions.

The Poisson bracket (3.37) in the following form

$$\begin{aligned}\{F,G\} = &-\int_\Omega\Big\{\left[F_\rho\left(\nabla\cdot G_{\boldsymbol{V}}\right)-\left(\nabla\cdot F_{\boldsymbol{V}}\right)G_\rho\right]-\left[\rho^{-1}\left(\nabla\times\boldsymbol{V}\right)\cdot\left(F_{\boldsymbol{V}}\times G_{\boldsymbol{V}}\right)\right]\\ &-\left[\boldsymbol{B}^*\cdot\rho^{-1}(F_{\boldsymbol{V}}\times(\nabla\times G_{\boldsymbol{B}^*}))+\boldsymbol{B}^*\cdot\rho^{-1}(\left(\nabla\times F_{\boldsymbol{B}^*}\right)\times G_{\boldsymbol{V}})\right]\end{aligned}$$

$$+d_i\left[\boldsymbol{B}^*\cdot\rho^{-1}(\,(\nabla\times F_{\boldsymbol{B}^*})\times(\nabla\times G_{\boldsymbol{B}^*})\,)\right]$$
$$-d_e^2\left[(\nabla\times\boldsymbol{V})\cdot\rho^{-1}(\,(\nabla\times F_{\boldsymbol{B}^*})\times(\nabla\times G_{\boldsymbol{B}^*})\,)\right]\Big\}d^3x, \tag{3.50}$$

directly satisfies the antisymmetry using the standard vector calculus identities without the needs of boundary conditions.

The boundary conditions required for the Jacobi's identity can be easily identified through the proof of the permutation law (3.27). We found that the required boundary conditions to prove the Jacobi's identity are

$$\boldsymbol{n}\times\boldsymbol{A}^*|_{\partial\Omega}=0\Longleftrightarrow\boldsymbol{n}\cdot\boldsymbol{B}^*|_{\partial\Omega}=0,$$

$$\boldsymbol{n}\times\boldsymbol{V}|_{\partial\Omega}=0$$

In order to obtain the equations of motions, we shall use the adjoint representation

$$\frac{d}{dt}F=\{F,\mathscr{H}\}, \tag{3.51}$$

which needs a specific choose of the functional F in order to represent the dynamical variables of the system, i.e., ρ, $\boldsymbol{V}$ and $\boldsymbol{B}^*$, and the gradient of the Hamiltonian. The later is given in (3.24), which require the following boundary condition

$$\boldsymbol{n}\times\boldsymbol{B}|_{\partial\Omega}=0.$$

Then, defining the functional F in terms of the delta function as

$$F=\int_\Omega f\;\delta\left(\boldsymbol{x}-\boldsymbol{x}_0\right)d^3x, \tag{3.52}$$

where f represents the dynamical variables. The delta function will use to eliminate the integrals from the both sides of the above equation of motion (3.51).

To drive the continuity equation (3.20), the functional F is

$$F = \int_{\Omega} \rho \; \delta \left(\boldsymbol{x} - \boldsymbol{x}_0 \right) d^3x,$$

and since the functional derivative F_ρ appears only once in the Poisson bracket (3.50), equation (3.51) yields

$$\frac{\partial \rho}{\partial t} = -\nabla \cdot \left(\rho \boldsymbol{V} \right),$$

which no integrations by parts are used, and then no boundary conditions are needed.

In order to drive the momentum equation (3.21), we follow a very similar procedure. Looking at the bracket (3.50), we can see that there are three terms involving $F_{\boldsymbol{V}}$,

$$\left(\nabla \cdot F_{\boldsymbol{V}} \right) \mathscr{H}_\rho + \rho^{-1} \left(\nabla \times \boldsymbol{V} \right) \cdot \left(F_{\boldsymbol{V}} \times \mathscr{H}_{\boldsymbol{V}} \right) + \boldsymbol{B}^* \cdot \rho^{-1} (F_{\boldsymbol{V}} \times \left(\nabla \times \mathscr{H}_{\boldsymbol{B}^*} \right)),$$

where the first term only needs integration by parts, which require the following boundary condition

$$\boldsymbol{n} \cdot F_{\boldsymbol{V}} |_{\partial \Omega} = 0,$$

for all functionals. Thus, using standard vector calculus identities, we have

$$\begin{aligned} \frac{\partial \boldsymbol{V}}{\partial t} &= -\left(\nabla \times \boldsymbol{V} \right) \times \boldsymbol{V} + \rho^{-1} \left(\nabla \times \boldsymbol{B} \right) \times \boldsymbol{B}^* \\ &\quad -\nabla \left(h + \frac{V^2}{2} + d_e^2 \frac{\left(\nabla \times \boldsymbol{B} \right)^2}{2\rho^2} \right), \end{aligned}$$

Finally, derivation of the generalized Ohms law (3.22) required integrations by parts for all of the rest three terms of the bracket (3.50)

$$\boldsymbol{B}^* \cdot \rho^{-1}(\,(\nabla \times F_{\boldsymbol{B}^*}) \times \mathscr{H}_{\boldsymbol{V}}) - d_i \boldsymbol{B}^* \cdot \rho^{-1}(\,(\nabla \times F_{\boldsymbol{B}^*}) \times (\nabla \times \mathscr{H}_{\boldsymbol{B}^*})\,)$$
$$+ d_e^2\,(\nabla \times \boldsymbol{V}) \cdot \rho^{-1}(\,(\nabla \times F_{\boldsymbol{B}^*}) \times (\nabla \times \mathscr{H}_{\boldsymbol{B}^*})\,),$$

which needs the following boundary condition

$$\boldsymbol{n} \times F_{\boldsymbol{B}^*}|_{\partial\Omega} = 0,$$

to yield

$$\begin{aligned} \frac{\partial \boldsymbol{B}^*}{\partial t} &= \nabla \times (\boldsymbol{V} \times \boldsymbol{B}^*) - d_i \nabla \times \left(\rho^{-1}\,(\nabla \times \boldsymbol{B}) \times \boldsymbol{B}^*\right) \\ &\quad + d_e^2 \nabla \times \left(\rho^{-1}\,(\nabla \times \boldsymbol{B}) \times (\nabla \times \boldsymbol{V})\right). \end{aligned}$$

For the invariants of the extended MHD given in Sec. 3.4, we found that the required boundary conditions can be given as

$$\boldsymbol{n} \cdot \boldsymbol{B}^*|_{\partial\Omega} = 0,$$

$$\boldsymbol{n} \times \boldsymbol{V}|_{\partial\Omega} = 0.$$

To summarize the above calculations, it should be noted that, the Poisson bracket (3.50) with the the following boundary condition

$$\boldsymbol{n} \cdot \boldsymbol{B}^*|_{\partial\Omega} = 0, \tag{3.53}$$

$$\boldsymbol{n} \times \boldsymbol{V}|_{\partial\Omega} = 0., \tag{3.54}$$

define a Poisson algebra. Also, for some limited class of observables that satisfies the following boundary conditions

$$\boldsymbol{n} \times F_{\boldsymbol{B}^*}|_{\partial\Omega} = 0, \tag{3.55}$$

$$\boldsymbol{n} \cdot F_{\boldsymbol{V}}|_{\partial\Omega} = 0, \tag{3.56}$$

for all the functionals, we can convert the Poisson bracket (3.50) to the conventional form

$$\{F, G\} = \langle F_u, \mathcal{J} G_u \rangle \,, \tag{3.57}$$

where Poisson operator $\mathcal{J}$ is defined by (3.25). Then we can directly recover the extended MHD equations of motion.

3.6 Macroscopic limits of extended MHD

3.6.1 Hall MHD

The Hall MHD system of equations is an approximate two-fluid model, in which electrons are considered to be completely inertia-less, and then the magnetic field lines are frozen in the electron fluid, whilst ions are considered to be decoupled from the magnetic field lines. To see the relation to the extended MHD, we present the formulation.

Upon setting the electron skin depth $d_e = 0$ (neglecting electron inertia), in the extended MHD model (3.19)-(3.21), we obtain the normalized Hall MHD equations,

$$\frac{\partial \rho}{\partial t} = -\nabla \cdot (\rho \boldsymbol{V}) \,, \tag{3.58}$$

$$\frac{\partial \boldsymbol{V}}{\partial t} = -\left(\nabla \times \boldsymbol{V}\right) \times \boldsymbol{V} + \rho^{-1}\left(\nabla \times \boldsymbol{B}\right) \times \boldsymbol{B} - \nabla\left(h + \frac{V^2}{2}\right), \quad (3.59)$$

,

$$\frac{\partial \boldsymbol{B}}{\partial t} = \nabla \times \left(\boldsymbol{V} \times \boldsymbol{B}\right) - d_i \nabla \times \left(\rho^{-1}\left(\nabla \times \boldsymbol{B}\right) \times \boldsymbol{B}\right). \quad (3.60)$$

In Hall MHD, the state vector is $u = (\rho, \boldsymbol{V}, \boldsymbol{B})^t$, and the energy is

$$\mathscr{H}_H := \int_\Omega \left\{\rho\left(\frac{V^2}{2} + U\left(\rho\right)\right) + \frac{B^2}{2}\right\} d^3x. \quad (3.61)$$

Also, under the same condition the extended MHD Poisson operator (3.25) reduces into

$$\mathcal{J}_H = \begin{pmatrix} 0 & -\nabla\cdot & 0 \\ -\nabla & -\frac{(\nabla\times\boldsymbol{V})\times\circ}{\rho} & \frac{(\nabla\times\circ)\times\boldsymbol{B}}{\rho} \\ 0 & \nabla\times\frac{(\circ\times\boldsymbol{B})}{\rho} & -d_i\nabla\times\left(\frac{(\nabla\times\circ)\times\boldsymbol{B}}{\rho}\right) \end{pmatrix}, \quad (3.62)$$

3.6.1.1 Poisson bracket and Jacobi's identity for Hall MHD

The noncanonical Poisson bracket of the Hall MHD system is given as

$$\begin{aligned} \{F, G\} \;=\; & -\int_\Omega \Big\{ \left[F_\rho \nabla \cdot G_{\boldsymbol{V}} + F_{\boldsymbol{V}} \cdot \nabla G_\rho\right] + \left[F_{\boldsymbol{V}} \cdot \rho^{-1}\left(\left(\nabla \times \boldsymbol{V}\right) \times G_{\boldsymbol{V}}\right)\right] \\ & - \left[\boldsymbol{B} \cdot \rho^{-1}\left(F_{\boldsymbol{V}} \times \left(\nabla \times G_{\boldsymbol{B}}\right)\right) + \boldsymbol{B} \cdot \rho^{-1}\left(\left(\nabla \times F_{\boldsymbol{B}}\right) \times G_{\boldsymbol{V}}\right)\right] \\ & + d_i\left[\boldsymbol{B} \cdot \rho^{-1}\left(\left(\nabla \times F_{\boldsymbol{B}}\right) \times \left(\nabla \times G_{\boldsymbol{B}}\right)\right)\right] \Big\} d^3x. \end{aligned} \quad (3.63)$$

The Poisson bracket of Hall MHD can be rewritten in terms of the generating bracket (3.26) as

$$\begin{aligned} \{F, G\} \;=\; & [F, G]^{\boldsymbol{V}}_{\boldsymbol{V},\boldsymbol{V}} + [F, G]^{\boldsymbol{A}}_{\boldsymbol{V},\boldsymbol{A}} + [F, G]^{\boldsymbol{A}}_{\boldsymbol{A},\boldsymbol{V}} - d_i\,[F, G]^{\boldsymbol{A}}_{\boldsymbol{A},\boldsymbol{A}} \\ & + \int_\Omega \left[F_\rho \nabla \cdot G_{\boldsymbol{V}} + F_{\boldsymbol{V}} \cdot \nabla G_\rho\right] d^3x. \end{aligned} \quad (3.64)$$

After similar calculations as (3.42), we may write the Hall MHD Jacobi identity as

$$
\begin{aligned}
&\{E,\{F,G\}\}+\circlearrowleft= \\
&\Big[E,[F,G]^{\boldsymbol{V}}_{\boldsymbol{V},\boldsymbol{V}}\Big]^{\boldsymbol{V}}_{\boldsymbol{V},\boldsymbol{V}}+\Big[G,[E,F]^{\boldsymbol{V}}_{\boldsymbol{V},\boldsymbol{V}}\Big]^{\boldsymbol{V}}_{\boldsymbol{V},\boldsymbol{V}}+\Big[F,[G,E]^{\boldsymbol{V}}_{\boldsymbol{V},\boldsymbol{V}}\Big]^{\boldsymbol{V}}_{\boldsymbol{V},\boldsymbol{V}} \\
&+\Big[E,[F,G]^{\boldsymbol{A}}_{\boldsymbol{V},\boldsymbol{V}}\Big]^{\boldsymbol{A}}_{\boldsymbol{A},\boldsymbol{A}}+\Big[G,[E,F]^{\boldsymbol{A}}_{\boldsymbol{A},\boldsymbol{V}}\Big]^{\boldsymbol{A}}_{\boldsymbol{V},\boldsymbol{A}}+\Big[F,[G,E]^{\boldsymbol{A}}_{\boldsymbol{V},\boldsymbol{A}}\Big]^{\boldsymbol{A}}_{\boldsymbol{V},\boldsymbol{A}} \\
&+\Big[E,[F,G]^{\boldsymbol{A}}_{\boldsymbol{V},\boldsymbol{A}}\Big]^{\boldsymbol{A}}_{\boldsymbol{V},\boldsymbol{A}}+\Big[G,[E,F]^{\boldsymbol{A}}_{\boldsymbol{V},\boldsymbol{V}}\Big]^{\boldsymbol{A}}_{\boldsymbol{A},\boldsymbol{A}}+\Big[F,[G,E]^{\boldsymbol{A}}_{\boldsymbol{A},\boldsymbol{V}}\Big]^{\boldsymbol{A}}_{\boldsymbol{V},\boldsymbol{A}} \\
&+\Big[E,[F,G]^{\boldsymbol{A}}_{\boldsymbol{A},\boldsymbol{V}}\Big]^{\boldsymbol{A}}_{\boldsymbol{V},\boldsymbol{A}}+\Big[G,[E,F]^{\boldsymbol{A}}_{\boldsymbol{V},\boldsymbol{A}}\Big]^{\boldsymbol{A}}_{\boldsymbol{V},\boldsymbol{A}}+\Big[F,[G,E]^{\boldsymbol{A}}_{\boldsymbol{V},\boldsymbol{V}}\Big]^{\boldsymbol{A}}_{\boldsymbol{A},\boldsymbol{A}} \\
&-d_i\Big[\Big[E,[F,G]^{\boldsymbol{A}}_{\boldsymbol{A},\boldsymbol{A}}\Big]^{\boldsymbol{A}}_{\boldsymbol{V},\boldsymbol{A}}+\Big[G,[E,F]^{\boldsymbol{A}}_{\boldsymbol{V},\boldsymbol{A}}\Big]^{\boldsymbol{A}}_{\boldsymbol{A},\boldsymbol{A}}+\Big[F,[G,E]^{\boldsymbol{A}}_{\boldsymbol{A},\boldsymbol{V}}\Big]^{\boldsymbol{A}}_{\boldsymbol{A},\boldsymbol{A}}\Big] \\
&-d_i\Big(\Big[E,[F,G]^{\boldsymbol{A}}_{\boldsymbol{A},\boldsymbol{V}}\Big]^{\boldsymbol{A}}_{\boldsymbol{A},\boldsymbol{A}}+\Big[G,[E,F]^{\boldsymbol{A}}_{\boldsymbol{A},\boldsymbol{A}}\Big]^{\boldsymbol{A}}_{\boldsymbol{V},\boldsymbol{A}}+\Big[F,[G,E]^{\boldsymbol{A}}_{\boldsymbol{V},\boldsymbol{A}}\Big]^{\boldsymbol{A}}_{\boldsymbol{A},\boldsymbol{A}}\Big) \\
&-d_i\Big(\Big[E,[F,G]^{\boldsymbol{A}}_{\boldsymbol{V},\boldsymbol{A}}\Big]^{\boldsymbol{A}}_{\boldsymbol{A},\boldsymbol{A}}+\Big[G,[E,F]^{\boldsymbol{A}}_{\boldsymbol{A},\boldsymbol{V}}\Big]^{\boldsymbol{A}}_{\boldsymbol{A},\boldsymbol{A}}+\Big[F,[G,E]^{\boldsymbol{A}}_{\boldsymbol{A},\boldsymbol{A}}\Big]^{\boldsymbol{A}}_{\boldsymbol{V},\boldsymbol{A}}\Big) \\
&+d_i^2\Big(\Big[E,[F,G]^{\boldsymbol{A}}_{\boldsymbol{A},\boldsymbol{A}}\Big]^{\boldsymbol{A}}_{\boldsymbol{A},\boldsymbol{A}}+\Big[G,[E,F]^{\boldsymbol{A}}_{\boldsymbol{A},\boldsymbol{A}}\Big]^{\boldsymbol{A}}_{\boldsymbol{A},\boldsymbol{A}}+\Big[F,[G,E]^{\boldsymbol{A}}_{\boldsymbol{A},\boldsymbol{A}}\Big]^{\boldsymbol{A}}_{\boldsymbol{A},\boldsymbol{A}}\Big) \\
&+O(\partial^2),
\end{aligned}
\tag{3.65}
$$

which, by Lemma1, vanishes, proving Jacobi's identity.

3.6.1.2 Hall MHD Casimir invariants

The Hall MHD has three independent Casimir invariants given by

- magnetic helicity

$$C_1^H = \frac{1}{2}\int_\Omega \boldsymbol{A}\cdot\boldsymbol{B}\,d^3x, \tag{3.66}$$

- ion helicity

$$C_2^H = \frac{1}{2}\int_\Omega (\boldsymbol{A}+d_i\boldsymbol{V})\cdot(\boldsymbol{B}+d_i\nabla\times\boldsymbol{V})\,d^3x, \tag{3.67}$$

- total mass

$$C_3^H = \int_\Omega \rho \, d^3x, \tag{3.68}$$

and the independent invariant, which is a result of the combination of the magnetic and ion canonical helicities

- combined cross and fluid helicities

$$C_4^H = \frac{1}{2}\int_\Omega \boldsymbol{V}\cdot(2\boldsymbol{B} + d_i \nabla\times\boldsymbol{V})\, d^3x,, \tag{3.69}$$

We can easily show that the Casimir invariants (3.66) and (3.67) are the reductions of the extended MHD Casimir invariants (3.44), (3.45) , respectively, whilst the dependent invariant (3.69) from (3.48), in the limit of $d_e \to 0$.

3.6.2 Inertial MHD

The inertial MHD model is obtained by setting the ion skin depth $d_i = 0$ (neglecting Hall drift) in the extended MHD model, which yields

$$\frac{\partial \rho}{\partial t} = -\nabla\cdot(\rho \boldsymbol{V}), \tag{3.70}$$

$$\begin{aligned}\frac{\partial \boldsymbol{V}}{\partial t} &= -(\nabla\times\boldsymbol{V})\times\boldsymbol{V} + \rho^{-1}(\nabla\times\boldsymbol{B})\times\boldsymbol{B}^* \\ &\quad -\nabla\left(h + \frac{V^2}{2} + d_e^2\frac{(\nabla\times\boldsymbol{B})^2}{2\rho^2}\right),\end{aligned} \tag{3.71}$$

$$\frac{\partial \boldsymbol{B}^*}{\partial t} = \nabla\times(\boldsymbol{V}\times\mathbf{B}^*) + d_e^2\nabla\times\left(\rho^{-1}(\nabla\times\boldsymbol{B})\times(\nabla\times\boldsymbol{V})\right). \tag{3.72}$$

The energy is

$$\mathscr{H}_{inertial} := \int_\Omega \left\{ \rho \left(\frac{V^2}{2} + U(\rho) \right) + \frac{B^2}{2} + d_e^2 \frac{(\nabla \times \boldsymbol{B})^2}{2\rho} \right\} d^3x. \quad (3.73)$$

With respect to the state vector $u = (\rho, \boldsymbol{V}, \boldsymbol{B}^*)^t$, the Poisson operator of the inertial MHD is

$$\mathcal{J}_{inertial} = \begin{pmatrix} 0 & -\nabla\cdot & 0 \\ -\nabla & -\frac{(\nabla\times\boldsymbol{V})\times\circ}{\rho} & \frac{(\nabla\times\circ)\times\boldsymbol{B}^*}{\rho} \\ 0 & \nabla\times\frac{(\circ\times\boldsymbol{B}^*)}{\rho} & d_e^2\nabla\times\left(\frac{(\nabla\times\circ)\times(\nabla\times\boldsymbol{V})}{\rho}\right) \end{pmatrix}. \quad (3.74)$$

It may appear unphysical to drop d_i while retaining d_e since electron inertia length scale is much less than the Hall length scale. However, this limit may be valid when the timescale of current changes is much shorter than the electrons gyro period [79].

3.6.2.1 Poisson bracket and Jacobi's identity for inertial MHD

The Poisson bracket of the inertial MHD system is written as

$$\begin{aligned} \{F,G\} \;=\; -\int_\Omega \Big\{ & [F_\rho \nabla\cdot G_{\boldsymbol{V}} + F_{\boldsymbol{V}}\cdot\nabla G_\rho] - \left[\rho^{-1}(\nabla\times\boldsymbol{V})\cdot(F_{\boldsymbol{V}}\times G_{\boldsymbol{V}})\right] \\ & - \left[\boldsymbol{B}^*\cdot\rho^{-1}(F_{\boldsymbol{V}}\times(\nabla\times G_{\boldsymbol{B}^*})) + \boldsymbol{B}^*\cdot\rho^{-1}((\nabla\times F_{\boldsymbol{B}^*})\times G_{\boldsymbol{V}})\right] \\ & - d_e^2\left[(\nabla\times\boldsymbol{V})\cdot\rho^{-1}((\nabla\times F_{\boldsymbol{B}^*})\times(\nabla\times G_{\boldsymbol{B}^*}))\right] \Big\} d^3x. \end{aligned} \quad (3.75)$$

Using the generating bracket (3.26), the inertial MHD Poisson bracket (3.75) can be written as

$$\begin{aligned} \{F,G\} \;=\; & [F,G]^{\boldsymbol{V}}_{\boldsymbol{V},\boldsymbol{V}} + [F,G]^{\boldsymbol{A}^*}_{\boldsymbol{V},\boldsymbol{A}^*} + [F,G]^{\boldsymbol{A}^*}_{\boldsymbol{A}^*,\boldsymbol{V}} + d_e^2\,[F,G]^{\boldsymbol{V}}_{\boldsymbol{A}^*,\boldsymbol{A}^*} \\ & + \int_\Omega [F_\rho\nabla\cdot G_{\boldsymbol{V}} + F_{\boldsymbol{V}}\cdot\nabla G_\rho]\, d^3x. \end{aligned} \quad (3.76)$$

Then, the Jacobi identity for the inertial MHD can be obtained directly from (3.43) by imposing the limit $d_i = 0$, which gives

$$
\begin{aligned}
&\{E,\{F,G\}\} + \circlearrowleft = \\
&\Big[E,[F,G]^{\boldsymbol{V}}_{\boldsymbol{V},\boldsymbol{V}}\Big]^{\boldsymbol{V}}_{\boldsymbol{V},\boldsymbol{V}} + \Big[G,[E,F]^{\boldsymbol{V}}_{\boldsymbol{V},\boldsymbol{V}}\Big]^{\boldsymbol{V}}_{\boldsymbol{V},\boldsymbol{V}} + \Big[F,[G,E]^{\boldsymbol{V}}_{\boldsymbol{V},\boldsymbol{V}}\Big]^{\boldsymbol{V}}_{\boldsymbol{V},\boldsymbol{V}} \\
&+ \Big[E,[F,G]^{\boldsymbol{A}^*}_{\boldsymbol{V},\boldsymbol{V}}\Big]^{\boldsymbol{A}^*}_{\boldsymbol{A}^*,\boldsymbol{A}^*} + \Big[G,[E,F]^{\boldsymbol{A}^*}_{\boldsymbol{A}^*,\boldsymbol{V}}\Big]^{\boldsymbol{A}^*}_{\boldsymbol{V},\boldsymbol{A}^*} + \Big[F,[G,E]^{\boldsymbol{A}^*}_{\boldsymbol{V},\boldsymbol{A}^*}\Big]^{\boldsymbol{A}^*}_{\boldsymbol{V},\boldsymbol{A}^*} \\
&+ \Big[E,[F,G]^{\boldsymbol{A}^*}_{\boldsymbol{V},\boldsymbol{A}^*}\Big]^{\boldsymbol{A}^*}_{\boldsymbol{V},\boldsymbol{A}^*} + \Big[G,[E,F]^{\boldsymbol{A}^*}_{\boldsymbol{V},\boldsymbol{V}}\Big]^{\boldsymbol{A}^*}_{\boldsymbol{A}^*,\boldsymbol{A}^*} + \Big[F,[G,E]^{\boldsymbol{A}^*}_{\boldsymbol{A}^*,\boldsymbol{V}}\Big]^{\boldsymbol{A}^*}_{\boldsymbol{V},\boldsymbol{A}^*} \\
&+ \Big[E,[F,G]^{\boldsymbol{A}^*}_{\boldsymbol{A}^*,\boldsymbol{V}}\Big]^{\boldsymbol{A}^*}_{\boldsymbol{V},\boldsymbol{A}^*} + \Big[G,[E,F]^{\boldsymbol{A}^*}_{\boldsymbol{V},\boldsymbol{A}^*}\Big]^{\boldsymbol{A}^*}_{\boldsymbol{V},\boldsymbol{A}^*} + \Big[F,[G,E]^{\boldsymbol{A}^*}_{\boldsymbol{V},\boldsymbol{V}}\Big]^{\boldsymbol{A}^*}_{\boldsymbol{A}^*,\boldsymbol{A}^*} \\
&+d_e^2\Big(\Big[E,[F,G]^{\boldsymbol{V}}_{\boldsymbol{A}^*,\boldsymbol{A}^*}\Big]^{\boldsymbol{V}}_{\boldsymbol{V},\boldsymbol{V}} + \Big[G,[E,F]^{\boldsymbol{V}}_{\boldsymbol{V},\boldsymbol{A}^*}\Big]^{\boldsymbol{V}}_{\boldsymbol{A}^*,\boldsymbol{V}} + \Big[F,[G,E]^{\boldsymbol{V}}_{\boldsymbol{A}^*,\boldsymbol{V}}\Big]^{\boldsymbol{V}}_{\boldsymbol{A}^*,\boldsymbol{V}} \Big) \\
&+d_e^2\Big(\Big[E,[F,G]^{\boldsymbol{V}}_{\boldsymbol{A}^*,\boldsymbol{V}}\Big]^{\boldsymbol{V}}_{\boldsymbol{A}^*,\boldsymbol{V}} + \Big[G,[E,F]^{\boldsymbol{V}}_{\boldsymbol{A}^*,\boldsymbol{A}^*}\Big]^{\boldsymbol{V}}_{\boldsymbol{V},\boldsymbol{V}} + \Big[F,[G,E]^{\boldsymbol{V}}_{\boldsymbol{V},\boldsymbol{A}^*}\Big]^{\boldsymbol{V}}_{\boldsymbol{A}^*,\boldsymbol{V}} \Big) \\
&+d_e^2\Big(\Big[E,[F,G]^{\boldsymbol{V}}_{\boldsymbol{V},\boldsymbol{A}^*}\Big]^{\boldsymbol{V}}_{\boldsymbol{A}^*,\boldsymbol{V}} + \Big[G,[E,F]^{\boldsymbol{V}}_{\boldsymbol{A}^*,\boldsymbol{V}}\Big]^{\boldsymbol{V}}_{\boldsymbol{A}^*,\boldsymbol{V}} + \Big[F,[G,E]^{\boldsymbol{V}}_{\boldsymbol{A}^*,\boldsymbol{A}^*}\Big]^{\boldsymbol{V}}_{\boldsymbol{V},\boldsymbol{V}} \Big) \\
&+d_e^2\Big(\Big[E,[F,G]^{\boldsymbol{A}^*}_{\boldsymbol{A}^*,\boldsymbol{A}^*}\Big]^{\boldsymbol{A}^*}_{\boldsymbol{A}^*,\boldsymbol{A}^*} + \Big[G,[E,F]^{\boldsymbol{A}^*}_{\boldsymbol{A}^*,\boldsymbol{A}^*}\Big]^{\boldsymbol{A}^*}_{\boldsymbol{A}^*,\boldsymbol{A}^*} + \Big[F,[G,E]^{\boldsymbol{A}^*}_{\boldsymbol{A}^*,\boldsymbol{A}^*}\Big]^{\boldsymbol{A}^*}_{\boldsymbol{A}^*,\boldsymbol{A}^*} \Big) \\
&\quad + O(\partial^2).
\end{aligned}
\tag{3.77}
$$

As in the previous cases, $O(\partial^2)$ terms cancels. Hence, Lemma1, we obtain Jacobi's identity.

3.6.2.2 Inertial MHD Casimir invariants

Akin to the extended and Hall MHD, the inertial MHD has three independent Casimir invariants:

- modified cross helicity

$$C_1^{in} = \int_\Omega \boldsymbol{V}\cdot\boldsymbol{B}^* d^3x, \tag{3.78}$$

- electron canonical helicity

$$C_4^{in} = \frac{1}{2}\int_\Omega \boldsymbol{P}^\star\cdot(\nabla\times\boldsymbol{P}^\star)\, d^3x, \tag{3.79}$$

where $\boldsymbol{P}^{\star} = \boldsymbol{V} \pm \frac{1}{d_e}\boldsymbol{A}^{*}$.

- total mass helicity

$$C_3^{in} = \int_{\Omega} \rho \, d^3x. \tag{3.80}$$

The combination of the Casimir invariants (3.78) and (3.79) yields

- combined modified magnetic helicity and fluid helicity

$$C_2^{in} = \frac{1}{2}\int_{\Omega} \left[\boldsymbol{A}^{*} \cdot \boldsymbol{B}^{*} + d_e^2 \boldsymbol{V} \cdot (\nabla \times \boldsymbol{V})\right] d^3x, \tag{3.81}$$

The first Casimir (3.78) comes from (3.44) by multiply the latter by $-\frac{d_i}{2d_e^2}$, and then sitting $d_i \to 0$. Further, (3.79) obtained by setting $d_i = 0$ in (3.49). The last Casimir is identical to (3.47), and also can be directly obtained by neglecting d_i in (3.45).

3.6.3 Indeal MHD

Finally, neglecting both the ion and electron skin depths concurrently yields the plasma physics simplest model, ideal MHD. Notice that, Hamiltonian structure of the ideal MHD was first given in [117]. The governing equations are composed as follow

$$\frac{\partial \rho}{\partial t} = -\nabla \cdot (\rho \boldsymbol{V}), \tag{3.82}$$

$$\frac{\partial \boldsymbol{V}}{\partial t} = -(\nabla \times \boldsymbol{V}) \times \boldsymbol{V} + \rho^{-1}(\nabla \times \boldsymbol{B}) \times \boldsymbol{B} - \nabla\left(h + \frac{V^2}{2}\right), \tag{3.83}$$

$$\frac{\partial \boldsymbol{B}}{\partial t} = \nabla \times (\boldsymbol{V} \times \mathbf{B}). \tag{3.84}$$

Furthermore, it was shown that the ideal MHD dynamical equations (3.82), (3.83), and (3.84), conserve the energy:

$$\mathscr{H}_{ideal} := \int_{\Omega} \left\{ \rho \left(\frac{V^2}{2} + U(\rho) \right) + \frac{B^2}{2} \right\} d^3x. \tag{3.85}$$

The dynamical variable in ideal MHD is $u = (\rho, \boldsymbol{V}, \boldsymbol{B})^t$.

The ideal MHD Poisson operator has the form

$$\mathcal{J}_{ideal} = \begin{pmatrix} 0 & -\nabla\cdot & 0 \\ -\nabla & -\frac{(\nabla\times\boldsymbol{V})\times\circ}{\rho} & \frac{(\nabla\times\circ)\times\boldsymbol{B}}{\rho} \\ 0 & \nabla\times\frac{(\circ\times\boldsymbol{B})}{\rho} & 0 \end{pmatrix}. \tag{3.86}$$

3.6.3.1 Poisson bracket and Jacobi's identity for ideal MHD

The ideal MHD has a Poisson bracket given as

$$\begin{aligned} \{F,G\} &= -\int_{\Omega} \Big\{ [F_\rho \nabla\cdot G_{\boldsymbol{V}} + F_{\boldsymbol{V}}\cdot\nabla G_\rho] - \left[\rho^{-1}(\nabla\times\boldsymbol{V})\cdot(F_{\boldsymbol{V}}\times G_{\boldsymbol{V}})\right] \\ &\quad - \left[\boldsymbol{B}\cdot\rho^{-1}(F_{\boldsymbol{V}}\times(\nabla\times G_{\boldsymbol{B}})) + \boldsymbol{B}\cdot\rho^{-1}((\nabla\times F_{\boldsymbol{B}})\times G_{\boldsymbol{V}})\right] \Big\} d^3x. \end{aligned} \tag{3.87}$$

Poisson bracket (3.87) can be written in terms of the generating bracket (3.26), as

$$\{F,G\} = [F,G]^{\boldsymbol{V}}_{\boldsymbol{V},\boldsymbol{V}} + [F,G]^{\boldsymbol{A}}_{\boldsymbol{V},\boldsymbol{A}} + [F,G]^{\boldsymbol{A}}_{\boldsymbol{A},\boldsymbol{V}} + \int_{\Omega} [F_\rho \nabla\cdot G_{\boldsymbol{V}} + F_{\boldsymbol{V}}\cdot\nabla G_\rho]\, d^3x. \tag{3.88}$$

Also, so, the Jacobi identity for the ideal MHD in terms of the generating bracket (3.26) can be written as

$$\{E,\{F,G\}\} + \circlearrowleft =$$

$$
\begin{aligned}
&\Big[E,[F,G]^{\boldsymbol{V}}_{\boldsymbol{V},\boldsymbol{V}}\Big]^{\boldsymbol{V}}_{\boldsymbol{V},\boldsymbol{V}}+\Big[G,[E,F]^{\boldsymbol{V}}_{\boldsymbol{V},\boldsymbol{V}}\Big]^{\boldsymbol{V}}_{\boldsymbol{V},\boldsymbol{V}}+\Big[F,[G,E]^{\boldsymbol{V}}_{\boldsymbol{V},\boldsymbol{V}}\Big]^{\boldsymbol{V}}_{\boldsymbol{V},\boldsymbol{V}}\\
&+\Big[E,[F,G]^{\boldsymbol{A}}_{\boldsymbol{V},\boldsymbol{V}}\Big]^{\boldsymbol{A}}_{\boldsymbol{A},\boldsymbol{A}}+\Big[G,[E,F]^{\boldsymbol{A}}_{\boldsymbol{A},\boldsymbol{V}}\Big]^{\boldsymbol{A}}_{\boldsymbol{V},\boldsymbol{A}}+\Big[F,[G,E]^{\boldsymbol{A}}_{\boldsymbol{V},\boldsymbol{A}}\Big]^{\boldsymbol{A}}_{\boldsymbol{V},\boldsymbol{A}}\\
&+\Big[E,[F,G]^{\boldsymbol{A}}_{\boldsymbol{V},\boldsymbol{A}}\Big]^{\boldsymbol{A}}_{\boldsymbol{V},\boldsymbol{A}}+\Big[G,[E,F]^{\boldsymbol{A}}_{\boldsymbol{V},\boldsymbol{V}}\Big]^{\boldsymbol{A}}_{\boldsymbol{A},\boldsymbol{A}}+\Big[F,[G,E]^{\boldsymbol{A}}_{\boldsymbol{A},\boldsymbol{V}}\Big]^{\boldsymbol{A}}_{\boldsymbol{V},\boldsymbol{A}}\\
&+\Big[E,[F,G]^{\boldsymbol{A}}_{\boldsymbol{A},\boldsymbol{V}}\Big]^{\boldsymbol{A}}_{\boldsymbol{V},\boldsymbol{A}}+\Big[G,[E,F]^{\boldsymbol{A}}_{\boldsymbol{V},\boldsymbol{A}}\Big]^{\boldsymbol{A}}_{\boldsymbol{V},\boldsymbol{A}}+\Big[F,[G,E]^{\boldsymbol{A}}_{\boldsymbol{V},\boldsymbol{V}}\Big]^{\boldsymbol{A}}_{\boldsymbol{A},\boldsymbol{A}}\\
&+O(\partial^2). \qquad (3.89)
\end{aligned}
$$

Thus, the Jacobi's identity (3.89) verified by using the advantages of Lemma1.

3.6.3.2 Ideal MHD Casimir invariants

It is well known that the ideal MHD has the following Casimir invariants:

- Magnetic helicity

$$C_1^i = \frac{1}{2}\int_\Omega \boldsymbol{V}\cdot\boldsymbol{B}\, d^3x, \qquad (3.90)$$

- Cross helicity

$$C_2^i = \int_\Omega \boldsymbol{V}\cdot\boldsymbol{B}\, d^3x, \qquad (3.91)$$

- Total mass

$$C_3^i = \int_\Omega \rho\, d^3x. \qquad (3.92)$$

Chapter 4

Alfvén waves as creations on Casimir leaves of extended MHD

4.1 Alfvén waves

Alfvén waves are the most typical electromagnetic phenomena in magnetized plasmas. In particular, nonlinear Alfvén waves deeply influence various plasma regimes in laboratory as well as in space, which have a crucial role in plasma heating [14, 65, 105], turbulence [22, 57, 154], reconnection [131], etc. An interesting property of the Alfvén waves, the amplitudes as well as wave forms are totally arbitrary when they propagate on a homogenous ambient magnetic field [44, 66]. In fact, we often observe large-amplitude Alfvén waves in orderly propagation (for example Ref. [121]). To put it in theoretical language, the set A of Alfvén waves after an appropriate transformation (see Ref. [100]), is a closed linear subspace, i.e., every linear combination of the members of A gives solution to the fully nonlinear wave equation. Needless to say, the set of general solutions to a linear equation is, by definition, a linear subspace. However, it is remarkable that the nonlinear MHD equation has such a linear subspace A of solutions.

Here we investigate the underlying mechanism producing such solutions in the context of a more accurate framework, generalized MHD. When

we take into account dispersion effects (we consider both ion and electron inertial effects [1, 79]), the wave forms are no longer arbitrary (remember that the ideal MHD model is dispersion free). Yet, we find that the generalized MHD system has a linear subspace of nonlinear solutions. The Casimir invariants of the system are the root cause of this interesting property [176].

We start by giving Linear dispersion relation of extended MHD models, e.g., ideal, Hall, and extended MHD. We derive nonlinear wave solutions of the extended MHD Models by putting the problem in the perspective of Hamiltonian mechanics. Via constructing equilibrium solutions (so-called Beltrami equilibrium) on Casimir leaves, we derive nonlinear wave solutions. The dispersion relation is exactly that of the linear theory, while the wave amplitude may be arbitrarily large. The wave function is composed of two components bearing distinct length scales.

4.2 Linear dispersion relation of extended MHD

In this section, we shall construct the linear theory for the extended MHD equations (3.19), (3.20) and (3.21), see Sec. 3.2.1. Then we shall discuses the limits to the Hall and ideal MHD models.

To look for the linear dispersion relation we split the fields to their ambient and fluctuating parts, as

$$\left.\begin{aligned} \boldsymbol{V} &= \boldsymbol{v}, \\ \boldsymbol{B} &= \hat{e}_z + \boldsymbol{b}, \\ \rho &= 1 + \widetilde{\rho}, \end{aligned}\right\} \tag{4.1}$$

where $\boldsymbol{B}_0 = \hat{e}_z$ is the ambient magnetic field, $\rho_0 = 1$ is the equilibrium density, which all equilibrium quantities are given in normalized units and the ambient flow is considered to be zero. The perturbed quantities are proportional to $\exp(i\boldsymbol{k}\cdot\boldsymbol{r} - i\omega t)$, where ω is the frequency and $\boldsymbol{k}$ is the wavevector. Notice that the total pressure is considered to be barotropic and adiabatic, i.e., it obeys the relation

$$p = s\rho^{\nu}, \tag{4.2}$$

where s is the proportional constant and ν is the adiabatic index. Then the perturbed equation of state may be given as

$$\nabla\widetilde{p} = C_s^2\nabla\widetilde{\rho}, \tag{4.3}$$

where $C_s \propto \sqrt{\nu}$ is the speed of sound. It is evident from the above relations that the incompressible limit is corresponding to an infinite adiabatic index ν and so an infinite speed of sound C_s.

Now, substituting the ansatz (4.1) along with (4.3) in the linearized equations of the extended MHD system (3.19)-(3.21), yields, respectively,

$$\widetilde{\rho} = \frac{\boldsymbol{k}\cdot\boldsymbol{v}}{\omega}, \tag{4.4}$$

$$\begin{aligned} -\omega\boldsymbol{v} &= (\boldsymbol{k}\times\boldsymbol{b})\times\hat{e}_z - \frac{C_s}{\omega}\boldsymbol{k}\,(\boldsymbol{k}\cdot\boldsymbol{v}) \\ &= (k_z\boldsymbol{b} - \boldsymbol{k}b_z) - \frac{C_s}{\omega}\boldsymbol{k}\,(\boldsymbol{k}\cdot\boldsymbol{v})\,, \end{aligned} \tag{4.5}$$

$$\begin{aligned} -\omega\left[1 + d_e^2k^2\right]\boldsymbol{b} &= \boldsymbol{k}\times(\boldsymbol{v}\times\hat{e}_z) - id_i\boldsymbol{k}\times([\boldsymbol{k}\times\boldsymbol{b}]\times\hat{e}_z) - \frac{C_s}{\omega}\boldsymbol{k}\,(\boldsymbol{k}\cdot\boldsymbol{v}) \\ &= (k_z\boldsymbol{v} - (\boldsymbol{k}\cdot\boldsymbol{v})\,\hat{e}_z) - id_ik_z\,(\boldsymbol{k}\times\boldsymbol{b})\,, \end{aligned} \tag{4.6}$$

where we used the vector calculus identities along with the notations

$$\boldsymbol{b}^* = \left[1 + d_e^2 k^2\right] \boldsymbol{b}. \tag{4.7}$$

The notation $\boldsymbol{k} \cdot \boldsymbol{b} = 0$ is also used, which came from the fact that the magnetic field must be divergence-free. Taking the dot product from the LHS of (4.5) with $\boldsymbol{k}$, we get

$$\boldsymbol{k} \cdot \boldsymbol{v} = \frac{\omega k^2 b_z}{\omega^2 - C_s^2 k^2} \tag{4.8}$$

The z-component of (4.5) and (4.6), respectively, are

$$\omega v_z = \frac{C_s}{\omega} k_z \left(\boldsymbol{k} \cdot \boldsymbol{v}\right) \tag{4.9}$$

$$-\omega \left[1 + d_e^2 k^2\right] b_z = \left(k_z v_z - \left(\boldsymbol{k} \cdot \boldsymbol{v}\right)\right) - i d_i k_z j_z \tag{4.10}$$

where $j_z = \left(\boldsymbol{k} \times \boldsymbol{b}\right) \cdot \hat{e}_z$.

Combining (4.9) and (4.10), we end up with

$$\omega \left[1 + d_e^2 k^2\right] b_z = k^2 b_z \left(\frac{\left(\omega^2 - C_s^2 k_z^2\right)}{\omega \left(\omega^2 - C_s^2 k^2\right)}\right) + i d_i k_z j_z. \tag{4.11}$$

By taking the cross product on both sides of (4.5) and (4.6) with $\boldsymbol{k}$ and then calculating the z-component, this leads us to

$$-\omega \left(\boldsymbol{k} \times \boldsymbol{v}\right) \cdot \hat{e}_z = k_z b_z, \tag{4.12}$$

$$-\omega \left[1 + d_e^2 k^2\right] j_z = \left(\boldsymbol{k} \times \boldsymbol{v}\right) \cdot \hat{e}_z + i d_i k^2 k_z j_z. \tag{4.13}$$

Thus, we can express j_z as

$$j_z = -i \frac{d_i \omega k^2 k_z b_z}{\left(\omega^2 \left[1 + d_e^2 k^2\right] - k_z^2\right)} \tag{4.14}$$

Substituting (4.14) into (4.11), we ends up with the linear dispersion relation of the extended MHD,

$$\left[\Gamma\omega^2 - k_z^2\right]\left[\Gamma\omega^4 - \left(1+\Gamma C_s^2\right)k^2\omega^2 + C_s^2k^2k_z^2\right] = d_i^2\omega^2k^2k_z^2\left(\omega^2 - C_s^2k^2\right), \tag{4.15}$$

where $\Gamma = [1 + d_e^2k^2]$. We note that the first term in the LHS of (4.15) gives the Alfvén dispersion relation and the second term gives the fast and slow magneto-acoustic dispersion relations when individually set to zero, which both are modified by the electron inertia effect. These two terms are coupled together by the RHS term of (4.15), which arises from the Hall effect.

Now, a few general observations regarding this dispersion relation (4.15) are in order.

- When the electron skin depth ignored ($d_e \to 0$), the dispersion relation (4.15) reduces to the Hall MHD dispersion relation [44, 122], which reads

$$\left[\omega^2 - k_z^2\right]\left[\omega^4 - \left(1+C_s^2\right)k^2\omega^2 + C_s^2k^2k_z^2\right] = d_i^2\omega^2k^2k_z^2\left(\omega^2 - C_s^2k^2\right). \tag{4.16}$$

- When both the electron and ion skin depths ignored (d_e and $d_i \to 0$) in (4.15), the results is the dispersion relation of the ideal MHD [44],

$$\left[\omega^2 - k_z^2\right]\left[\omega^4 - \left(1+C_s^2\right)k^2\omega^2 + C_s^2k^2k_z^2\right] = 0. \tag{4.17}$$

- When $C_s \to \infty$ (incompressible fluid), the dispersion relation (4.15) have the solutions,

$$\omega = \frac{-k_z}{(1+d_e^2k^2)}\left[\pm d_i k \mp \sqrt{\frac{d_i^2k^2}{4}+(1+d_e^2k^2)}\right] \tag{4.18}$$

- When $C_s = 0$ (cold plasma) or $C_s \to \infty$ (incompressible fluid), the dispersion relation (4.15) for parallel propagation ($k_z = k$) possesses the same solutions,

$$\omega = \frac{-k}{(1+d_e^2k^2)}\left[\pm d_i k \mp \sqrt{\frac{d_i^2k^2}{4}+(1+d_e^2k^2)}\right] \tag{4.19}$$

- In the case of warm plasma, which the sound speed is finite, the dispersion relation (4.15) has six solutions. In Fig. 4.1, the three positive frequency solutions are plotted against wavenumber k. To do that, we first introduce the angle θ to be the angle between the ambient magnetic field and the wave vector, so that $k_z = k\cos(\theta)$. Figs. 4.1a - 4.1d, shows the dispersion relations of three mode obtained from (4.15), for parallel propagation ($\theta^\circ = 0$)and different sound speed. The values of the sound speed are chosen relative to the Alfvén speed ($V_A = 1$ in normalized units). The dispersion relation of the sound wave ($\omega = C_s k$), plotted as a reference to identify the coupling and the converting between the different modes. We note that for $C_s << V_A$ the sound wave (orange line) is uncoupled from the fast and slow magnetoacoustic waves (red and blue lines respectively), and the sound mode survives only for very low and very high frequency, which is evanescent in between, as shown in Fig.4.1a. As the sound speed increased, different coupling arises between the three different modes, as

shown in Figs. 4.1b, 4.1c and 4.1d. We also observe the conversion of the solutions from mode to another as the sound speed change. Figs. 4.1e and 4.1f shows the interaction of the mode for two examples of oblique propagations ($\theta^\circ = 15$ and $\theta^\circ = 85$).

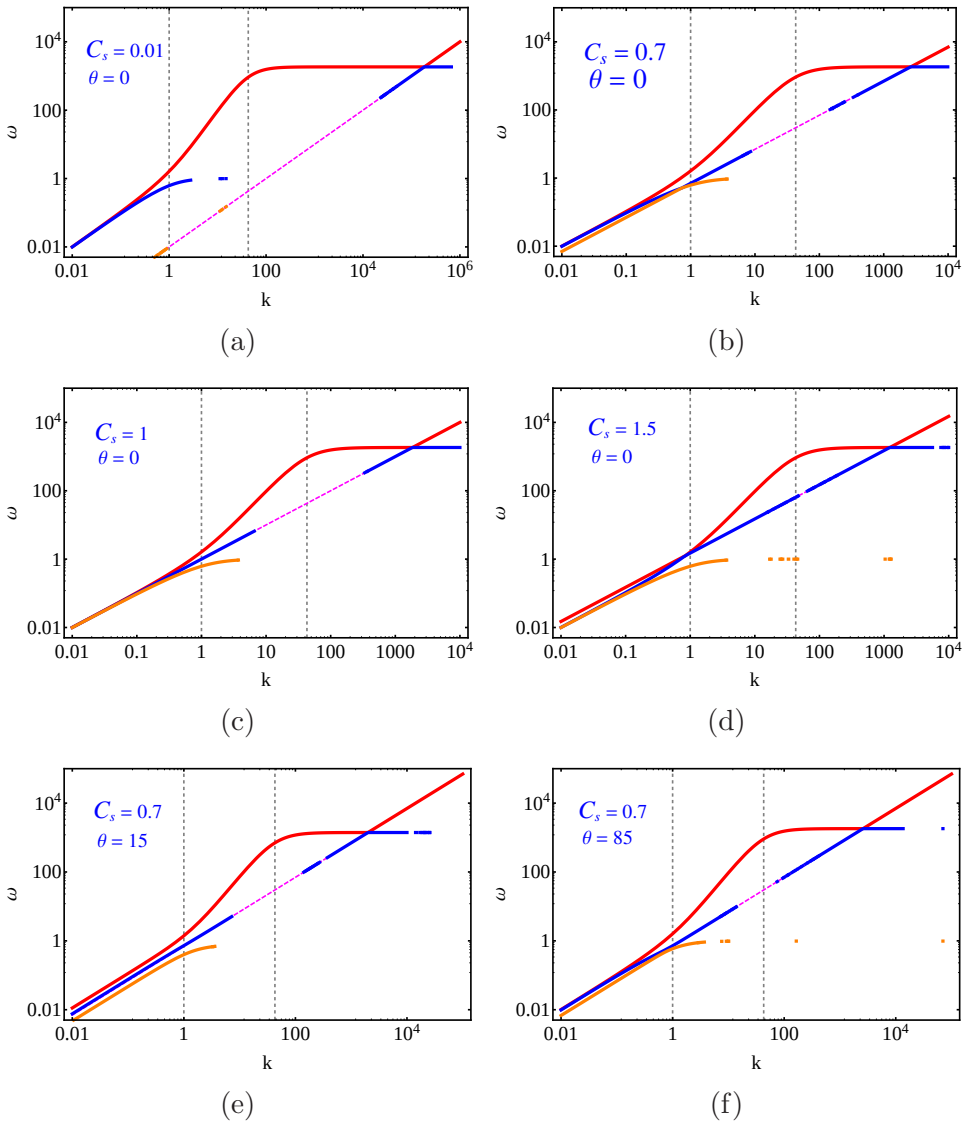

Figure 4.1: The dispersion relation in warm Plasmas governed by the extended MHD for fixed ion skin depth $d_i = 1$ and electron skin depth $d_e = 0.0233$. Figs. (a), (b), (c) and (d), for parallel propagation $\theta = 0$ and different value of the sound speed C_s. Figs. (e) and (f), For oblique propagation $\theta^\circ = 15$ and $\theta^\circ = 85$ and fixed sound speed $C_s = 0.7$. The dashed magenta line is the sound wave dispersion relation ($\omega = C_s k$), which used as a reference. The two vertical dashed lines separate the ideal, Hall and electron inertia regimes respectively (when viewed from left to right).

4.3 Nonlinear Alfvén waves

4.3.1 Nonlinear Alfvén waves in ideal MHD

Here we consider an ideal MHD plasma obeying the dynamical equations (3.82), (3.83) and (3.84), see Sec. 3.6.3, which the Hamiltonian structure ideal MHD is presented. The existence of Casimir invariants is the signature of the noncanonicality, by which the orbits in the phase space are restricted to stay on the Casimir leaves (the level-sets of the Casimir invariants) [116]. The equilibrium points are, then, the stationary points of the Hamiltonian (energy) on the Casimir leaves. The cross helicity $C_2^i = \int_\Omega \boldsymbol{V} \cdot \boldsymbol{B}\, d^3x$ (see Sec. 3.6.3.2) is one of the Casimir invariants of MHD, which is relevant to the present purpose of constructing nonlinear Alfvén waves.

Minimizing the Hamiltonian (3.85) with the constraint on C_2^i, we obtain

$$\boldsymbol{V} = \pm \boldsymbol{B}. \tag{4.20}$$

Evidently, every $\boldsymbol{B}$, being combined with $\boldsymbol{V} = \pm\boldsymbol{B}$, is an equilibrium ($\partial_t = 0$) solution of the ideal incompressible MHD equations.

We can convert these equilibrium stats to Alfvén waves propagating on a homogeneous ambient magnetic field $\boldsymbol{B}_0$ (which can be arbitrarily chosen) [176]. Let us rewrite $\boldsymbol{B}$ and $\boldsymbol{V} = \pm\boldsymbol{B}$ as

$$\boldsymbol{B} = \boldsymbol{B}_0 + \boldsymbol{b}, \quad \boldsymbol{V} = \pm\boldsymbol{B}_0 + \boldsymbol{v}. \tag{4.21}$$

Boosting the coordinate $\boldsymbol{x} \to \boldsymbol{x} \mp \boldsymbol{B}_0 t$, we find that the decomposed component (which is the wave component) satisfies

$$\frac{\partial \boldsymbol{v}}{\partial t} = -(\nabla \times \boldsymbol{v}) \times \boldsymbol{v} + (\nabla \times \boldsymbol{b}) \times (\boldsymbol{b} + \boldsymbol{B}_0) - \nabla(V^2/2 + P), \tag{4.22}$$

$$\frac{\partial \boldsymbol{b}}{\partial t} = \nabla \times [\boldsymbol{v} \times (\boldsymbol{b} + \boldsymbol{B}_0)], \tag{4.23}$$

which are exactly the Alfvén wave equations with an ambient field $\boldsymbol{B}_0$. Notice that the wave component $\boldsymbol{b}$ and $\boldsymbol{v}$ propagate with the Alfvén velocity $\pm\boldsymbol{B}_0$.

4.3.2 Nonlinear Alfvén waves in Hall MHD

We consider a collisionless plasma consisting of a completely magnetized electrons and a partially magnetized ions. This plasma is governed by the Hall MHD, which the dynamical equations are (3.58)-(3.60). The Hamiltonian structure of Hall MHD has been discussed in Sec.3.6.1, which the equations of motion are shown to conserve the energy,

$$\mathscr{H}_H := \int_\Omega \left\{ \rho \left(\frac{V^2}{2} + U(\rho) \right) + \frac{B^2}{2} \right\} d^3x. \tag{4.24}$$

Also, it is shown that the Hall MHD Poisson bracket possess the following Casimir invariants;

$$C_1^H = \frac{1}{2} \int_\Omega \boldsymbol{A} \cdot \boldsymbol{B} \, d^3x, \tag{4.25}$$

$$C_2^H = \frac{1}{2} \int_\Omega (\boldsymbol{A} + d_i \boldsymbol{V}) \cdot (\boldsymbol{B} + d_i \nabla \times \boldsymbol{V}) \, d^3x, \tag{4.26}$$

$$C_3^H = \int_\Omega \rho \, d^3x, \tag{4.27}$$

We can invoke the method of [176,177] to construct nonlinear wave solutions by the Casimir invariants and the Hamiltonian. We first construct energy-

Casimir equilibrium by extremizing

$$\mathscr{H}_{\mu}(u) = \mathscr{H}(u) - \sum_{n=1}^{3} \mu_n C_n(u). \tag{4.28}$$

Using the energy (4.24) along with the Casimir invariants (4.25)-(4.27) in (4.28), the Euler-Lagrange equation $\partial_u \mathscr{H}_{\mu} = 0$ can read as follow:

- the functional derivative with respect to $\boldsymbol{B}$ gives

$$\nabla \times \boldsymbol{B} = (\mu_1 + \mu_2)\boldsymbol{B} + d_i \mu_2 \nabla \times \boldsymbol{V}, \tag{4.29}$$

- the functional derivative with respect to $\boldsymbol{V}$ gives

$$\rho \boldsymbol{V} = d_i \mu_2 (\boldsymbol{B} + d_i \nabla \times \boldsymbol{V}), \tag{4.30}$$

- the functional derivative with respect to ρ gives

$$\frac{V^2}{2} + h(\rho) - \mu_3 = 0, \tag{4.31}$$

  where μ_1, μ_2 and μ_3 are Lagrange multipliers.

Assuming that the system incorporated incompressible flow ($\nabla \cdot \boldsymbol{V} = 0$) with a constant mass density $\rho = 1$, equations (4.29) and (4.30) combine to yield a double-curl Beltrami equation

$$\nabla \times \nabla \times \boldsymbol{B} - \left(\mu_1 + \frac{1}{d_i^2 \mu_2}\right) \nabla \times \boldsymbol{B} + \frac{1}{d_i^2}\left(1 + \frac{\mu_1}{\mu_2}\right) \boldsymbol{B} = 0. \tag{4.32}$$

This can be factorized in terms of a single Beltrami as

$$(curl - \lambda_+)(curl - \lambda_-)\boldsymbol{B} = 0, \tag{4.33}$$

where the eigenvalues $\lambda_{\pm}$ are determined by

$$\left.\begin{aligned} \lambda_+ + \lambda_- &= \mu_1 + \tfrac{1}{d_i^2 \mu_2}, \\ \lambda_+ \lambda_- &= \tfrac{1}{d_i^2}\left(1 + \tfrac{\mu_1}{\mu_2}\right). \end{aligned}\right\} \tag{4.34}$$

Equation (4.33) shows that the general solution of the double-curl Beltrami (4.32) can be given by a linear combination of two curl operator eigenfunctions, such as

$$\boldsymbol{B} = a_+ \boldsymbol{G}_+ + a_- \boldsymbol{G}_-, \tag{4.35}$$

with $\boldsymbol{G}_{\pm}$ are the eigenfunctions of the operator $((curl - \lambda_{\pm})\,\boldsymbol{G}_{\pm} = 0)$ and $a_{\pm}$ are arbitrary constants.

Let us now use solution (4.35) along with the equilibrium equations (4.29) and (4.30) to define the corresponding flow field solution. This leads us to

$$\boldsymbol{V} = d_i a_+ \left(\lambda_+ - \mu_1\right) \boldsymbol{G}_+ + d_i a_- \left(\lambda_- - \mu_1\right) \boldsymbol{G}_-. \tag{4.36}$$

Now, we are in a position to construct the nonlinear wave solutions of the Hall MHD. Let us first setting one of the Beltrami eigenvalues to be zero, i.e., $\lambda_- = 0$ which implies that the corresponding eigenfunction $\boldsymbol{G}_- = \boldsymbol{G}_0$ constant (harmonic field). Then, equations (4.34), (4.35) and (4.36), become, respectively,

$$\left.\begin{aligned} \mu_1 &= -\mu_2 = \mu_{_H}, \\ \lambda_+ &= \lambda_{_H} = \mu_{_H} - \tfrac{1}{d_i^2 \mu_{_H}}, \end{aligned}\right\} \tag{4.37}$$

$$\boldsymbol{B} = a_0 \boldsymbol{G}_0 + a_{_H} \boldsymbol{G}_{_H}, \tag{4.38}$$

$$\boldsymbol{V} = -d_i a_0 \mu_{_H} \boldsymbol{G}_0 - \frac{a_{_H}}{d_i \mu_{_H}} \boldsymbol{G}_{_H}, \tag{4.39}$$

where the index H indicates the Hall MHD.

Considering that the harmonic field to be the ambient magnetic field, i.e., $\boldsymbol{G}_0 = \boldsymbol{B}_0 = \hat{z}$ in normalized units with $a_0 = 1$. Thus, we can look to the solutions (4.38) and (4.39) as consisting of an ambient component and wave component. Thence, those solutions can be rewritten as

$$\boldsymbol{B} \;=\; \hat{z} + \boldsymbol{b}, \qquad\qquad \boldsymbol{V} = -d_i\, \mu_{_H}\, \hat{z} + \boldsymbol{v}, \tag{4.40}$$

where

$$\boldsymbol{b} \;=\; -d_i \mu_{_H}\, \boldsymbol{v}. \tag{4.41}$$

It is important to note that equations (4.40) and (4.41) are representing the Beltrami stationary solutions satisfying

$$0 \;=\; \nabla \times (\boldsymbol{V} \times \boldsymbol{B}) - d_i \nabla \times \left(\rho^{-1} \left(\nabla \times \boldsymbol{B}\right) \times \boldsymbol{B}\right), \tag{4.42}$$

$$0 \;=\; \nabla \times [\boldsymbol{V} \times (\boldsymbol{B} + \boldsymbol{V})] + (1 - d_i)\, \nabla \times ((\nabla \times \boldsymbol{B}) \times \boldsymbol{B}), \tag{4.43}$$

Boosting the system under Galilean-transformation, which gives the coordinate of a point in the moving reference frame (moves with uniform velocity) as measured from the fixed frame, yields the new coordinates:

$$(x, y, z) \longmapsto (x, y, \xi) := (x, y, z + d_i\, \mu_{_H}\, t)\,.$$

where $t \mapsto \tau := t$ and $z \mapsto \xi := z + d_i\, \mu_{_H}\, t$. The transformations of derivatives with respect to the coordinates are

$$\nabla_{x,y,z} \mapsto \widetilde{\nabla}_{x,y,\xi}, \qquad\qquad \frac{\partial}{\partial t} \mapsto \frac{\partial}{\partial \tau} + d_i\, \mu_{_H}\, \frac{\partial}{\partial \xi}$$

where for 3-vector $\boldsymbol{X}$ (with $\nabla \cdot \boldsymbol{X} = 0$),

$$-\mu_{_H} \frac{\partial \boldsymbol{X}}{\partial \xi} = \nabla \times (\mu_{_H} \hat{z} \times \boldsymbol{X}),$$

is true. Upon using (4.40), we can boost the equilibrium system (4.42) and (4.43) in to

$$\frac{\partial \boldsymbol{b}}{\partial \tau} = \widetilde{\nabla} \times [\left(\boldsymbol{v} - \widetilde{\nabla} \times \boldsymbol{b}\right) \times \boldsymbol{B}], \tag{4.44}$$

$$\frac{\partial \left(\boldsymbol{b} + \widetilde{\nabla} \times \boldsymbol{v}\right)}{\partial \tau} = \widetilde{\nabla} \times [\boldsymbol{v} \times \left(\boldsymbol{B} + \widetilde{\nabla} \times \boldsymbol{v}\right)] + (1 - d_i)\, \widetilde{\nabla} \times \left(\left(\widetilde{\nabla} \times \boldsymbol{b}\right) \times \boldsymbol{B}\right). \tag{4.45}$$

Hence, the stationary solutions appear to propagate along the direction of the ambient magnetic field as observed in the moving frame, which forms the exact nonlinear Alfvén waves solution of the incompressible Hall MHD. The waves propagate with phase velocity $d_i\, \mu_{_H}$, whilst the Beltrami eigenvalue $\lambda_{_H} = k$ in boosted frame is shown as a wave number. We use equation(4.37) to find an expression for $\mu_{_H}$. We end up with

$$\mu_{_{H\pm}} = \frac{k}{2} \pm \sqrt{\frac{k^2}{4} + \frac{1}{d_i^2}}. \tag{4.46}$$

Then, the nonlinear dispersion relation reads as

$$\omega_{_{H\pm}} = d_i k \left[\frac{k}{2} \pm \sqrt{\frac{k^2}{4} + \frac{1}{d_i^2}}\right], \tag{4.47}$$

In Fig. 4.2 the dispersion relation (4.47) is plotted for $d_i = 1$. The positive branch ($\omega_{_{H+}}$) represents by red line (top) corresponding to the *whistler* mode, whilst the negative branch ($\omega_{_{H-}}$) represents by blue line (bottom) corresponding to the shear ion cyclotron waves, which saturates to the ion cyclotron frequency.

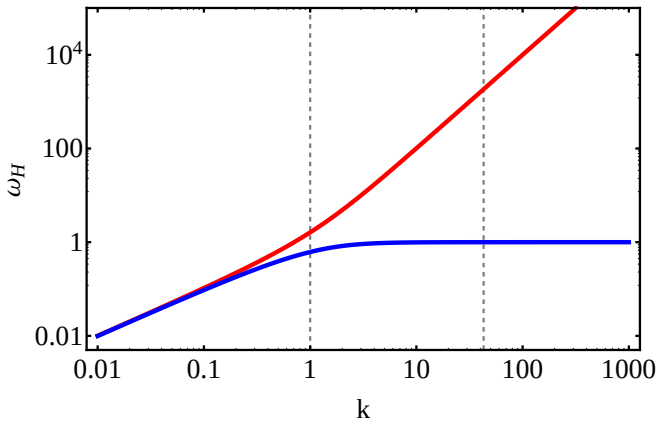

Figure 4.2: Hall MHD dispersion relation profile for $d_i = 1$. The two vertical dashed lines separate the ideal, Hall and electron inertia regimes respectively (when viewed from left to right).

4.3.3 Nonlinear Alfvén waves in extended MHD

Now we will proceed to extend our analysis to generalized MHD. We will follow the method described in Sec. 4.3.2. In this section, we seek to study the effect of the inclusion of the electron inertia on the propagation of waves. To focus on the electron inertia effect and for sake of simplicity, we start by changing the normalization of the extended MHD equations given in Sec. 3.1.2, in which the magnetic field is normalized to the ambient filed B_0, the velocity to the Alfvén speed ($V_A = B_0/\sqrt{\mu_0\rho_0}$), time to the ion gyroperiod ω_{ci}^{-1}, and the space variables to the ion skin depth d_i. After some manipulations the extended MHD equations in the new normalized variables are comprise of

$$\begin{aligned} \frac{\partial \rho}{\partial t} &= -\nabla \cdot (\rho \boldsymbol{V}), \\ \frac{\partial \boldsymbol{V}}{\partial t} &= -(\nabla \times \boldsymbol{V}) \times \boldsymbol{V} + \rho^{-1} (\nabla \times \boldsymbol{B}) \times \boldsymbol{B}^* \end{aligned} \tag{4.48}$$

$$- \nabla \left(h + V^2/2 + d_e^2 \left(\nabla \times \boldsymbol{B} \right)^2 / 2\rho^2 \right), \tag{4.49}$$

$$\frac{\partial \boldsymbol{B}^*}{\partial t} = \nabla \times \left(\boldsymbol{V} \times \mathbf{B}^* \right) - \nabla \times \left(\rho^{-1} \left(\nabla \times \boldsymbol{B} \right) \times \boldsymbol{B}^* \right) + d_e^2 \nabla \times \left(\rho^{-1} \left(\nabla \times \boldsymbol{B} \right) \times \left(\nabla \times \boldsymbol{V} \right) \right), \tag{4.50}$$

where

$$\boldsymbol{B}^* = \boldsymbol{B} + d_e^2 \nabla \times \rho^{-1} \left(\nabla \times \boldsymbol{B} \right), \tag{4.51}$$

As shown in Sec. 3.4, the extended MHD has six helicities. Here we choose three helicities to build the equilibrium. It should be noted here that, any combinations of the helicities yield the same equilibrium (We should use at least three different helicities; one for each fluid (electrons and ions) and the conservation of mass). The extended MHD invariants are

$$C_1 = \int_\Omega \boldsymbol{B}^* \cdot \left(\boldsymbol{V} - \frac{1}{2d_e^2} \boldsymbol{A}^* \right) d^3x, \tag{4.52}$$

$$C_2 = \frac{1}{2} \int_\Omega \left[\boldsymbol{B}^* \cdot \boldsymbol{A}^* + d_e^2 \boldsymbol{V} \cdot \left(\nabla \times \boldsymbol{V} \right) \right] d^3x, \tag{4.53}$$

$$C_3 = \int_\Omega \rho \, d^3x, \tag{4.54}$$

with the total energy

$$\mathscr{H} = \int_\Omega \left\{ \rho \left(\frac{|\boldsymbol{V}|^2}{2} + U\left(\rho\right) \right) + \frac{\boldsymbol{B} \cdot \boldsymbol{B}^*}{2} \right\} d^3x. \tag{4.55}$$

4.3.3.1 Beltrami equilibria

To construct the Beltrami equilibria, we start from the energy-Casimir functional of the extended MHD system, which reads as

$$\mathscr{H}_\mu \left(u \right) = \mathscr{H} \left(u \right) - \sum_{n=1}^{3} \mu_n C_n \left(u \right). \tag{4.56}$$

The critical points on the Casimir leaves are found by setting $\partial_u \mathscr{H}_\mu = 0$ which yields

$$\nabla \times \boldsymbol{B} = \mu_1 \nabla \times \boldsymbol{V} + \left(\mu_2 - \frac{\mu_1}{d_e^2}\right) \boldsymbol{B}^*, \tag{4.57}$$

$$\rho \boldsymbol{V} = \mu_1 \boldsymbol{B}^* + \mu_2 d_e^2 \nabla \times \boldsymbol{V}, \tag{4.58}$$

$$\frac{V^2}{2} + h(\rho) + d_e^2 \frac{(\nabla \times \boldsymbol{B})^2}{2\rho^2} - \mu_3 = 0, \tag{4.59}$$

where μ_1, μ_2 and μ_3 are Lagrange multipliers. Notice that (4.59) is Bernoulli's equation. Now, consider the incompressible flow ($\nabla \cdot \boldsymbol{V} = 0$) with a constant mass density $\rho = 1$. Then, combining (4.57) and (4.58) with the aid of (4.51), we get the triple curl Beltrami equation,

$$\nabla \times \nabla \times \nabla \times \boldsymbol{B} - \eta_1 \nabla \times \nabla \times \boldsymbol{B} + \eta_2 \nabla \times \boldsymbol{B} - \eta_3 \boldsymbol{B} = 0, \tag{4.60}$$

where

$$\begin{aligned}
\eta_1 &= \left(2 - \frac{\mu_1}{d_e^2 \mu_2}\right) / \Delta, \\
\eta_2 &= \left(\mu_2 + \frac{1}{d_e^2 \mu_2} - \frac{\mu_1}{d_e^2}\left(1 + \frac{\mu_1}{\mu_2}\right)\right) / \Delta, \\
\eta_3 &= \left(1 - \frac{\mu_1}{d_e^2 \mu_2}\right) / \left(d_e^2 \Delta\right), \\
\Delta &= d_e^2 \left[\mu_2 - \frac{\mu_1}{d_e^2}\left(1 + \frac{\mu_1}{\mu_2}\right)\right].
\end{aligned}$$

The general solution of (4.60) can be expressed in terms of a single Beltrami fields $\boldsymbol{G}_l$ $(l = 0, 1, 2)$, such that

$$\begin{aligned}
(curl - \lambda_l)\, \boldsymbol{G}_l &= 0 \qquad (in \ \ \Omega), \\
\boldsymbol{n} \cdot \boldsymbol{G}_l &= 0 \qquad (on \ \ \Omega)
\end{aligned}$$

for more details see Refs. [100, 180]. Then, (4.60) can be written as

$$(curl - \lambda_0)(curl - \lambda_1)(curl - \lambda_2)\boldsymbol{B} = 0, \tag{4.61}$$

where the eigenvalues λ_0, λ_1 and λ_2 are given by

$$\left.\begin{aligned} \lambda_0 + \lambda_1 + \lambda_2 &= \eta_1, \\ \lambda_0\lambda_1 + \lambda_1\lambda_2 + \lambda_2\lambda_0 &= \eta_2, \\ \lambda_0\lambda_1\lambda_2 &= \eta_3. \end{aligned}\right\} \tag{4.62}$$

Now constructing the general solution, which is the linear combination of three eigenfunctions given as,

$$\boldsymbol{B} = a_0\boldsymbol{G}_0 + a_1\boldsymbol{G}_1 + a_2\boldsymbol{G}_2, \tag{4.63}$$

where a_l's are arbitrary constants. Substituting in (4.57) and (4.58), the corresponding flow is given by

$$\begin{aligned} \boldsymbol{V} &= \left[\sigma\left(1 + d_e^2\lambda_0^2\right) + \frac{d_e^2\mu_2}{\mu_1}\lambda_0\right] a_0\boldsymbol{G}_0 \\ &+ \left[\sigma\left(1 + d_e^2\lambda_1^2\right) + \frac{d_e^2\mu_2}{\mu_1}\lambda_1\right] a_1\boldsymbol{G}_1 \\ &+ \left[\sigma\left(1 + d_e^2\lambda_2^2\right) + \frac{d_e^2\mu_2}{\mu_1}\lambda_2\right] a_2\boldsymbol{G}_2, \end{aligned} \tag{4.64}$$

where $\sigma = \mu_1 + \mu_2\left(1 - \frac{d_e^2\mu_2}{\mu_1}\right)$.

Now, setting one of the Beltrami eigenvalues equal to zero ($\lambda_0 = 0$)(which implies that the corresponding eigenfunction is a harmonic field), yields a special class of Beltrami solutions, see Ref. [176]. Letting $\lambda_0 = 0$, three consequences immediately follow from (4.62),

$$\left.\begin{aligned} \mu_1 = d_e^2\mu_2 &= \mu, \\ \lambda_1 + \lambda_2 &= \eta_1, \\ \lambda_1\lambda_2 &= \eta_2. \end{aligned}\right\} \tag{4.65}$$

Now, solving (4.65) yields

$$\lambda_{\pm} = \frac{1}{2\mu d_e^2}\left[-1 \pm \sqrt{1 - 4d_e^2\left(\mu^2 - 1\right)}\right], \tag{4.66}$$

where we chose $\lambda_+ = \lambda_1$ and $\lambda_- = \lambda_2$. Under this conditions the general flow solution becomes

$$\boldsymbol{V} = \mu a_0 \boldsymbol{G}_0 + \frac{1}{\mu}\left(a_1 \boldsymbol{G}_1 + a_2 \boldsymbol{G}_2\right). \tag{4.67}$$

Based on the geometry ($xyz-plane/space$), the eigenfunctions $\boldsymbol{G}_1$ and $\boldsymbol{G}_2$ are naturally sinusoidal functions. To satisfy the single Beltrami condition, the eigenfunctions are given in the form of a circularly polarized wave;

$$\boldsymbol{G}_1 = \begin{pmatrix} \sin\left(\lambda_1 z\right) \\ \cos\left(\lambda_1 z\right) \\ 0 \end{pmatrix}, \qquad \boldsymbol{G}_2 = \begin{pmatrix} \sin\left(\lambda_2 z\right) \\ \cos\left(\lambda_2 z\right) \\ 0 \end{pmatrix}.$$

An immediate generalization to a more complex Beltrami field, so called ABC flow is possible [cf. [97]]. These $\boldsymbol{V}$ and $\boldsymbol{B}$ have oscillatory amplitudes, thus the Bernoulli condition (4.59) demands a non-constant $h\left(\rho\right)$. We assume that the sound velocity is sufficiently large so that ρ may be assumed to be constant and consistent to (4.60). On the other hand, Beltrami solutions (4.63) and (4.67) imply that the magnetic field and the flow velocity are not necessarily aligned, unless $\mu = \pm 1$. Additionally, we observe that the solutions are expressed as a combination of three Beltrami eigenfunctions $\boldsymbol{G}_l$, in which two of them have a large scale (compared with the electron skin depth d_e), whereas the third is in scale hierarchy of d_e. Since in the Hall MHD limit $d_e \to 0$, one of the eigenvalues ($\lambda_+ \to \left(1 - \mu^2\right)/\mu$) is finite, whilst the other ($\lambda_- \to -\infty$) is singular and therefore the corresponding eigenstate $\boldsymbol{G}_2$ is divergent; see Figs. 4.3. This singularity can be

removed by setting the arbitrary constant (a_2) associated with the divergent eigenstate ($\boldsymbol{G}_2$) to zero.

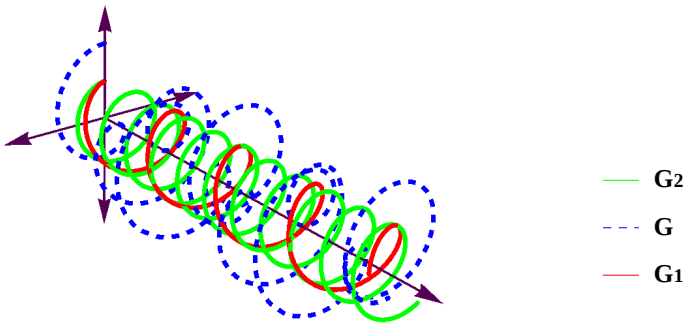

(a)

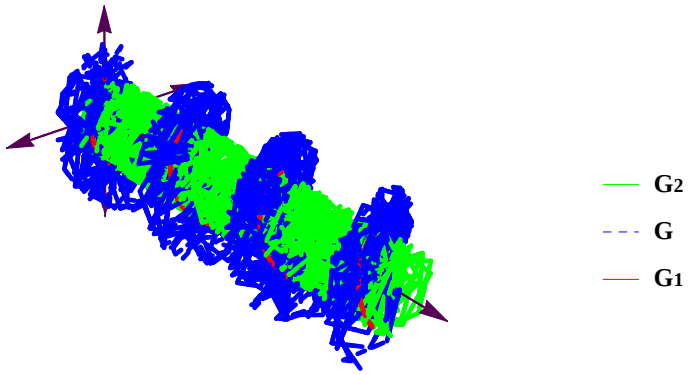

(b)

Figure 4.3: The profiles of the eigenfunctions $\boldsymbol{G}_1$, $\boldsymbol{G}_2$ and their superposition $\boldsymbol{G} = a_1\boldsymbol{G}_1 + a_2\boldsymbol{G}_2$ for $\mu = 2$, $a_1 = a_2 = 1$; (a) $d_e = 0.26$ and (b) $d_e = 10^{-8}$.

4.3.3.2 Exact wave solutions of the extended MHD

To examine the propagation of the wave component, we assume that $\boldsymbol{G}_0$ serve as an ambient field. Now, setting $\boldsymbol{G}_0 = \hat{z}$ and $a_0 = 1$, ($\boldsymbol{G}_0$ represents the normalized ambient magnetic field). From (4.67) the corresponding ambient flow is $\boldsymbol{V}_0 = \mu\ \hat{z}$. The magnetic and flow fields become

$$\boldsymbol{B} \;=\; \boldsymbol{b} + \hat{z}, \qquad\qquad \boldsymbol{V} = \boldsymbol{v} + \mu\hat{z}, \tag{4.68}$$

where

$$\boldsymbol{b} \;=\; \mu\boldsymbol{v}. \tag{4.69}$$

Let us show explicitly that the Beltrami solution (4.68)-(4.69) can be modified to wave solution by boosting the coordinate. The Beltrami solution is the stationary solution satisfying

$$0 = \nabla \times [\,(\boldsymbol{V} - \nabla \times \boldsymbol{B}) \times \boldsymbol{B}^*], \tag{4.70}$$

$$0 = \nabla \times [\boldsymbol{V} \times (\boldsymbol{B}^* + \nabla \times \boldsymbol{V})\,], \tag{4.71}$$

$$\nabla \cdot \boldsymbol{V} = 0, \tag{4.72}$$

$$\nabla \cdot \boldsymbol{B} = 0, \qquad\qquad \nabla \cdot \boldsymbol{B}^* = 0. \tag{4.73}$$

Transforming the system under Galilean-boost yields the new coordinates:

$$(x, y, z) \longmapsto (x, y, \xi) := (x, y, z - \mu t)\,.$$

where $t \mapsto \tau := t$ and $z \mapsto \xi := z - \mu t$. The transformations of derivatives with respect to the coordinates are

$$\nabla_{x,y,z} \mapsto \widetilde{\nabla}_{x,y,\xi}, \qquad \frac{\partial}{\partial t} \mapsto \frac{\partial}{\partial \tau} - \mu \frac{\partial}{\partial \xi}$$

where for 3-vector $\boldsymbol{X}$ (with $\nabla \cdot \boldsymbol{X} = 0$), $-\mu \frac{\partial \boldsymbol{X}}{\partial \xi} = \nabla \times (\mu \hat{z} \times \boldsymbol{X})$ is true. Using (4.68), equations (4.70) and (4.71) can be boosted in the new coordinates into

$$\frac{\partial \boldsymbol{B}^*}{\partial \tau} = \widetilde{\nabla} \times \Big[\Big(\boldsymbol{v} - \widetilde{\nabla} \times \boldsymbol{B} \Big) \times \boldsymbol{B}^* \Big], \tag{4.74}$$

$$\frac{\partial \Big(\boldsymbol{B}^* + \widetilde{\nabla} \times \boldsymbol{v} \Big)}{\partial \tau} = \widetilde{\nabla} \times \Big[\boldsymbol{v} \times \Big(\boldsymbol{B}^* + \widetilde{\nabla} \times \boldsymbol{v} \Big) \Big], \tag{4.75}$$

which are the Alfvén wave equations with a homogeneous ambient field $\boldsymbol{B}_0 = \hat{z}$. Thence, on the boosted frame, the fluctuating parts of the previous stationary solution appears as propagating waves, which forms an exact solution of the incompressible extended MHD equations. Here, we notice that the wave components are a superposition of two Beltrami eigenfunctions, which implies that only a definite wave functions (sinusoidal functions), can propagate with fixed shape. Further, the phase velocity here is given by μ, which from (4.65) may be written as

$$\mu_\pm = \frac{1}{(1 + d_e^2 k^2)} \left[-\frac{k}{2} \pm \sqrt{\frac{k^2}{4} + (1 + d_e^2 k^2)} \right], \tag{4.76}$$

where the eigenvalue $k := \lambda_1$ or λ_2, serves as the wave number. Then, the corresponding circularly polarized wave dispersion relation ($\omega = -\mu \, (\hat{z} \cdot \boldsymbol{k})$), which in the case $\boldsymbol{k} = k \, \hat{z}$ reads as

$$\omega_\pm = \frac{-k}{(1 + d_e^2 k^2)} \left[-\frac{k}{2} \pm \sqrt{\frac{k^2}{4} + (1 + d_e^2 k^2)} \right]. \tag{4.77}$$

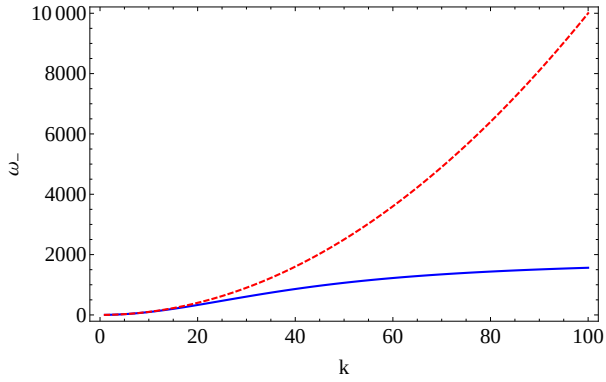

(a)

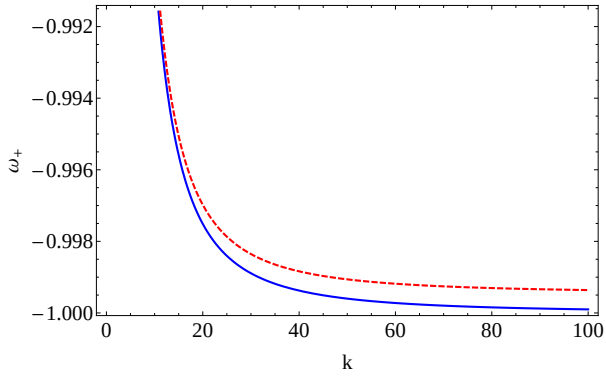

(b)

Figure 4.4: Normalized dispersion relation profiles for $d_e = 0$ (dashed-red) and $d_e = 0.0233$ (blue); (a) (ω_-) and (b) (ω_+) .

which represents the dispersion relation of the fully nonlinear wave solutions. In the limit $(d_e \to 0)$, (4.77) is reduced to the dispersion relation of exact solution of Hall MHD [97, 176]. We also observe that the inclusion of the electron inertia effect not only modifies waves modes, remove the singularities associated with the exact solution of Hall MHD, but also captured more of the physics of the full two-fluid model; see Figs. 4.4.

On the limiting cases of the nonlinear waves We shall now investigate the various regimes of interest, and list the expressions for (4.76) and

(4.77) accordingly.

1. First, consider the limit $k \ll 1$, which in *dimensional* units is tantamount to stating that $kd_i \ll 1$. This indicates that we are operating in the ideal MHD domain, and we arrive at

$$\mu_{\pm} \to \pm 1, \qquad \omega_{\pm} \to \mp k \left(\widehat{\mathbf{e}}_{B_\circ} \cdot \widehat{\mathbf{e}}_z \right), \tag{4.78}$$

   which corresponds to the shear Alfvén waves of ideal MHD (that are co- and counter-propagating).

2. Next, consider the case where Hall effects are important, but electron inertia can still be neglected, i.e. the Hall regime. In this instance, the conditions (in the dimensionless units) are given by $k > 1$ and $d_e^2 k^2 \ll 1$. The dispersion relations reduce to

$$\begin{aligned} \mu_+ &\to 1/k, \qquad & \omega_+ &\to -1 \left(\widehat{\mathbf{e}}_{B_\circ} \cdot \widehat{\mathbf{e}}_z \right), \\ \mu_- &\to -k, \qquad & \omega_- &\to k^2 \left(\widehat{\mathbf{e}}_{B_\circ} \cdot \widehat{\mathbf{e}}_z \right), \end{aligned} \tag{4.79}$$

   implying that ω_+ is the magnetosonic-cyclotron branch since ω_+ is the ion gyrofrequency. On the other hand, ω_- is the shear-whistler mode, as seen from the dispersion relation.

   We record important features of the Hall regime before moving on to the next case. As opposed to the ideal MHD regime, or the electron inertia one (discussed below), the Hall regime is bounded strictly from below *and* above. As a consequence, the range is somewhat 'narrow' and care must be taken when investigating it in greater detail. Secondly, it may appear as though the whistler mode ω_- is unbounded

as it is proportional to k^2. However, this is incorrect since we have implicitly assumed that the inequality $d_e^2 k^2 \ll 1$ is applicable. In turn, this suggests that the whistler mode is rendered invalid when considering frequencies higher than the electron gyrofrequency.

3. The third regime of interest is when electron inertia effects become important, even dominant. This regime requires that the conditions $k \gg 1$ and $d_e^2 k^2 \gg 1$ be met. In this instance, we find that

$$\mu_\pm \to \theta_\pm / k, \qquad \omega_\pm \to -\theta_\pm \left(\widehat{\mathbf{e}}_{B_\circ} \cdot \widehat{\mathbf{e}}_z \right), \tag{4.80}$$

where $\theta_\pm = \left(-1 \pm \sqrt{1 + 4d_e^2} \right) / 2d_e^2$. By substituting the relation $d_e^2 \ll 1$, in terms of the normalized variables, into the expression for $\theta_\pm$, we note that θ_- approximates the normalized electron gyrofrequency, whilst θ_+ approximates the normalized ion gyrofrequency. It is important to recognize that $\theta_\pm$ depends on the dimensionless electron skin depth, and thereby gives rise to a direct relationship between the electron skin depth and $\omega_\pm$, i.e. the ion or electron gyrofrequency (for θ_+ and θ_- respectively).

Thus, the magnetosonic-cyclotron branch in the electron inertia regime approaches the same limit as its Hall counterpart; this is seen by comparing the expressions for ω_+ in both cases. However, the dispersion relation for the whistler-mode branch in Hall MHD (given by ω_-), is such that it would diverge for $k \to \infty$. The role of electron inertia in this case is to impose a strict upper bound (viz. the electron gyrofrequency) on the frequency attainable by this whistler-mode.

Chapter 5

Nonlinear helicons

5.1 What is helicons?

Helicons (synonymously-called whistlers) are low frequency (compared with the electron cyclotron frequency) circularly polarized electromagnetic waves propagating along an ambient magnetic field. The word *helicon* was first used by Arigrain [5] in 1960 to describe low frequency electromagnetic waves that propagate along a strong applied magnetic field in a solid state plasmas. Helicons have variety of applications such as plasma sources [27,40,88,150], spacecraft propulsion [4,38,153,164] as well as in laboratory plasma experiments [157, 158]. The linear theory of helicon waves has been studied in great detail for a particular frequency range much lower than electron cyclotron frequency and much higher than the ion cyclotron frequency, in which the ions are considered immobile (see [28, 42, 43], and references therein). While early theory ignored electron mass, Boswell [26] found that finite electron inertia gives rise of a second quasi-electrostatic waves called Trivelpiece-Gould (TG) waves [167].

5.2 Linear theory

Consider a homogenous incompressible plasma in cylindrical geometry. If the ion motion is neglected, the extended MHD (see Sec. 3.2.1) will

reduced to

$$\frac{\partial \boldsymbol{B}^*}{\partial t} = -d_i \nabla \times ((\nabla \times \boldsymbol{B}) \times \boldsymbol{B}^*) \tag{5.1}$$

where

$$\boldsymbol{B}^* = \boldsymbol{B} + d_e^2 \nabla \times (\nabla \times \boldsymbol{B}) . \tag{5.2}$$

linearize (5.1) about the equilibrium $\boldsymbol{B}_0 = \hat{z}$ (in normalized units), as

$$\boldsymbol{B} = \hat{z} + \boldsymbol{b}. \tag{5.3}$$

The resultant equation is

$$-i\omega \left(\boldsymbol{b} + d_e^2 \nabla \times \nabla \times \boldsymbol{b} \right) = -d_i \nabla \times [(\nabla \times \boldsymbol{b}) \times \hat{z}] . \tag{5.4}$$

Note that, solutions of the form

$$\boldsymbol{F} = \boldsymbol{f}(r) \exp[i(m\theta + kz - \omega t)], \tag{5.5}$$

are considered.

Using vector identity the right hand side of the above equation can be written as

$$\nabla \times [(\nabla \times \boldsymbol{b}) \times \hat{z}] = ik \nabla \times \boldsymbol{b}. \tag{5.6}$$

Now, equation (5.4) can be rewritten as

$$d_e^2 \omega \nabla \times \nabla \times \boldsymbol{b} - d_i k \nabla \times \boldsymbol{b} + \omega \boldsymbol{b} = 0. \tag{5.7}$$

equation (5.7) can be factored as

$$(curl - \beta_1) (curl - \beta_2) \boldsymbol{b} = 0, \tag{5.8}$$

where the eigenvalues β_1 and β_2 are given by

$$\left.\begin{aligned} \beta_1 + \beta_2 &= \tfrac{d_i k}{d_e^2 \omega}, \\ \beta_1 \beta_2 &= \tfrac{1}{d_e^2}. \end{aligned}\right\} \tag{5.9}$$

The general solution of (5.8) is therefore the sum of the solutions of

$$\nabla \times \boldsymbol{b} = \beta_1 \boldsymbol{b}, \tag{5.10}$$

$$\nabla \times \boldsymbol{b} = \beta_2 \boldsymbol{b}. \tag{5.11}$$

where

$$\beta_{1,2} = \frac{d_i k}{2 d_e^2 \omega} \left[1 \mp \sqrt{1 - 4 \frac{d_e^2 \omega^2}{d_i^2 k^2}} \right], \tag{5.12}$$

which is obtained by solving equations (5.9) for β. It is worth here remarking that the root β_1 with $(-)$ sign represents helicon mode, whilst β_2 with $(+)$ represents TG mode.

5.2.1 Beltrami field in cylindrical geometry

Our problem now is turned to solve the single Beltrami field

$$(curl - \beta)\, \boldsymbol{G} = 0 \qquad (in \;\; \Omega), \tag{5.13}$$

$$\boldsymbol{n} \cdot \boldsymbol{G} = 0 \qquad (on \;\; \Omega), \tag{5.14}$$

where $\boldsymbol{G}$ is a solenoidal vector field.

Taking the *curl* of (5.13), using the vector calculus identity, and invoking (5.14), we obtain the vector Helmholtz equation

$$\nabla^2 \boldsymbol{G} + \beta^2 \boldsymbol{G} = 0. \tag{5.15}$$

To solve the vector Helmholtz equation we use the tricky method introduced by Hansen [64], in which the vector field $\boldsymbol{G}$ could be written as a linear combination of three fields,

$$\boldsymbol{L} = \nabla\psi, \tag{5.16}$$

$$\boldsymbol{T} = \nabla \times (\psi \boldsymbol{a}), \tag{5.17}$$

$$\boldsymbol{S} = \nabla \times \nabla \times (\psi \boldsymbol{a}), \tag{5.18}$$

where $\boldsymbol{a}$ is either a position vector or a constant unit vector and ψ is a scalar function satisfied the scalar Helmholtz equation

$$\nabla^2\psi + \beta^2\psi = 0. \tag{5.19}$$

Then the general solution of equation (5.15) is

$$\boldsymbol{G} = c_1\boldsymbol{L} + c_2\boldsymbol{T} + c_3\boldsymbol{S}. \tag{5.20}$$

where c's are arbitrary constant.

Before proceeding further, we want to notice that, it is not necessary that every solution of equation (5.15) to be a solution of equation (5.13), however, the reverse is true. To ensure that the general solution (5.20) is also a solution of (5.13) we need to subject it to the constraint given by (5.14) which implies that the vector field is solenoidal ($\nabla \cdot \boldsymbol{G}$). Looking to (5.16)-(5.18) we can observe that the term $\boldsymbol{L}$ does not contribute to the vector field $\boldsymbol{G}$ since the curl of $\boldsymbol{L}$ vanishes ($\nabla \times \boldsymbol{L} = 0$). Then, (5.20) becomes

$$\boldsymbol{G} = c_2\boldsymbol{T} + c_3\boldsymbol{S}. \tag{5.21}$$

Substituting (5.21) into the single Beltrami (5.13) yields

$$\begin{aligned} \nabla \times \boldsymbol{G} &= \beta \boldsymbol{G}, \\ c_2 \nabla \times \nabla \times \psi \boldsymbol{a} + c_3 \nabla \times \nabla \times \nabla \times \psi \boldsymbol{a} &= \beta c_2 \nabla \times \psi \boldsymbol{a} + \beta c_3 \nabla \times \nabla \times \psi \boldsymbol{a}, \\ c_2 \nabla \times \nabla \times \psi \boldsymbol{a} + \beta^2 c_3 \nabla \times \psi \boldsymbol{a} &= \beta c_2 \nabla \times \psi \boldsymbol{a} + \beta c_3 \nabla \times \nabla \times \psi \boldsymbol{a}, \end{aligned} \tag{5.22}$$

which implies $c_2 = \lambda c_3 = 1$. Therefore, the general solution of (5.13) is

$$\boldsymbol{G} = \beta \nabla \times \psi \boldsymbol{a} + \nabla \times \nabla \times \psi \boldsymbol{a}. \tag{5.23}$$

In cylindrical coordinates, the above form of the solution is often known as the Chandrasekhar-Kendall eigenfunctions, although they did not provide the explicit form of the solution in [37]. The completeness of the Chandrasekhar-Kendall eigenfunctions was investigated in [175]. The solutions to the Helmholtz equation (5.19) in cylindrical coordinates (r, θ, z) is

$$\boldsymbol{G} = \beta \nabla \psi \times \hat{z} + \nabla \times (\nabla \psi \times \hat{z}), \tag{5.24}$$

with

$$\psi = J_m(\gamma r)\, e^{i(m\theta + kz)}, \tag{5.25}$$

where J_m serves the Bessel function of the first kind of order m and $\gamma^2 = \beta^2 - k^2$ (γ here serve as a transverse wave number). Note that we here consider only the choice of $\boldsymbol{a} = \hat{z}$. Then,

$$\boldsymbol{L} = \nabla \psi,$$

$$= \left[\frac{\partial}{\partial r}\left(J_m\left(\gamma r\right)\right)\hat{r} + \frac{im}{r}J_m\left(\gamma r\right)\hat{\theta} + ikJ_m\left(\gamma r\right)\hat{z}\right]e^{i(m\theta+kz)}, \quad (5.26)$$

$$\boldsymbol{T} = \nabla\psi \times \hat{z},$$

$$= \left[\frac{im}{r}J_m\left(\gamma r\right)\hat{r} - \frac{\partial}{\partial r}\left(J_m\left(\gamma r\right)\right)\hat{\theta}\right]e^{i(m\theta+kz)}, \quad (5.27)$$

$$\boldsymbol{S} = \nabla \times \left(\nabla\psi \times \hat{z}\right),$$

$$= \left[ik\frac{\partial}{\partial r}\left(J_m\left(\gamma r\right)\right)\hat{r} - \frac{mk}{r}J_m\left(\gamma r\right)\hat{\theta} + \gamma^2 J_m\left(\gamma r\right)\hat{z}\right]e^{i(m\theta+kz)} \quad (5.28)$$

Therefore, the general solution (5.24) becomes

$$\begin{aligned}\boldsymbol{G} = &\left\{\left[\lambda\frac{im}{r}J_m\left(\gamma r\right) + ik\frac{\partial}{\partial r}\left(J_m\left(\gamma r\right)\right)\right]\hat{r}\right.\\ &-\left[\frac{mk}{r}J_m\left(\gamma r\right) + \lambda\frac{\partial}{\partial r}\left(J_m\left(\gamma r\right)\right)\right]\hat{\theta}\\ &\left.+\gamma^2 J_m\left(\gamma r\right)\hat{z}\right\}e^{i(m\theta+kz)}. \quad (5.29)\end{aligned}$$

Then the components of the general solution of equation (5.8) are

$$\begin{aligned}b_r(r) = &\left(\frac{iA_1}{\gamma_1^2}\right)\left[\frac{m\beta_1}{r}J_m(\gamma_1 r) + k\frac{\partial J_m(\gamma_1 r)}{\partial r}\right]\\ &+\left(\frac{iA_2}{\gamma_2^2}\right)\left[\frac{m\beta_2}{r}J_m(\gamma_2 r) + k\frac{\partial J_m(\gamma_2 r)}{\partial r}\right], \quad (5.30)\end{aligned}$$

$$\begin{aligned}b_\theta(r) = &-\left(\frac{A_1}{\gamma_1^2}\right)\left[\frac{mk}{r}J_m(\gamma_1 r) + \beta_1\frac{\partial J_m(\gamma_1 r)}{\partial r}\right]\\ &-\left(\frac{A_2}{\gamma_2^2}\right)\left[\frac{mk}{r}J_m(\gamma_2 r) + \beta_2\frac{\partial J_m(\gamma_2 r)}{\partial r}\right], \quad (5.31)\end{aligned}$$

$$b_z\left(r\right) = A_1 J_m\left(\gamma_1 r\right) + A_2 J_m\left(\gamma_2 r\right) \quad (5.32)$$

where A_1 and A_2 are the arbitrary constants, which serve here as wave amplitudes.

Before concluding this part, we point out that different boundary conditions and the corresponding dispersion relation will be discussed in Sec. 5.3.5.

5.2.2 Verification of solutions

The above solution has to verify two equations; the first one is the divergence free condition ($\nabla \cdot \boldsymbol{B} = 0$) and the second one is the double Beltrami equation (5.7). Since the general solution of (5.7) is a linear combination of the eigenfunctions of a single Beltrami equation, so we need only to verify the solution of a single Beltrami equation ($\nabla \times \boldsymbol{b} = \beta \boldsymbol{b}$). The solution has the form

$$\begin{aligned}\boldsymbol{b} = \Bigg\{ & \left(\frac{iA}{\gamma^2}\right)\left[\frac{m\beta}{r}J_m(\gamma r) + k\frac{\partial J_m(\gamma r)}{\partial r}\right]\hat{r} \\ & -\left(\frac{A}{\gamma^2}\right)\left[\frac{mk}{r}J_m(\gamma r) + \beta\frac{\partial J_m(\gamma r)}{\partial r}\right]\hat{\theta} \\ & +AJ_m(\gamma r)\,\hat{z}\Bigg\} e^{i(m\theta+kz-\omega t)}. \end{aligned} \tag{5.33}$$

$$\begin{aligned}\nabla \cdot \boldsymbol{b} &= \frac{\partial b_r}{\partial r} + \frac{b_r}{r} + \frac{1}{r}\frac{\partial b_\theta}{\partial \theta} + \frac{\partial b_z}{\partial z} \\ &= -\frac{m\beta}{r^2}J_m(\gamma r) + \frac{m\beta}{r}\frac{\partial}{\partial r}J_m(\gamma r) + k\frac{\partial^2}{\partial r^2}J_m(\gamma r) + \frac{m\beta}{r^2}J_m(\gamma r) \\ &\quad + \frac{k}{r}\frac{\partial}{\partial r}J_m(\gamma r) - \frac{m^2 k\beta}{r^2}J_m(\gamma r) - \frac{m\beta}{r}\frac{\partial}{\partial r}J_m(\gamma r) + k\gamma^2 J_m(\gamma r) \\ &= 0. \end{aligned} \tag{5.34}$$

$$\begin{aligned}\nabla \times \boldsymbol{b} &= \left[\frac{1}{r}\frac{\partial b_z}{\partial \theta} + \frac{\partial b_\theta}{\partial z}\right]\hat{r} + \left[\frac{\partial b_r}{\partial z} - \frac{\partial b_z}{\partial r}\right]\hat{\theta} + \left[\frac{1}{r}\frac{\partial (r b_\theta)}{\partial r} - \frac{1}{r}\frac{\partial b_r}{\partial \theta}\right]\hat{z} \\ &= \left\{\frac{imA}{r}J_m(\gamma r) + \left(\frac{ikA}{\gamma^2}\right)\left[\frac{mk}{r}J_m(\gamma r) + \beta\frac{\partial J_m(\gamma r)}{\partial r}\right]\right\}\hat{r} \\ &- \left\{\left(\frac{kA}{\gamma^2}\right)\left[\frac{m\beta}{r}J_m(\gamma r) + k\frac{\partial J_m(\gamma r)}{\partial r}\right] - A\frac{\partial J_m(\gamma r)}{\partial r}\right\}\hat{\theta} \\ &+ \left\{\left(\frac{A}{\gamma^2}\right)\left[\frac{m^2\beta}{r^2}J_m(\gamma r) + \frac{mk}{r}\frac{\partial J_m(\gamma r)}{\partial r}\right]\right. \\ &\quad \left. -\left(\frac{A}{\gamma^2}\right)\left[\frac{mk}{r}\frac{\partial J_m(\gamma r)}{\partial r} - \frac{mk}{r^2}J_m(\gamma r) + \beta\frac{\partial^2 J_m(\gamma r)}{\partial r^2}\right]\right. \end{aligned}$$

$$
\begin{aligned}
& -\left(\frac{A}{\gamma^2}\right)\left[\frac{mk}{r^2}J_m(\gamma r)+\frac{\beta}{r}\frac{\partial J_m(\gamma r)}{\partial r}\right]\Bigg\}\hat{z} \\
= \; & \beta\Bigg\{\left(\frac{iA}{\gamma^2}\right)\left[\frac{m\beta}{r}J_m(\gamma r)+k\frac{\partial J_m(\gamma r)}{\partial r}\right]\hat{r} \\
& -\left(\frac{A}{\gamma^2}\right)\left[\frac{mk}{r}J_m(\gamma r)+\beta\frac{\partial J_m(\gamma r)}{\partial r}\right]\hat{\theta} \\
& +A\; J_m\left(\gamma r\right)\hat{z}\Bigg\}e^{i(m\theta+kz-\omega t)} \\
= \; & \beta\boldsymbol{b}. \qquad (5.35)
\end{aligned}
$$

5.3 Nonlinear theory

5.3.1 Incompressible extended MHD

The equations of extended MHD (see Sec. 3.2.1) after some algebraic manipulations can be cast in the incompressible limit into the following form:

$$
\begin{aligned}
\frac{\partial \boldsymbol{B}^*}{\partial t} &= \nabla\times\left[(\boldsymbol{V}-d_i\nabla\times\boldsymbol{B})\times\boldsymbol{B}^*\right] \\
&\quad +d_e^2\nabla\times\left((\nabla\times\boldsymbol{B})\times(\nabla\times\boldsymbol{V})\right), \qquad (5.36)
\end{aligned}
$$

$$
\begin{aligned}
\frac{\partial\left(\boldsymbol{B}^*+\nabla\times\boldsymbol{V}\right)}{\partial t} &= \nabla\times\left[\boldsymbol{V}\times\left(\boldsymbol{B}^*+\nabla\times\boldsymbol{V}\right)+\left(1-d_i\right)(\nabla\times\boldsymbol{B})\times\boldsymbol{B}^*\right] \\
&\quad +d_e^2\nabla\times\left((\nabla\times\boldsymbol{B})\times(\nabla\times\boldsymbol{V})\right), \qquad (5.37)
\end{aligned}
$$

where

$$
\boldsymbol{B}^*=\boldsymbol{B}+d_e^2\nabla\times\rho^{-1}\left(\nabla\times\boldsymbol{B}\right). \qquad (5.38)
$$

The extended MHD system is endowed with a Hamiltonian structure [1]. On the phase space of state variables $u=(\boldsymbol{V},\boldsymbol{B}^*)$, we can define a Poisson bracket, which has two independent Casimir invariants (existence of Casimir

invariants make the Poisson bracket *noncanonical*):

$$C_1 = \frac{1}{2}\int_\Omega \left(\boldsymbol{A}^* - \frac{2d_e^2}{d_i}\boldsymbol{V}\right)\cdot\boldsymbol{B}^* d^3x, \tag{5.39}$$

$$C_2 = \frac{1}{2}\int_\Omega \Big[(\boldsymbol{A}^* + d_i\boldsymbol{V})\cdot(\boldsymbol{B}^* + d_i\nabla\times\boldsymbol{V}) + d_e^2\boldsymbol{V}\cdot(\nabla\times\boldsymbol{V})\Big] d^3x, \tag{5.40}$$

The energy is given by

$$E = \int_\Omega \left\{\frac{|\boldsymbol{V}|^2}{2} + \frac{\boldsymbol{B}\cdot\boldsymbol{B}^*}{2}\right\} d^3x. \tag{5.41}$$

Writing E in terms of u gives the Hamiltonian.

5.3.2 Beltrami equilibria

Now we follow the method described in Sec. 4.3.3. We first construct energy-Casimir equilibrium by extremizing

$$\mathscr{E}_\mu(u) = E(u) - \sum_{n=1}^{2}\mu_n C_n(u). \tag{5.42}$$

The Euler-Lagrange equation $\partial_u\mathscr{E}_\mu = 0$ reads

$$\nabla\times\boldsymbol{B} = (\mu_1+\mu_2)\boldsymbol{B}^* + \left(d_i\mu_2 - \frac{d_e^2}{d_i}\mu_1\right)\nabla\times\boldsymbol{V}, \tag{5.43}$$

$$\rho\boldsymbol{V} = \left(d_i\mu_2 - \frac{d_e^2}{d_i}\mu_1\right)\boldsymbol{B}^* + \left(d_i^2+d_e^2\right)\mu_2\nabla\times\boldsymbol{V}, \tag{5.44}$$

where μ_1 and μ_2 are Lagrange multipliers. Equations (5.43) and (5.44) combine to yield a triple-curl Beltrami equation

$$\nabla\times\nabla\times\nabla\times\boldsymbol{B} - \alpha_1\nabla\times\nabla\times\boldsymbol{B} + \alpha_2\nabla\times\boldsymbol{B} - \alpha_3\boldsymbol{B} = 0, \tag{5.45}$$

where

$$\begin{aligned}
\alpha_1 &= \left[\left(d_i^2+d_e^2\right)\mu_2+d_e^2\left(\mu_1+\mu_2\right)\right]/\Delta,\\
\alpha_2 &= \left[1+\left(d_i^2+d_e^2\right)\left(\mu_1+\mu_2\right)\mu_2-\left(d_i\mu_2-\frac{d_e^2}{d_i}\mu_1\right)^2\right]/\Delta,\\
\alpha_3 &= \left[\mu_1+\mu_2\right]/\Delta,\\
\Delta &= d_e^2\left[\left(d_i^2+d_e^2\right)\mu_2\left(\mu_1+\mu_2\right)-\left(d_i\mu_2-\frac{d_e^2}{d_i}\mu_1\right)^2\right].
\end{aligned}$$

Equation (5.45) can be factored as

$$\left(curl-\lambda_0\right)\left(curl-\lambda_1\right)\left(curl-\lambda_2\right)\boldsymbol{B}=0, \tag{5.46}$$

where the eigenvalues λ_0, λ_1 and λ_2 are given by

$$\left.\begin{aligned}
\lambda_0+\lambda_1+\lambda_2&=\alpha_1,\\
\lambda_0\lambda_1+\lambda_1\lambda_2+\lambda_2\lambda_0&=\alpha_2,\\
\lambda_0\lambda_1\lambda_2&=\alpha_3.
\end{aligned}\right\} \tag{5.47}$$

The general solution of (5.46) can be written as a linear combination of three Beltrami eigenfunctions [179]:

$$\boldsymbol{B}=\sum_{l=0}^{2}a_l\boldsymbol{G}_l, \tag{5.48}$$

where $\boldsymbol{G}_l$'s are the Beltrami eigenfunctions satisfying ($\nabla\times\boldsymbol{G}_l=\lambda_l\boldsymbol{G}_l$), and a_l's are arbitrary constants. By substituting (5.48) into (5.43) and (5.44), the corresponding flow is given by

$$\boldsymbol{V} = \sum_{l=0}^{2}\left[\sigma\left(1+d_e^2\lambda_l^2\right)+\frac{\left(d_i^2+d_e^2\right)\mu_2}{\left(d_i\mu_2-\frac{d_e^2}{d_i}\mu_1\right)}\lambda_l\right]a_l\boldsymbol{G}_l, \tag{5.49}$$

where $\sigma=\left(d_i\mu_2-\frac{d_e^2}{d_i}\mu_1\right)-\frac{\left(d_i^2+d_e^2\right)(\mu_1+\mu_2)\mu_2}{\left(d_i\mu_2-\frac{d_e^2}{d_i}\mu_1\right)}$.

We make a special choice for one of the Beltrami eigenvalues to set $\lambda_0 = 0$. Then, the corresponding eigenfunction becomes a harmonic field. Two consequences immediately follow from (5.47):

$$\left.\begin{aligned} \mu_1 = -\mu_2 = \mu, \\ \lambda_1 + \lambda_2 = \alpha_1, \\ \lambda_1 \lambda_2 = \alpha_2. \end{aligned}\right\} \tag{5.50}$$

Now, solving (5.50) yields

$$\lambda_{1,2} = \frac{d_i}{2 d_e^2 \mu_\star} \left[1 \mp \sqrt{1 - \frac{4 d_e^2}{d_i^2} \left(\mu_\star^2 - 1 \right)} \right], \tag{5.51}$$

where $\mu_\star = \left(d_i^2 + d_e^2 \right) \mu / d_i$. Under this condition the general flow solution becomes

$$\boldsymbol{V} = -\mu_\star a_0 \boldsymbol{G}_0 - \frac{1}{\mu_\star} \left(a_1 \boldsymbol{G}_1 + a_2 \boldsymbol{G}_2 \right). \tag{5.52}$$

We can write down the Beltrami solutions explicitly, for example, in the cylindrical coordinates:

$$\boldsymbol{B} = a_0 \boldsymbol{G}_0 + \boldsymbol{b}, \qquad \boldsymbol{V} = -\mu_\star a_0 \boldsymbol{G}_0 + \boldsymbol{v}, \tag{5.53}$$

$$\boldsymbol{v} = \frac{-1}{\mu_\star} \boldsymbol{b}. \tag{5.54}$$

where

$$\begin{aligned} \boldsymbol{b} &= a_1 \boldsymbol{G}_1 + a_2 \boldsymbol{G}_2 \\ &= \left\{ \sum_{l=1}^{2} a_l \left(\lambda_l \frac{im}{r} J_m \left(\gamma_l r \right) + ik \frac{\partial}{\partial r} \left(J_m \left(\gamma_l r \right) \right) \right) \hat{r} \right. \\ &\quad - \sum_{l=1}^{2} a_l \left(\frac{mk}{r} J_m \left(\gamma_l r \right) + \lambda_l \frac{\partial}{\partial r} \left(J_m \left(\gamma_l r \right) \right) \right) \hat{\theta} \\ &\quad \left. + \sum_{l=1}^{2} a_l \gamma_l^2 J_m \left(\gamma_l r \right) \hat{z} \right\} e^{i(m\theta + kz)}, \end{aligned} \tag{5.55}$$

where $\gamma_l^2 = \lambda_l^2 - k^2$ measures the transverse wave numbers, k is the axial wave number and J_m is the Bessel function of first kind of order m.

5.3.3 Nonlinear helicon waves

We can derive wave solutions from the forgoing equilibrium solutions. Evidently (5.53)-(5.55) are equilibrium solutions satisfying

$$\begin{aligned} 0 &= \nabla \times [\,(\boldsymbol{V} - d_i \nabla \times \boldsymbol{B}) \times \boldsymbol{B}^*], && (5.56) \\ 0 &= \nabla \times [\boldsymbol{V} \times (\boldsymbol{B}^* + \nabla \times \boldsymbol{V}) \\ &\quad + (1 - d_i)\,(\nabla \times \boldsymbol{B}) \times \boldsymbol{B}^*], && (5.57) \end{aligned}$$

$$\begin{aligned} \nabla \cdot \boldsymbol{V} &= 0, && (5.58) \\ \nabla \cdot \boldsymbol{B} &= 0, \qquad \nabla \cdot \boldsymbol{B}^* = 0. && (5.59) \end{aligned}$$

Here we assume that the harmonic field $\boldsymbol{G}_0$ represents the ambient magnetic field, and the other components $\boldsymbol{G}_1$ and $\boldsymbol{G}_2$ are "wave fields" propagating on $\boldsymbol{G}_0$. Setting $(\boldsymbol{G}_0 = \hat{z})$ and $(a_0 = 1)$, we write

$$\boldsymbol{B} = \hat{z} + \boldsymbol{b}, \qquad \boldsymbol{V} = -\mu_\star \hat{z} + \boldsymbol{v}, \tag{5.60}$$

Next, we transform the coordinates by Galilean-boost:

$$(r, \theta, z) \longmapsto (r, \theta, \xi) := (r, \theta, z + \mu_\star t)\,,$$

where $t \mapsto \tau := t$ and $z \mapsto \xi := z + \mu_\star t$. The derivatives transform as $\nabla_{r,\theta,z} \mapsto \widetilde{\nabla}_{r,\theta,\xi}$, and $\frac{\partial}{\partial t} \mapsto \frac{\partial}{\partial \tau} + \mu_\star \frac{\partial}{\partial \xi}$. For a 3-vector $\boldsymbol{R}$ such that $\nabla \cdot \boldsymbol{R} = 0$, we may calculate $-\mu_\star \frac{\partial \boldsymbol{R}}{\partial \xi} = \nabla \times (\mu_\star \hat{z} \times \boldsymbol{R})$. Applying the above coordinates

transformations along with (5.60), the equilibrium equations (5.56) and (5.57) transform into

$$\frac{\partial \boldsymbol{b}^*}{\partial \tau} = \widetilde{\nabla} \times \Big[\Big(\boldsymbol{v} - d_i \widetilde{\nabla} \times \boldsymbol{b} \Big) \times \boldsymbol{B}^* \Big], \tag{5.61}$$

$$\begin{aligned} \frac{\partial \Big(\boldsymbol{b}^* + \widetilde{\nabla} \times \boldsymbol{v} \Big)}{\partial \tau} &= \widetilde{\nabla} \times \Big[\boldsymbol{v} \times \Big(\boldsymbol{B}^* + \widetilde{\nabla} \times \boldsymbol{v} \Big) \\ &\quad + (1 - d_i) \Big(\widetilde{\nabla} \times \boldsymbol{b} \Big) \times \boldsymbol{B}^* \Big], \end{aligned} \tag{5.62}$$

which read as wave equations. Hence, our triple Beltrami solution, which is now denoted as (5.60), can be regarded as a wave solution propagating on the ambient field $\boldsymbol{B}_0 = \hat{z}$.

Let us extract wave characteristic quantities from the Beltrami solutions; we put

$$\boldsymbol{B} = \hat{z} + \boldsymbol{b}\, e^{-i\omega t}, \qquad \boldsymbol{V} = \boldsymbol{v}\, e^{-i\omega t}, \tag{5.63}$$

$$\boldsymbol{v} = \left(\frac{-k}{\omega} \right) \boldsymbol{b}, \tag{5.64}$$

where $\boldsymbol{b}$ is given by (5.55). Equation (5.64) determines the relation between the the magnetic and velocity fields in the wave. Note that here $\mu_\star$ serves as the phase velocity. We can rewrite the eigenvalues equation (5.51) in terms of the frequency ($\omega = k\mu_\star$) as

$$\lambda_{1,2} = \frac{d_i k}{2 d_e^2 \omega} \left[1 \mp \sqrt{1 - 4 \frac{d_e^2}{d_i^2} \left(\frac{\omega^2}{k^2} - 1 \right)} \right]. \tag{5.65}$$

The eigenvalues (5.65) are identical to the eigenvalues obtained from the linear analysis (when the ions are considered immobile), except for the last term under the square-root. This term recovers the ion inertia effect, yielding an ion cyclotron wave mode (cf. Fig.5.1) which has been ignored in previous studies.

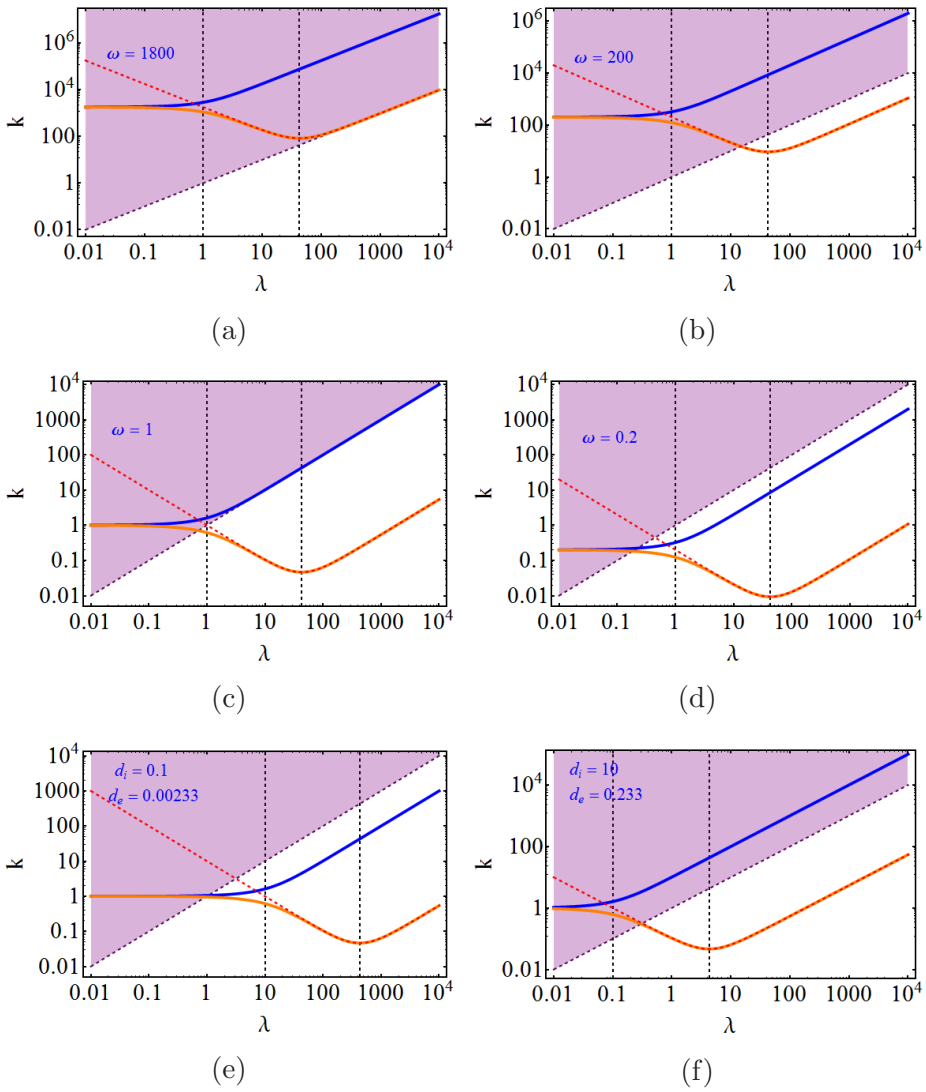

Figure 5.1: The relation between k (axial wave number) and λ (Beltrami eigenvalue measuring the reciprocal length scale of wave field variation). In (a), (b), (c) and (d), $d_i = 1$ and $d_e = 0.0233$ are fixed, while ω is changed as a parameter. In (e) and (f), $\omega = 1$ is fixed, while the skin depths are changed. The shaded region above the dashed line of $k = \lambda$ is the evanescent domain. The dashed red curve shows the limit of immobile ions given by (5.12). The regime of $\lambda < 1/d_i$ may be approximated by ideal MHD, and the regime of $1/d_i < \lambda < 1/d_e$ by Hall MHD, while the electron inertia plays important role in the regime of $1/d_e < \lambda$.

In Fig. 5.1 $k-\lambda$ diagrams are presented in which the helicon and TG modes are represented by an "orange line" and the ion cyclotron mode by a "blue line". We have inserted two vertical dashed lines in each plot to separate the ideal ($\lambda < 1/d_i$), Hall ($1/d_i < \lambda < 1/d_e$) and the electron inertia ($\lambda > 1/d_e$) domains. Notice that the ion cyclotron mode arises when λ or k is negative. Figs. 5.1a-5.1d are the $k-\lambda$ curves for different values of the applied magnetic field. We can observe that for $\omega > 1800$ in normalized units all modes become evanescent (no propagation). As the value of ω decreases the helicon and TG modes appeared, when it reaches a definite value ($\omega \leq 1$ in normalized units) a third mode arises. We also observed a particular coupling between the different modes, a for the values of $k < \omega$ the coupling occurs between Helicon and TG waves, whilst the ion cyclotron wave is coupled with the TG wave for the values of $k > \omega$. To examine the effect of the plasma density, we plot the $k-\lambda$ relation for two different values of the skin depth; see. Figs. 5.1e and 5.1f). The change of the plasma density (thus, the skin depth) strongly influences the waves coupling.

5.3.4 Electric field and energy deposition

We shall now compute the electric field $\boldsymbol{E}$ using Faraday's law (3.17) and the generalized Ohm's law (3.16). Generalized Oham's law (3.16) enabled us to calculate the z-component of the electric field E_z while the transverse components $\boldsymbol{E}_\perp$ could be computed using (3.17).

From equation (3.16), we obtain the follow:

$$\boldsymbol{E} = d_i \left(\nabla \times \boldsymbol{B}\right) \times \boldsymbol{B}^* - \boldsymbol{V} \times \boldsymbol{B}^* + d_e^2 \frac{\partial}{\partial t} \boldsymbol{J}, \tag{5.66}$$

where $\boldsymbol{B}^* = \boldsymbol{B} + d_e^2 \nabla \times \nabla \times \boldsymbol{B}$. Substituting the solutions (5.63)-(5.55) into (5.66), the resultant equation is

$$\boldsymbol{E} = d_i \left(\nabla \times \boldsymbol{b}\right) \times \boldsymbol{b}^* + d_i \left(\nabla \times \boldsymbol{b}\right) \times \hat{z} - \boldsymbol{v} \times \boldsymbol{b}^* - \boldsymbol{v} \times \hat{z} + d_e^2 \frac{\partial}{\partial t} \boldsymbol{J}, \quad (5.67)$$

where $\boldsymbol{b}^* = \boldsymbol{b} + d_e^2 \times \nabla \times \boldsymbol{b}$. Then, using Beltrami condition ($\nabla \times \boldsymbol{b} = \lambda \boldsymbol{b}$) and (5.64) in (5.67) yields

$$E_z = -i\omega d_e^2 \lambda b_z \left(r\right). \quad (5.68)$$

The transverse components could be calculated from (3.17) as follow:

$$\nabla \times \boldsymbol{E} = i\omega \boldsymbol{b}. \quad (5.69)$$

The r-component of (5.69) is

$$\begin{aligned} \frac{1}{r}\frac{\partial E_z}{\partial \theta} - \frac{\partial E_\theta}{\partial z} &= i\omega b_r, \\ \frac{im}{r} E_z - ikE_\theta &= i\omega b_r, \end{aligned} \quad (5.70)$$

which leads us to

$$E_\theta = -\frac{\omega}{k}\left(b_r + \frac{imd_e^2\lambda}{r} b_z\right). \quad (5.71)$$

Similarly, θ-component of (5.69) is

$$\begin{aligned} \frac{\partial E_r}{\partial z} - \frac{\partial E_z}{\partial r} &= i\omega b_\theta, \\ ikE_r - \frac{\partial E_z}{\partial r} &= i\omega b_\theta, \end{aligned} \quad (5.72)$$

which leads us to

$$E_r = \frac{\omega}{k}\left(b_\theta - d_e^2 \lambda b_z\right). \quad (5.73)$$

Notice that equations (5.68), (5.71) and (5.73) satisfy the z-component of (5.69).

We now in the position to compute the energy deposition. Since the transverse components of the electric field and magnetic field are perpendicular, and hence, only the z-component will contribute to the energy loss. Then the rate of losing energy is

$$-\frac{dW}{dt} = \langle \boldsymbol{J} \cdot \boldsymbol{E} \rangle = \langle J_z E_z \rangle \,. \tag{5.74}$$

From (5.55) The current density is given by

$$\begin{aligned} \boldsymbol{J} &= \nabla \times \boldsymbol{B} \\ &= \lambda_1 a_1 \boldsymbol{G}_1 + \lambda_2 a_2 \boldsymbol{G}_2 \\ &= \boldsymbol{J}_{\lambda_1} + \boldsymbol{J}_{\lambda_2}. \end{aligned} \tag{5.75}$$

where the Beltrami $\nabla \times \boldsymbol{B} = \lambda \boldsymbol{B}$ is used.

Then, the real part of the J_z is

$$Re\,(J_z) = \Big[a_1 \lambda_1 \gamma_1^2 J_m\,(\gamma_1 r) + a_2 \lambda_2 \gamma_2^2 J_m\,(\gamma_2 r) \Big] \cos\,(\Theta)\,, \tag{5.76}$$

and for electric field is

$$\begin{aligned} Re\,(E_z) &= \omega d_e^2 \Big[a_1 \lambda_1 \gamma_1^2 J_m\,(\gamma_1 r) + a_2 \lambda_2 \gamma_2^2 J_m\,(\gamma_2 r) \Big] \sin\,(\Theta)\,, \\ &= d_2^2 \frac{d}{dt} Re\,(J_z)\,, \end{aligned} \tag{5.77}$$

where $\Theta = [m\theta + kz - \omega t]$. Thus,

$$-\frac{dW}{dt} = \langle J_z E_z \rangle = 0. \tag{5.78}$$

Equations (5.78) shows that the energy loss rate for collisionless plasma is zero, because of the 90° phase difference between the current J_z and the electric field E_z. Including resistivity would make a nonzeo energy loss, since in this case the current and the electric field ($\boldsymbol{E} = \eta \boldsymbol{J}$) are parallel, where η is plasma resistivity.

5.3.5 Dispersion relation

5.3.5.1 Bounded plasma

Conducting boundary: Considering the case of a plasma rod of radius a bounded by a perfectly conducting material, the boundary condition here is that the tangential components of the electric field should be zero, which yield $E_z = E_\theta = 0$ at the boundary.

Applying those boundary to (5.68) and (5.71), yield respectively,

$$a_1 \gamma_1^2 J_m(\gamma_1 a) + a_2 \gamma_2^2 J_m(\gamma_2 a) = 0, \tag{5.79}$$

$$\begin{aligned} &a_1 \left(\lambda_1 \frac{m}{a} J_m(\gamma_1 a) + k \frac{\partial}{\partial r} \left(J_m(\gamma_1 r) \right) |_{r=a} \right) \\ &+ a_2 \left(\lambda_2 \frac{m}{a} J_m(\gamma_2 a) + k \frac{\partial}{\partial r} \left(J_m(\gamma_2 r) \right) |_{r=a} \right) = 0. \end{aligned} \tag{5.80}$$

Then the dispersion relation can be given by the following determinant

$$\begin{vmatrix} a_1 \gamma_1^2 J_m(\gamma_1 a) & a_2 \gamma_2^2 J_m(\gamma_2 a) \\ a_1 \left[\frac{\lambda_1 m}{a} J_m(\gamma_1 a) + k \frac{\partial J_m(\gamma_1 r)}{\partial r} |_{r=a} \right] & a_2 \left[\frac{\lambda_2 m}{a} J_m(\gamma_2 a) + k \frac{\partial J_m(\gamma_2 r)}{\partial r} |_{r=a} \right] \end{vmatrix} = 0. \tag{5.81}$$

Insulating boundary: Considering a plasma column confined by an insulating tube of radius a, the boundary condition here requires the calculation of the fields in the vacuum region.

In the vacuum region there are no conducting currents, which means

$$\boldsymbol{J} = 0 = \nabla \times \boldsymbol{b}. \tag{5.82}$$

Taking the curl of (5.82) yields

$$\nabla \times \nabla \times \boldsymbol{b} = 0, \tag{5.83}$$

Since $(\nabla \cdot \boldsymbol{b} = 0)$, then

$$\nabla^2 \boldsymbol{b} = 0, \tag{5.84}$$

The vacuum fields are therefore given by

$$b_r = -\frac{ia_3}{k}\frac{\partial}{\partial r}K_m(kr), \tag{5.85}$$

$$b_\theta = \frac{a_3 m}{rk}K_m(kr), \tag{5.86}$$

$$b_z = a_3 K_m(kr), \tag{5.87}$$

where K_m is the modified Bessel function of the second kind of order m. Connecting the vacuum fields (5.85) to the plasma fields (5.55) at the boundary yield the dispersion relation

$$\begin{vmatrix} a_1\left[\frac{\lambda_1 m}{a}J_m(\gamma_1 a) + k\frac{\partial J_m(\gamma_1 r)}{\partial r}\big|_{r=a}\right] & a_2\left[\frac{\lambda_2 m}{a}J_m(\gamma_2 a) + k\frac{\partial J_m(\gamma_2 r)}{\partial r}\big|_{r=a}\right] & -\frac{a_3}{k}\frac{\partial K_m(kr)}{\partial r} \\ -a_1\left[\frac{mk}{a}J_m(\gamma_1 a) + \lambda_1\frac{\partial J_m(\gamma_1 r)}{\partial r}\big|_{r=a}\right] & -a_2\left[\frac{mk}{a}J_m(\gamma_2 a) + \lambda_2\frac{\partial J_m(\gamma_1 r)}{\partial r}\big|_{r=a}\right] & \frac{a_3 m}{ak}K_m(ka) \\ a_1\gamma_1^2 J_m(\gamma_1 a) & a_2\gamma_2^2 J_m(\gamma_2 a) & a_3 K_m(ka) \end{vmatrix} = 0. \tag{5.88}$$

Before moving farther, we refer the reader to [28, 42, 43, 47, 80] for in-depth discussions of these Boundary conditions.

5.3.6 The partitions of the wave energy

As an interesting property of the nonlinear solution (5.48), the coefficients a_1 and a_2 can be arbitrarily chosen to combine two Beltrami eigenfunctions. Here we study how they are determined by physical conditions. One possible, conventional argument is to relate such coefficients to boundary conditions on the electromagnetic field. However, it is known that boundary conditions fall short of determining the coefficients (in the linear theory) [27, 41, 48]. We can approach the problem from a different angle; based on our Hamiltonian formalism, we can invoke the Casimir invariants (helicities) to quantify the coefficients. Inserting the solution (5.63)-(5.64) into (5.39) and (5.40), we obtain the helicities represented in terms of a_1 and a_2 (and other plasma parameters). Numerically inverting this somewhat involved relation, we obtain the ratio a_1/a_2, as well as the energy partition, as functions of the helicities.

The auxiliary relation between the magnetic and flow fields (5.64) is used to determine the wave energy partition. First, we used the recurrence relations

$$\frac{m}{r}J_m(\gamma r) = \frac{\gamma}{2}\left(J_{m-1}(\gamma r) + J_{m+1}(\gamma r)\right),$$
$$\frac{\partial}{\partial r}J_m(\gamma r) = \frac{\gamma}{2}\left(J_{m-1}(\gamma r) - J_{m+1}(\gamma r)\right),$$

in the fluctuated magnetic field equation (5.55), which yield

$$\begin{aligned}\boldsymbol{b} &= \Big\{ \sum_{l=1}^{2} i a_l \Big((\lambda_l + k)\, J_{m-1}(\gamma_l r) + (\lambda_l - k)\, J_{m+1}(\gamma_l r) \Big) \hat{r} \\ &\quad - \sum_{l=1}^{2} a_l \Big((\lambda_l + k)\, J_{m-1}(\gamma_l r) - (\lambda_l - k)\, J_{m+1}(\gamma_l r) \Big) \hat{\theta} \\ &\quad + \sum_{l=1}^{2} a_l \gamma_l^2 J_m(\gamma_l r)\, \hat{z} \Big\} e^{i[m\theta + kz - \omega t]}, \end{aligned} \tag{5.89}$$

where the arbitrary constants are redefined as $a_1 = \frac{a_1\gamma_1}{2}$ and $a_2 = \frac{a_2\gamma_2}{2}$. The real part of the magnetic field can be read as

$$\begin{aligned}\boldsymbol{b} &= -\sum_{l=1}^{2} i a_l \Big((\lambda_l + k)\, J_{m-1}(\gamma_l r) + (\lambda_l - k)\, J_{m+1}(\gamma_l r) \Big) \sin(m\theta + kz - \omega t) \hat{r} \\ &\quad - \sum_{l=1}^{2} a_l \Big((\lambda_l + k)\, J_{m-1}(\gamma_l r) - (\lambda_l - k)\, J_{m+1}(\gamma_l r) \Big) \cos(m\theta + kz - \omega t) \hat{\theta} \\ &\quad + \sum_{l=1}^{2} a_l \gamma_l^2 J_m(\gamma_l r) \cos(m\theta + kz - \omega t) \hat{z}. \end{aligned} \tag{5.90}$$

To determine the free parameters in the above equation, we used the invariants of the system (5.39), (5.40) and (5.41). We start by defining the element of volume in cylindrical coordinates as

$$d^3x = r\, dr\, d\theta\, dz,$$

where $0 \le r \le a$, $0 \le \theta \le 2\pi$ and $-L \le z \le L$, a is the cylinder radius and L is the cylinder half length. Assume that

$$L = \frac{\pi n}{k}, \tag{5.91}$$

where n is an integer. This yields the following integration relations

$$\int_{-L}^{L} \cos\Big(\frac{n\pi}{L}x\Big) \cos\Big(\frac{m\pi}{L}x\Big) dx = \begin{cases} L & n = m \neq 0 \\ 0 & n \neq m \end{cases}$$

$$\int_{-L}^{L} \sin\left(\frac{n\pi}{L}x\right) \sin\left(\frac{m\pi}{L}x\right) dx = \begin{cases} L & n = m \neq 0 \\ 0 & n \neq m \end{cases}$$

$$\int_{-L}^{L} \sin\left(\frac{n\pi}{L}x\right) \cos\left(\frac{m\pi}{L}x\right) dx = 0$$

$$\int_{-L}^{L} \sin\left(\frac{n\pi}{L}x\right) dx = 0$$

$$\int_{-L}^{L} \cos\left(\frac{n\pi}{L}x\right) dx = 0$$

Starting by the Hamiltonian (energy) (5.41), which becomes

$$E = \int_{\Omega} \left\{ \frac{|\boldsymbol{v}|^2}{2} + \frac{\boldsymbol{B} \cdot \boldsymbol{B}^*}{2} \right\} d^3x, \tag{5.92}$$

$$= E_K + E_M. \tag{5.93}$$

the magnetic part is

$$E_M = \frac{1}{2} \int_0^a \int_0^{2\pi} \int_{-L}^{L} \boldsymbol{B} \cdot \boldsymbol{B}^* r \, dr \, d\theta \, dz, \tag{5.94}$$

where

$$\boldsymbol{B}^* = \hat{z} + \boldsymbol{b} + d_e^2 \nabla \times \nabla \times \boldsymbol{b}, \tag{5.95}$$

and $\boldsymbol{b}$ is given by the superposition of the solutions of two Beltrami equations

$$\boldsymbol{b} = a_1 \boldsymbol{G}_1 + a_2 \boldsymbol{G}_2.$$

Then,

$$\boldsymbol{b}^* = a_1 \left(1 + d_e^2 \lambda_1^2\right) \boldsymbol{G}_1 + a_2 \left(1 + d_e^2 \lambda_1^2\right) \boldsymbol{G}_2. \tag{5.96}$$

Use of the above information the magnetic energy can be written as

$$\begin{aligned}
E_M &= 2\pi L a_1^2\left(1+d_e^2\lambda_1^2\right)\int_0^a\Big[\left(\lambda_1+k\right)^2\left[J_{m-1}\left(\gamma_1 r\right)\right]^2 \\
&+\left(\lambda_1-k\right)^2\left[J_{m+1}\left(\gamma_1 r\right)\right]^2+2\gamma_1^2\left[J_m\left(\gamma_1 r\right)\right]^2\Big]rdr \\
&+2\pi L a_2^2\left(1+d_e^2\lambda_2^2\right)\int_0^a\Big[\left(\lambda_2+k\right)^2\left[J_{m-1}\left(\gamma_2 r\right)\right]^2 \\
&+\left(\lambda_2-k\right)^2\left[J_{m+1}\left(\gamma_2 r\right)\right]^2+2\gamma_2^2\left[J_m\left(\gamma_2 r\right)\right]^2\Big]rdr \\
&+2\pi L a_1 a_2\left[\left(1+d_e^2\lambda_1^2\right)+\left(1+d_e^2\lambda_2^2\right)\right]\times \\
&\int_0^a\Big[\left(\lambda_1+k\right)\left(\lambda_2+k\right)J_{m-1}\left(\gamma_1 r\right)J_{m-1}\left(\gamma_2 r\right) \\
&+\left(\lambda_1-k\right)\left(\lambda_2-k\right)J_{m+1}\left(\gamma_1 r\right)J_{m+1}\left(\gamma_2 r\right)+2\gamma_1\gamma_2 J_m\left(\gamma_1 r\right)J_m\left(\gamma_2 r\right)\Big]rdr.
\end{aligned} \tag{5.97}$$

The kinetic part of the energy is

$$E_K=\frac{1}{2}\int_0^a\int_0^{2\pi}\int_{-L}^{L}\boldsymbol{v}^2 r\,dr\,d\theta\,dz, \tag{5.98}$$

but,

$$\boldsymbol{v} = -\frac{k}{\omega}\boldsymbol{b}. \tag{5.99}$$

Then,

$$\begin{aligned}
E_K &= \frac{1}{2}\left(\frac{k}{\omega}\right)^2\int_0^a\int_0^{2\pi}\int_{-L}^{L}\boldsymbol{b}^2 r\,dr\,d\theta\,dz, \\
&= 2\pi L\left(\frac{k}{\omega}\right)^2 a_1^2\int_0^a\Big[\left(\lambda_1+k\right)^2\left[J_{m-1}\left(\gamma_1 r\right)\right]^2 \\
&+\left(\lambda_1-k\right)^2\left[J_{m+1}\left(\gamma_1 r\right)\right]^2+2\gamma_1^2\left[J_m\left(\gamma_1 r\right)\right]^2\Big]rdr \\
&+2\pi L\left(\frac{k}{\omega}\right)^2 a_2^2\int_0^a\Big[\left(\lambda_2+k\right)^2\left[J_{m-1}\left(\gamma_2 r\right)\right]^2 \\
&+\left(\lambda_2-k\right)^2\left[J_{m+1}\left(\gamma_2 r\right)\right]^2+2\gamma_2^2\left[J_m\left(\gamma_2 r\right)\right]^2\Big]rdr
\end{aligned}$$

$$+4\pi L\left(\frac{k}{\omega}\right)^2 a_1 a_2 \int_0^a \Big[(\lambda_1+k)(\lambda_2+k) J_{m-1}(\gamma_1 r) J_{m-1}(\gamma_2 r) + (\lambda_1-k)(\lambda_2-k) J_{m+1}(\gamma_1 r) J_{m+1}(\gamma_2 r) + 2\gamma_1\gamma_2 J_m(\gamma_1 r) J_m(\gamma_2 r) \Big] r dr. \tag{5.100}$$

Thus, the total energy may be written as

$$\begin{aligned} E &= \left[1 + d_e^2\lambda_1^2 + \left(\frac{k}{\omega}\right)^2\right] A_1^2 + \left[1 + d_e^2\lambda_2^2 + \left(\frac{k}{\omega}\right)^2\right] A_2^2 \\ &\quad +2\left[1 + \frac{d_e^2}{2}\left(\lambda_1^2+\lambda_2^2\right) + \left(\frac{k}{\omega}\right)^2\right] A_3^2, \end{aligned} \tag{5.101}$$

where

$$\begin{aligned} A_1^2 &= 2\pi L a_1^2 \int_0^a \Big[(\lambda_1+k)^2 \left[J_{m-1}(\gamma_1 r)\right]^2 \\ &\quad + (\lambda_1-k)^2 \left[J_{m+1}(\gamma_1 r)\right]^2 + 2\gamma_1^2 \left[J_m(\gamma_1 r)\right]^2 \Big] r dr, \\ &= 2\pi L a_1^2 X_1 \end{aligned} \tag{5.102}$$

$$\begin{aligned} A_2^2 &= 2\pi L a_2^2 \int_0^a \Big[(\lambda_2+k)^2 \left[J_{m-1}(\gamma_2 r)\right]^2 \\ &\quad + (\lambda_2-k)^2 \left[J_{m+1}(\gamma_2 r)\right]^2 + 2\gamma_2^2 \left[J_m(\gamma_2 r)\right]^2 \Big] r dr, \\ &= 2\pi L a_2^2 X_2 \end{aligned} \tag{5.103}$$

$$\begin{aligned} A_3^2 &= 2\pi L a_1 a_2 \int_0^a \Big[(\lambda_1+k)(\lambda_2+k) J_{m-1}(\gamma_1 r) J_{m-1}(\gamma_2 r) \\ &\quad + (\lambda_1-k)(\lambda_2-k) J_{m+1}(\gamma_1 r) J_{m+1}(\gamma_2 r) + 2\gamma_1\gamma_2 J_m(\gamma_1 r) J_m(\gamma_2 r) \Big] r dr, \\ &= 2\pi L a_1 a_2 X_3 \end{aligned} \tag{5.104}$$

are constants determined by the above integrals. The helicities C_1 and C_2 read

$$C_1 = \frac{1}{2}\int_\Omega \boldsymbol{B}^* \cdot \left(\boldsymbol{A}^* - \frac{2d_e^2}{d_i}\boldsymbol{v}\right) d^3x,$$

$$
\begin{aligned}
&= \left[\frac{(1+d_e^2\lambda_1^2)}{\lambda_1}+2\frac{d_e^2k}{d_i\omega}\right]\left(1+d_e^2\lambda_1^2\right)A_1^2 \\
&+\left[\frac{(1+d_e^2\lambda_2^2)}{\lambda_2}+2\frac{d_e^2k}{d_i\omega}\right]\left(1+d_e^2\lambda_2^2\right)A_2^2 \\
&+\Bigg[\left(\frac{1}{\lambda_1}+\frac{1}{\lambda_2}\right)\left(1+d_e^2\lambda_1^2\right)\left(1+d_e^2\lambda_2^2\right) \\
&+4\left(\frac{d_e^2k}{d_i\omega}\right)\left(1+\frac{d_e^2}{2}\left(\lambda_1^2+\lambda_2^2\right)\right)\Bigg]A_3^2, \qquad (5.105)
\end{aligned}
$$

and

$$
\begin{aligned}
C_2 &= \frac{1}{2}\int_\Omega\Big[(\boldsymbol{A}^*+d_i\boldsymbol{V})\cdot(\boldsymbol{B}^*+d_i\nabla\times\boldsymbol{V}) \\
&\quad +d_e^2\boldsymbol{V}\cdot(\nabla\times\boldsymbol{V})\Big]d^3x, \\
&= \left[\frac{\left(1+d_e^2\lambda_1^2\right)^2}{\lambda_1}-2d_i\left(\frac{k}{\omega}\right)\left(1+d_e^2\lambda_1^2\right)+\left(d_i^2+d_e^2\right)\lambda_1\left(\frac{kB}{\omega}\right)^2\right]A_1^2 \\
&\quad +\left[\frac{\left(1+d_e^2\lambda_2^2\right)^2}{\lambda_2}-2d_i\left(\frac{k}{\omega}\right)\left(1+d_e^2\lambda_2^2\right)+\left(d_i^2+d_e^2\right)\lambda_2\left(\frac{k}{\omega}\right)^2\right]A_2^2 \\
&\quad +\Bigg[\left(d_i^2+d_e^2\right)\left(\frac{kB}{\omega}\right)^2(\lambda_1+\lambda_2)-4d_i\left(\frac{k}{\omega}\right)\left(1+\frac{d_e^2}{2}\left(\lambda_1^2+\lambda_2^2\right)\right) \\
&\quad +\left(\frac{1}{\lambda_1}+\frac{1}{\lambda_2}\right)\left(1+d_e^2\lambda_1^2\right)\left(1+d_e^2\lambda_2^2\right)\Bigg]A_3^2, \qquad (5.106)
\end{aligned}
$$

At that point, we shall use the ratio of (5.105) and (5.106) to determine the ratio of the arbitrary constants a_1/a_2 numerically. Then, we flip the results and got the arbitrary constants ratio a_1/a_2 as a function of the helicities ratio C_1/C_2 (see Fig.5.2). Figure 5.2 shows how the helicon-TG energy ratio is changed by the helicities.

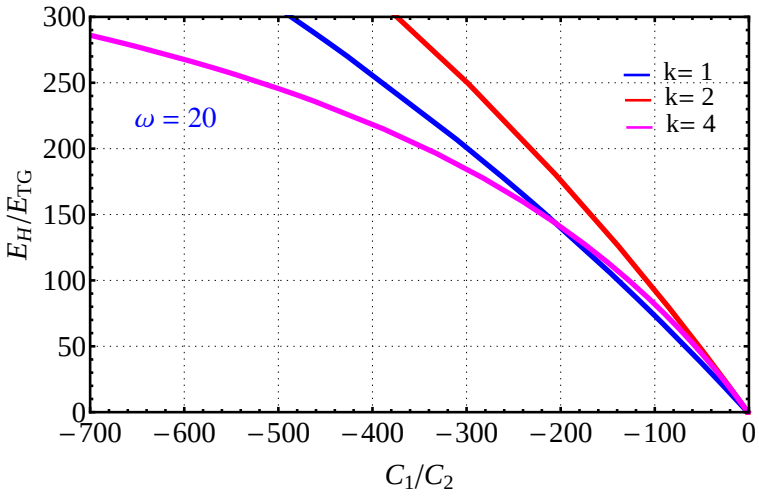

(a)

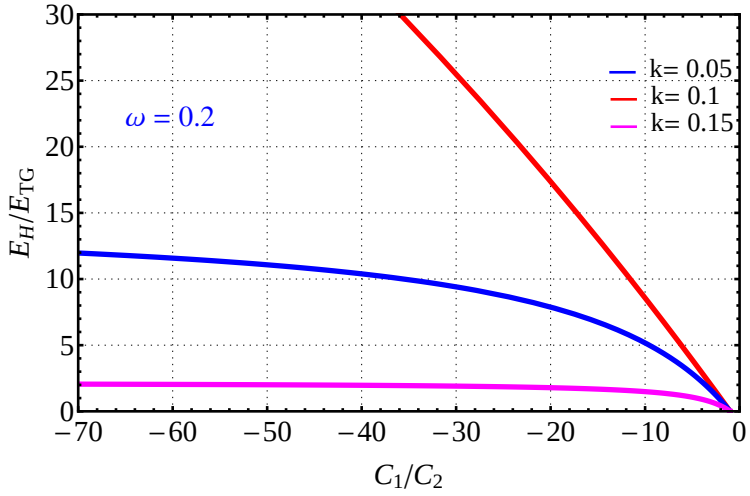

(b)

Figure 5.2: The relation between Helicon-TG energy ratio E_H/E_{TG} and the helicities ratio C_1/C_2. Here, we assume $d_i = 1$, $d_e = 0.0233$ and $m = 0$. In (a) $\omega = 20$, and (b) $\omega = 0.2$.

The Casimir invariants (5.39) and (5.40) can be related to the two-fluid (electrons and ions) helicities, respectively, in the one-fluid model limits. In two-fluid plasma consisting of electrons and ions, the invariants can be written as $\int_\Omega \boldsymbol{P}_{e,i}.\nabla \times \boldsymbol{P}_{e,i} d^3x$, where $\boldsymbol{P}_{e,i}$ is the canonical momentum for each specie ($\boldsymbol{P}_{e,i} = m_{e,i}\boldsymbol{V}_{e,i} + q_{e,i}\boldsymbol{A}$). At the one-fluid limit, the extended MHD invariants and the two-fluid helicities reduce into the same quantities. Since the helicity is the measure of the wave polarization, or the twist of the perturbed (generalized) magnetic field lines, this figure can be used for the practical purpose of designing the wave-launching system to optimize the wave energy partition.

Chapter 6

Extended MHD turbulence

6.1 Feasibility of extended MHD for modeling turbulence

Current measurements and analysis of the solar wind spectrum in the regime $L \lesssim d_e$ (sometimes interpreted as the 'dissipation' range) appear to suggest that a power law behavior, with a slope of approximately -4, is manifested [59, 134, 136, 151]; see also [135]. However, the measurements in the dissipation range are prone to instrumentation errors, as pointed out in [137], which has also led to other interpretations of the spectrum in its vicinity [9, 10]. Moreover, at these small scales, the magnetic fluctuations are not purely homogeneous and exhibit signs of intermittency [127]. On account of all the complexities inherent in solar wind turbulence, gaining a thorough understanding of this phenomenon is, arguably, one of the current major goals [31, 58].

It has become increasingly common to model the solar wind spectra at scales smaller than the ion (or electron) skin depth by means of (gyro)kinetic simulations [34, 73, 75, 132, 163] or hybrid fluid-kinetic models [35, 36, 128, 145, 170], but computational and analytic studies of the solar wind by means of Hall MHD are also quite common [108, 112, 147, 155]. However, it is incorrect to use Hall MHD to study the physics near the

electron skin depth (which equals the electron gyroradius when the electron plasma beta is around unity). For this reason, there have been several studies centred around electron MHD, which can include the effects of electron inertia [19, 21, 46, 53, 107, 120]. However, a chief limitation of electron MHD is the assumption of stationary ions. As a result, the model cannot be applied to systems where the mean velocity is significant.

Extended MHD is endowed with a mean flow, electron inertia and the Hall drift, it gives rise to both electron and Hall MHD as limiting cases [78]. For this reason, we shall employ it as our basic physical model in determining the energy and helicities spectra. Our method relies upon the construction of fully nonlinear Alfvén wave solutions for extended MHD, which are then used for computing the spectra. Notice that, the same solutions were constructed using a more general approach in Chapter 4; see Sec. 4.3.3. We demonstrate that our model reproduces many previous results, both experimental and theoretical; on the latter front, we show that it yields spectra that are distinct from those predicted by Hall MHD, and that are quite similar to the observational data from the solar wind [31, 136] and other collisionless plasmas [86].

6.2 Extended MHD: the mathematical preliminaries

In this Section, we present a brief overview of extended MHD, and discuss some of its chief mathematical properties.

Recalling the equations of extended MHD, see Sec. 3.2.1, which

comprise of the continuity equation

$$\frac{\partial \rho}{\partial t} = -\nabla \cdot (\rho \boldsymbol{V}), \tag{6.1}$$

the dynamical equation for the velocity,

$$\begin{aligned} \frac{\partial \boldsymbol{V}}{\partial t} = &- (\nabla \times \boldsymbol{V}) \times \boldsymbol{V} + \rho^{-1} (\nabla \times \boldsymbol{B}) \times \boldsymbol{B}^* \\ &-\nabla \left(h + \frac{V^2}{2} + d_e^2 \frac{(\nabla \times \boldsymbol{B})^2}{2\rho^2} \right), \end{aligned} \tag{6.2}$$

and the extended MHD Ohm's law

$$\begin{aligned} \frac{\partial \boldsymbol{B}^*}{\partial t} = &\nabla \times (\boldsymbol{V} \times \boldsymbol{B}^*) - \nabla \times \left(\rho^{-1} (\nabla \times \boldsymbol{B}) \times \boldsymbol{B}^* \right) \\ &+ d_e^2 \nabla \times \left(\rho^{-1} (\nabla \times \boldsymbol{B}) \times (\nabla \times \boldsymbol{V}) \right), \end{aligned} \tag{6.3}$$

where

$$\boldsymbol{B}^* = \mathbf{B} + d_e^2 \nabla \times \rho^{-1} (\nabla \times \boldsymbol{B}), \tag{6.4}$$

is the suitable dynamical variable (instead of the conventional magnetic field), and is widely used in electron MHD [60]. It is important to recognize that these equations have been normalized in Alfvénic units, as discussed in Sec. 4.3.3. Moreover, the length scales are normalized in units of the ion skin depth $\lambda_i = c/\omega_{pi}$ for the sake of simplicity, i.e. it amounts to setting $L = \lambda_i$. The incompressible limit of extended MHD is easily obtained by setting $\rho = 1$ in the normalized units.

It is well known that extended MHD [1, 78, 92] yields a conserved energy of the form

$$\begin{aligned} E &= \int_\Omega \left\{ \rho \left(\frac{|\boldsymbol{V}|^2}{2} + d_e^2 \frac{|\boldsymbol{J}|^2}{2\rho} + U(\rho) \right) + \frac{|\boldsymbol{B}|^2}{2} \right\} d^3x, \\ &= \int_\Omega \left\{ \rho \left(\frac{|\boldsymbol{V}|^2}{2} + U(\rho) \right) + \frac{\boldsymbol{B} \cdot \boldsymbol{B}^*}{2} \right\} d^3x, \end{aligned} \tag{6.5}$$

Moreover, extended MHD is endowed with the following helicities (see Sec. 3.4):

$$h_e = \frac{1}{2}\int_\Omega \left(\boldsymbol{A}^* - 2d_e^2\boldsymbol{V}\right)\cdot\boldsymbol{B}^* d^3x, \tag{6.6}$$

$$h_i = \frac{1}{2}\int_\Omega \left[(\boldsymbol{A}^*+\boldsymbol{V})\cdot(\boldsymbol{B}^*+\nabla\times\boldsymbol{V}) + d_e^2\boldsymbol{V}\cdot(\nabla\times\boldsymbol{V})\right] d^3x, \tag{6.7}$$

$$G = \frac{1}{2}\int_\Omega \left[\boldsymbol{A}^*\cdot\boldsymbol{B}^* + d_e^2\boldsymbol{V}\cdot(\nabla\times\boldsymbol{V})\right] d^3x, \tag{6.8}$$

$$K = \frac{1}{2}\int_\Omega \boldsymbol{V}\cdot[2\boldsymbol{B}^*+\nabla\times\boldsymbol{V}]\, d^3x, \tag{6.9}$$

$$C_\pm = \int_\Omega \boldsymbol{P}_\pm^*\cdot\left(\nabla\times\boldsymbol{P}_\pm^*\right) d^3x, \tag{6.10}$$

where $\boldsymbol{P}_\pm^* = \boldsymbol{V}+\theta_\pm\boldsymbol{A}^*$ and $\theta_\pm = \left(-1\pm\sqrt{1+4d_e^2}\right)/(2d_e^2)$ constitute the two constants. It should be noted that, for clarity, different notations have been chosen to define the above extended MHD invariants. Also, we do not mention here the conservation of mass (3.46) since it will not be used in the following calculations.

6.3 Nonlinear wave solutions of extended MHD

In this section, we shall derive a certain class of nonlinear wave solutions for incompressible extended MHD using an alternative approach equivalent to the one that discussed in Sec. 4.3.3. This is done by adopting an approach akin to the one outlined in [82, 96, 97].

6.3.1 The derivation of the nonlinear wave solutions

The equations of incompressible extended MHD can be manipulated, and thereby cast into the following form:

$$\frac{\partial \boldsymbol{B}^*}{\partial t} = \nabla \times [\,(\boldsymbol{V} - \nabla \times \boldsymbol{B}) \times \boldsymbol{B}^*], \tag{6.11}$$

$$\frac{\partial\,(\boldsymbol{B}^* + \nabla \times \boldsymbol{V})}{\partial t} = \nabla \times [\boldsymbol{V} \times (\boldsymbol{B}^* + \nabla \times \boldsymbol{V})\,], \tag{6.12}$$

along with the auxiliary condition

$$\nabla \times ((\nabla \times \boldsymbol{B}) \times (\nabla \times \boldsymbol{V})) = 0, \tag{6.13}$$

which will be commented on later. For now, it suffices to note that this term will obviously vanish when the magnetic and velocity fields are parallel (or anti-parallel) to one another. Furthermore, the condition (6.13) eliminates the last term on the RHS of (6.3), and thereby enables us to arrive at (6.11) and (6.12). The above equations must be supplemented with the incompressibility conditions

$$\nabla \cdot \boldsymbol{V} = 0, \tag{6.14}$$

$$\nabla \cdot \boldsymbol{B}^* = 0, \qquad \nabla \cdot \boldsymbol{B} = 0. \tag{6.15}$$

We shall now describe a class of nonlinear waves that were first derived and investigated in [82,96,97]; the electron inertia corrections that arise are explicitly displayed throughout.

Assuming that there is no ambient flow, we can split the velocity and magnetic field into the ambient and wave components, denoted by the subscript '$\circ$' and lowercase letters respectively, as follows

$$\mathbf{B} = \hat{\boldsymbol{e}}_{B_\circ} + \boldsymbol{b}, \qquad \boldsymbol{V} = \boldsymbol{v}, \tag{6.16}$$

where $\hat{\boldsymbol{e}}_{B_\circ}$ is the direction that the constant ambient field (in the normalized units) is oriented. Using the definition (6.4), we find that

$$\boldsymbol{B}^* = \hat{\boldsymbol{e}}_{B_\circ} + \boldsymbol{b}^*, \qquad \boldsymbol{b}^* = \boldsymbol{b} + d_e^2 \nabla \times (\nabla \times \boldsymbol{b})\,. \tag{6.17}$$

Substituting (6.16) and (6.17) into (6.11) and (6.12), the resultant equations are

$$\begin{aligned} \frac{\partial \boldsymbol{b}^*}{\partial t} &= \nabla \times [\,(\boldsymbol{v} - \nabla \times \boldsymbol{b}) \times \boldsymbol{b}^*] \\ &\quad + \nabla \times [\,(\boldsymbol{v} - \nabla \times \boldsymbol{b}) \times \hat{\boldsymbol{e}}_{B_\circ}], \end{aligned} \tag{6.18}$$

$$\begin{aligned} \frac{\partial\,(\boldsymbol{b}^* + \nabla \times \boldsymbol{v})}{\partial t} &= \nabla \times [\boldsymbol{v} \times (\boldsymbol{b}^* + \nabla \times \boldsymbol{v})\,] \\ &\quad + \nabla \times [\boldsymbol{v} \times \widehat{\boldsymbol{e}}_{B_\circ}]. \end{aligned} \tag{6.19}$$

Let us now suppose that the following (special) conditions were to be satisfied

$$\boldsymbol{b}^* = \frac{1}{\mu_1}\,(\boldsymbol{v} - \nabla \times \boldsymbol{b})\,, \tag{6.20}$$

$$\boldsymbol{b}^* + \nabla \times \boldsymbol{v} = \frac{1}{\mu_2}\boldsymbol{v}. \tag{6.21}$$

By substituting (6.20) and (6.21) into (6.18) and (6.19), the nonlinear terms are eliminated, leaving us with the following linear time-dependent equations:

$$\frac{\partial \boldsymbol{b}^*}{\partial t} = \mu_1 \nabla \times [\boldsymbol{b}^* \times \hat{\boldsymbol{e}}_{B_\circ}], \tag{6.22}$$

$$\frac{\partial \boldsymbol{v}}{\partial t} = \mu_2 \nabla \times [\boldsymbol{v} \times \hat{\boldsymbol{e}}_{B_\circ}], \tag{6.23}$$

which can be easily solved as they possess wave solutions of the form

$$\boldsymbol{b}^* = \mathbf{b}_k^* \ \exp\left[i\boldsymbol{k}\cdot\boldsymbol{x} + i\mu_1\left(\widehat{\boldsymbol{e}}_{B_\circ}\cdot\boldsymbol{k}\right)t\right], \tag{6.24}$$

$$\boldsymbol{v} = \mathbf{v}_k \ \exp\left[i\boldsymbol{k}\cdot\boldsymbol{x} + i\mu_2\left(\hat{\boldsymbol{e}}_{B_\circ}\cdot\boldsymbol{k}\right)t\right]. \tag{6.25}$$

But, in addition to satisfying (6.22) and (6.23), they must also meet the additional constraints imposed by (6.20) and (6.21). This necessitates $\mu_1 = \mu_2 = \mu$, and transforms (6.20) and (6.21) into

$$\boldsymbol{v}_k - \mu\boldsymbol{b}_k^* = i\boldsymbol{k}\times\boldsymbol{b}_k, \tag{6.26}$$

$$\boldsymbol{v}_k - \mu\boldsymbol{b}_k^* = i\mu\boldsymbol{k}\times\boldsymbol{v}_k. \tag{6.27}$$

These two equations imply that

$$\boldsymbol{b}_k = \mu\boldsymbol{v}_k, \tag{6.28}$$

which is a powerful relation between the fluctuating (wave) components of the flow and the magnetic field. This compact expression, along with (6.16), (6.24) and (6.25) will be shown to yield nonlinear Alfvén wave solutions of incompressible extended MHD. It has also been verified via back-substitution into the extended MHD equations.

Here, we wish to reiterate an important fact. It is the imposition of (6.20) and (6.21) that enables us to successfully handle the nonlinear terms inherent in (6.18) and (6.19). Thus, it appears as though the subsequent derivation, as exemplified by (6.22) and (6.23), is akin to a standard linear wave analysis. However, this is not merely a linear treatment, as the

relations (6.20) and (6.21), which were essential in "eliminating" the nonlinearities, are analyzed and addressed in the discussion preceding (6.26) and (6.27), and in the equations themselves.

Thus, our analysis does take into account all nonlinear terms, which are necessary in any study of turbulence as the latter involves scale-to-scale coupling. We observe that our use of the conditions (6.20) and (6.21) to eliminate the nonlinear contributions is a well-established approach [3, 82, 96, 98]. In fact, a similar result was also derived in [140] (see Footnote #30), and the general methodology behind these approaches can be traced to the classic text of [173].

A remarkable feature of (6.28) is that it satisfies the condition (6.13), which was one of the conditions that we'd imposed at the beginning of our analysis. As stated earlier, we refer the reader to [3] (see also [96]) for an alternative derivation, that does not rely upon this additional constraint for obtaining (6.28).

Let us now use (6.28) along with the expression $\boldsymbol{b}_k^* = \boldsymbol{b}_k - d_e^2 \boldsymbol{k} \times (\boldsymbol{k} \times \boldsymbol{b}_k)$, which follows from (6.17) and (6.24). We substitute these relations into either (6.26) or (6.27). This leads us to

$$\boldsymbol{k} \times (\boldsymbol{k} \times \boldsymbol{v}_k) + \frac{i}{d_e^2 \mu} \boldsymbol{k} \times \boldsymbol{v}_k = \frac{(\mu^2 - 1)}{d_e^2 \mu^2} \boldsymbol{v}_k, \tag{6.29}$$

which can be further simplified upon using a suitable vector calculus identity, and $\boldsymbol{k} \cdot \boldsymbol{v}_k = 0$. Thus, we end up with

$$\boldsymbol{k} \times \boldsymbol{v}_k = -i\alpha(k)\, \boldsymbol{v}_k, \tag{6.30}$$

where $\alpha\,(k)$ is given by

$$\alpha\,(k) = \frac{(1-\mu^2)}{\mu} - \mu d_e^2 k^2. \tag{6.31}$$

It is worth remarking that (6.30) is the Fourier transformed version of the Beltrami equation ($\nabla \times \mathbf{v} = \alpha \mathbf{v}$) with a non-constant α. We are now in a position to compute the final relation for α - this is done by taking the cross product of (6.30) with $\mathbf{k}$, and then using (6.30) once again. We find that

$$\alpha\,(k) = \pm k, \tag{6.32}$$

which can then be combined with (6.31) to solve for μ. The resulting equation is a quadratic, which leads to two solutions for μ (denoted by $\mu_\pm$) that are given by

$$\mu_\pm\,(k) = \frac{1}{(1+d_e^2k^2)}\left[-\frac{k}{2} \pm \sqrt{\frac{k^2}{4} + (1+d_e^2k^2)}\right], \tag{6.33}$$

and let us focus on the simple case wherein $\mathbf{k} = k\ \hat{z}$, following the path prescribed in [82, 97]. The frequency $\omega = -\mu\,(\hat{\boldsymbol{e}}_{B_\circ} \cdot \boldsymbol{k})$ reads as

$$\omega_\pm = \frac{-k}{(1+d_e^2k^2)}\left[-\frac{k}{2} \pm \sqrt{\frac{k^2}{4} + (1+d_e^2k^2)}\right](\hat{\boldsymbol{e}}_{B_\circ} \cdot \hat{z})\,. \tag{6.34}$$

The final expressions for (6.33) and (6.34) are identical to (4.76) and (4.77) obtained in Sec. 4.3.3.2.

Before concluding this part, we point out that each value of μ gives rise to two distinct fully nonlinear wave solutions that resemble the famous ABC equilibria. Also, we refer the reader to Sec. 4.3.3.2, for the discussion of the various limiting cases of the dispersion relation (6.34).

6.4 The spectral energy distributions for extended MHD

In this section, we shall focus on deriving the energy spectra for extended MHD by invoking a Kolmogorov-like hypothesis regarding the energy and generalized helicity cascades. We follow this up with pictorial representations of the various spectra.

6.4.1 Extended MHD invariants in Fourier space

We shall list the primary invariants of extended MHD, and give their Fourier representations. The total energy in extended MHD is given by

$$\begin{aligned} E &= \frac{1}{2}\int_{\Omega}\left\{|\boldsymbol{V}|^2+\boldsymbol{B}\cdot\boldsymbol{B}^*\right\}d^3x \\ &= \frac{1}{2}\sum_k\left\{|\boldsymbol{v}_k|^2+\left(1+d_e^2k^2\right)|\boldsymbol{b}_k|^2\right\}, \end{aligned} \tag{6.35}$$

and the relation $\mathbf{b}_k^* = \mathbf{b}_k - d_e^2\mathbf{k}\times(\mathbf{k}\times\mathbf{b}_k) = (1+d_e^2k^2)\,\boldsymbol{b}_k$ was used to simplify, and eventually obtain, the above expression.

Next, we shall consider the independent and dependent Casimir invariants of extended MHD, which are given in Sec. 6.2. We start by h_e (6.6) which can be viewed as analogous to the two-fluid electron helicity in the single-fluid limit. It is given by

$$\begin{aligned} h_e &= \frac{1}{2}\int_{\Omega}\left(\boldsymbol{A}^*-2d_e^2\boldsymbol{V}\right)\cdot\boldsymbol{B}^*\,d^3x, \\ &= \sum_k\left\{\frac{i\,(1+d_e^2k^2)}{2k^2}\,(\boldsymbol{k}\times\boldsymbol{b}_k)-d_e^2\boldsymbol{v}_k\right\} \\ &\qquad\cdot\quad\left\{\left(1+d_e^2k^2\right)\boldsymbol{b}_{-k}\right\}, \end{aligned} \tag{6.36}$$

where we have used $\boldsymbol{A}_k^* = (1 + d_e^2 k^2)\, \boldsymbol{A}_k$, along with the relations

$$\begin{aligned}
\boldsymbol{B}^* &= \nabla \times \boldsymbol{A}^*, \\
\boldsymbol{B} &= \nabla \times \boldsymbol{A}, \\
\boldsymbol{A}_k &= \frac{i}{k^2} \boldsymbol{k} \times \boldsymbol{b}_k,
\end{aligned}$$

the last of which follows from (6.28), (6.30) and (6.32) along with the use of suitable vector calculus identities.

The second invariant h_i (6.7) can be viewed as the two-fluid ion helicity in the single fluid limit. It is defined as follows:

$$\begin{aligned}
h_i &= \frac{1}{2} \int_\Omega \left[(\boldsymbol{A}^* + \boldsymbol{V}) \cdot (\boldsymbol{B}^* + \nabla \times \boldsymbol{V}) + d_e^2 \boldsymbol{V} \cdot (\nabla \times \boldsymbol{V}) \right] d^3x, \\
&= \frac{1}{2} \sum_k \left\{ \left\{ \frac{i\,(1 + d_e^2 k^2)}{k^2} (\boldsymbol{k} \times \boldsymbol{b}_k) + \boldsymbol{v}_k \right\} \right. \\
&\quad \cdot \left\{ \left(1 + d_e^2 k^2\right) \boldsymbol{b}_{-k} - i \boldsymbol{k} \times \boldsymbol{v}_{-k} \right\} \\
&\qquad \left. - i d_e^2 \boldsymbol{v}_k \cdot \boldsymbol{k} \times \boldsymbol{v}_{-k} \right\}.
\end{aligned} \tag{6.37}$$

Next, we consider the invariant G (6.8). It is given by

$$\begin{aligned}
G &= \frac{1}{2} \int_\Omega \left[\boldsymbol{B}^* \cdot \boldsymbol{A}^* + d_e^2 \boldsymbol{V} \cdot (\nabla \times \boldsymbol{V}) \right] d^3x, \\
&= \frac{1}{2} \sum_k \left\{ \frac{i\,(1 + d_e^2 k^2)^2}{k^2} (\boldsymbol{k} \times \boldsymbol{b}_k) \cdot \boldsymbol{b}_{-k} \right. \\
&\qquad \left. - i d_e^2 \boldsymbol{v}_k \cdot \boldsymbol{k} \times \boldsymbol{v}_{-k} \right\}.
\end{aligned} \tag{6.38}$$

Further, the invariant K (6.9) can be viewed as

$$\begin{aligned}
K &= \int_\Omega \boldsymbol{V} \cdot \left(\boldsymbol{B}_* + \frac{1}{2} \nabla \times \boldsymbol{V} \right) d^3x, \\
&= \sum_k \boldsymbol{v}_k \cdot \left\{ \left(1 + d_e^2 k^2\right) \boldsymbol{b}_{-k} - \frac{i}{2} \boldsymbol{k} \times \boldsymbol{v}_{-k} \right\}.
\end{aligned} \tag{6.39}$$

Finally, we consider the two generalized invariants given by (6.10). They can be expressed as follows:

$$\begin{aligned} C_{\pm} &= \frac{1}{2}\int_{\Omega}(\theta_{\pm}\boldsymbol{A}^{*}+\boldsymbol{V})\cdot(\theta_{\pm}\mathbf{B}^{*}+\nabla\times\boldsymbol{V})\,d^{3}x, \\ &= \frac{1}{2}\sum_{k}\left\{\frac{i\theta_{\pm}\left(1+d_{e}^{2}k^{2}\right)}{k^{2}}\left(\boldsymbol{k}\times\boldsymbol{b}_{k}\right)+\boldsymbol{v}_{k}\right\} \\ &\quad\cdot\quad\left\{\theta_{\pm}\left(1+d_{e}^{2}k^{2}\right)\boldsymbol{b}_{-k}-i\boldsymbol{k}\times\boldsymbol{v}_{-k}\right\}, \end{aligned} \tag{6.40}$$

where

$$|\theta_{\pm}| = \left|\frac{-1\pm\sqrt{1+4d_{e}^{2}}}{2d_{e}^{2}}\right| \approx \begin{cases} 1, & \text{for } \theta_{+} \quad (6.41) \\ \dfrac{1}{d_{e}^{2}}, & \text{for } \theta_{-} \quad (6.42) \end{cases}$$

as noted in Sec. 4.3.3.2. Here, we wish to reiterate that (6.38), (6.39) and (6.40) are not independent; they can be constructed as a special combinations of the independent Casimir invariants (6.36) and (6.37). Indeed, it is more 'natural' to regard (6.40) as the invariant helicities of extended MHD, on account of their similarity with magnetic helicity in terms of their structure.

6.4.2 The derivation of the spectra for extended MHD

We are now in a position to derive the various spectra of interest in the different regimes. To do so, we shall rely upon an approach based on the classical arguments presented by [79]. We shall adopt the notation and methodology outlined in [82] henceforth. In quantitative terms, we assume that the (total) energy cascade rate is the product of the energy (6.35) and the inverse of the eddy turnover time τ, the latter of which is given by $\tau = (k|v_k|)^{-1}$. Thus, the energy cascading rate, denoted by ϵ_E, is evaluated

to be

$$\epsilon_E = k|v_k|\Big(1+\mu^2\left(1+d_e^2k^2\right)\Big)\frac{|v_k^2|}{2}, \tag{6.43}$$

and we had invoked (6.28) to express (6.35) purely in terms of v_k. We introduce the omnidirectional spectral function $W_E(k)$ that corresponds to the kinetic energy per unit mass per unit wave vector k, and is thus found to equal

$$\begin{aligned} W_E(k) &= \frac{|v_k^2|}{k} \\ &= (2\epsilon_E)^{2/3}k^{-5/3}\Big[1+\mu^2\left(1+d_e^2k^2\right)\Big]^{-2/3}. \end{aligned} \tag{6.44}$$

Similarly, it is possible to define the omnidirectional spectral distribution function for the magnetic energy density $M_E(k)$. This can be related to $W_E(k)$ by means of (6.28), thereby yielding

$$M_E(k) = \mu^2 W_E(k) \tag{6.45}$$

A similar set of arguments, and scaling relations can be thus devised for the helicities. As pointed our earlier, only two of (6.36), (6.38) and (6.40) are truly independent. For the sake of completeness, however, we shall present the scaling relations for all of these helicities.

Let us start with (6.36) first. Assuming that the eddy turnover time is τ as before, we find that its cascading rate (ϵ_{h_e}) is

$$\epsilon_{h_e} = k|v_k|\left[\mu\left(1+d_e^2k^2\right)\left(\mu\frac{(1+d_e^2k^2)}{2k}-d_e^2\right)\right]|v_k^2|. \tag{6.46}$$

The associated kinetic and magnetic spectral energy can be computed in a similar manner, and they are given by

$$W_{h_e}(k) = (\epsilon_{h_e})^{2/3}\left[\mu\left(1+d_e^2k^2\right)\left(\mu\frac{(1+d_e^2k^2)}{2k}-d_e^2\right)\right]^{-2/3}k^{-5/3}, \tag{6.47}$$

$$M_{h_e}(k) = \mu^2 W_{h_e}(k). \tag{6.48}$$

Next, we consider the invariant (6.37) and repeat the above set of arguments and algebra. The cascading rate ϵ_{h_i} takes on the form

$$\epsilon_{h_i} = k|v_k|\Big[\Big(k+\mu\left(1+d_e^2k^2\right)\Big)^2 + d_e^2k^2\Big]\frac{|v_k^2|}{2k}, \tag{6.49}$$

and the spectral energies are

$$W_{h_i}(k) = \frac{(2\epsilon_{h_i})^{2/3}}{k}\left[\Big(k+\mu\left(1+d_e^2k^2\right)\Big)^2 + d_e^2k^2\right]^{-2/3}, \tag{6.50}$$

$$M_{h_i}(k) = \mu^2 W_{h_i}(k). \tag{6.51}$$

Again, we consider the invariant (6.38). The cascading rate ϵ_G has the form

$$\epsilon_G = k|v_k|\Big[d_e^2k^2 + \mu^2\left(1+d_e^2k^2\right)^2\Big]\frac{|v_k^2|}{2k}, \tag{6.52}$$

and the spectral energies are

$$W_G(k) = \frac{(2\epsilon_G)^{2/3}}{k}\Big[d_e^2k^2 + \mu^2\left(1+d_e^2k^2\right)^2\Big]^{-2/3}, \tag{6.53}$$

$$M_G(k) = \mu^2 W_G(k). \tag{6.54}$$

Further, the cascading of the invariant K (6.39) is

$$\epsilon_K = (kv_k)\left[\frac{k}{2}+\mu\left(1+d_e^2k^2\right)\right]v_k^2, \tag{6.55}$$

with

$$W_K(k) = (\epsilon_K)^{2/3}\left[\frac{k}{2}+\mu\left(1+d_e^2k^2\right)\right]^{-2/3}k^{-5/3}, \tag{6.56}$$

$$M_K(k) = \mu^2 W_K(k). \tag{6.57}$$

Moving on the generalized helicities (which are arguably the true analogs of the magnetic or fluid helicity), we find that the cascading rate $\epsilon_{C_\pm}$ is

$$\epsilon_{C_\pm} = k|v_k|\Big(k+\theta_\pm\mu\left(1+d_e^2k^2\right)\Big)^2\frac{|v_k^2|}{2k}, \tag{6.58}$$

leading us to the spectral energies

$$W_{C_\pm}(k) = \frac{\left(2\epsilon_{C_\pm}\right)^{2/3}}{k}\left[k + \theta_\pm \mu\left(1 + d_e^2 k^2\right)\right]^{-4/3}, \tag{6.59}$$

$$M_{C_\pm}(k) = \mu^2 W_{C_\pm}(k)\,. \tag{6.60}$$

We round off this section by pointing out the fact that there are *two* different values of μ that are given by (6.33). Hence, for each of the spectral energies, the two cases must be considered separately.

6.4.3 The kinetic and magnetic spectral plots

In Figs. 6.1 - 6.6, the kinetic and magnetic spectra, denoted by $W_\pm$ and $M_\pm$ respectively, have been plotted as a function of k (where $k := kd_i$). The '$\pm$' corresponds to the two values of μ given by (6.33). In each of the plots, we have included two vertical lines, which serve to separate the ideal ($k < 1$), Hall ($k > 1$ and $k < 1/d_e$) and electron inertia ($k > 1/d_e$) regions.

An inspection of (6.47) reveals that it blows up at approximately $k = 1/d_e$. This feature is not present in any of the other spectra. Hence, we observe the existence of singular behaviour in Fig. 6.2 that is absent in the rest of the figures. As we have reiterated earlier, we shall consider only Figs. 6.1 and 6.6 to be independent and of importance, since they represent the spectra arising from the energy and generalized helicity invariants.

In each of the figures, we have explicitly labelled certain spectral indices. The reason behind our logic is that we examine the ideal, Hall and electron inertia regimes in detail in Sec. 6.5, where we obtain the spectra for these limiting cases. These spectra are compared against the figures, thereby serving as a mutual consistency check.

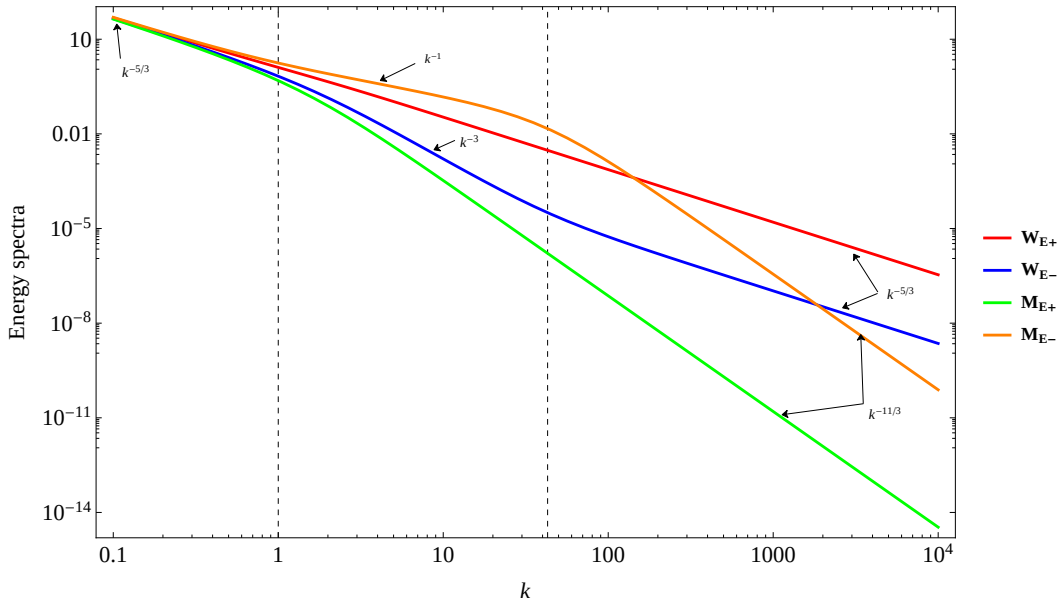

Figure 6.1: Here, W_{E_+} and W_{E_-} are the two values of (6.44) corresponding to μ_+ and μ_- respectively; the latter duo are given by (6.33). Recall that k has been normalized in units of $1/d_i$. The values of M_{E_+} and M_{E_-} are computed by means of (6.45). The two vertical dotted lines separate the ideal, Hall and electron inertia regimes respectively (when viewed from left to right).

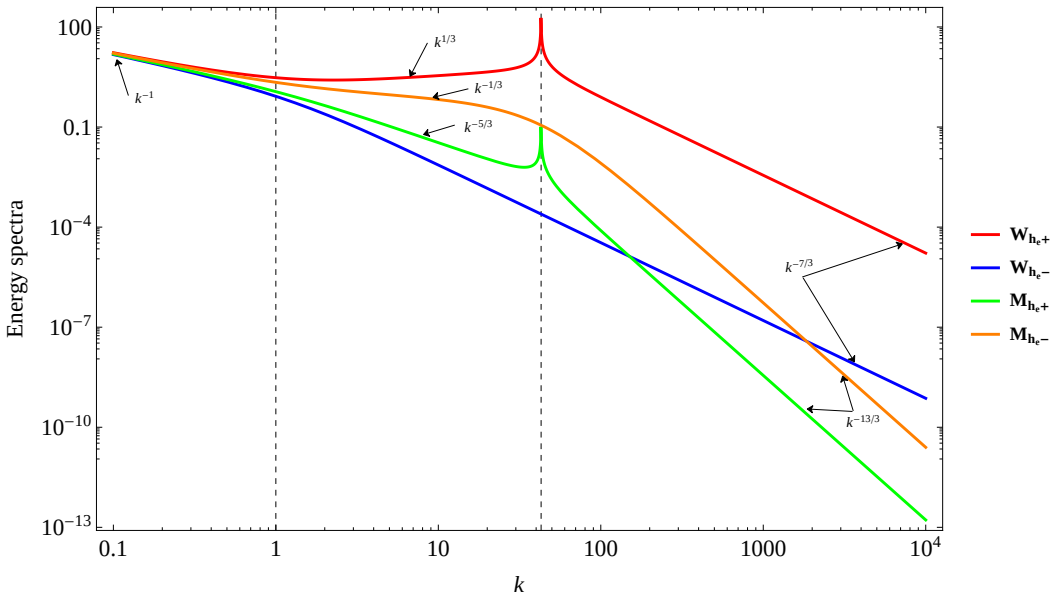

Figure 6.2: Here, W_{h_e+} and W_{h_e-} are the two values of (6.47) corresponding to μ_+ and μ_- respectively; the latter duo are given by (6.33). Recall that k has been normalized in units of $1/d_i$. The values of M_{h_e+} and M_{h_e-} are computed by means of (6.48). The two vertical dotted lines separate the ideal, Hall and electron inertia regimes respectively (when viewed from left to right).

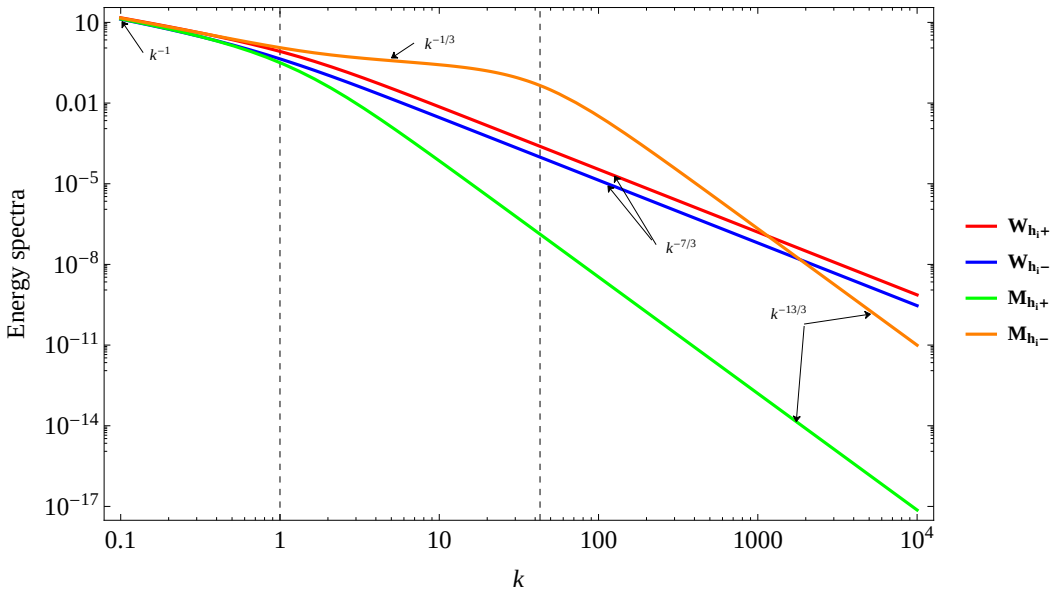

Figure 6.3: Here, W_{h_i+} and W_{h_i-} are the two values of (6.50) corresponding to μ_+ and μ_- respectively; the latter duo are given by (6.33). Recall that k has been normalized in units of $1/d_i$. The values of M_{h_i+} and M_{h_i-} are computed by means of (6.51). The two vertical dotted lines separate the ideal, Hall and electron inertia regimes respectively (when viewed from left to right).

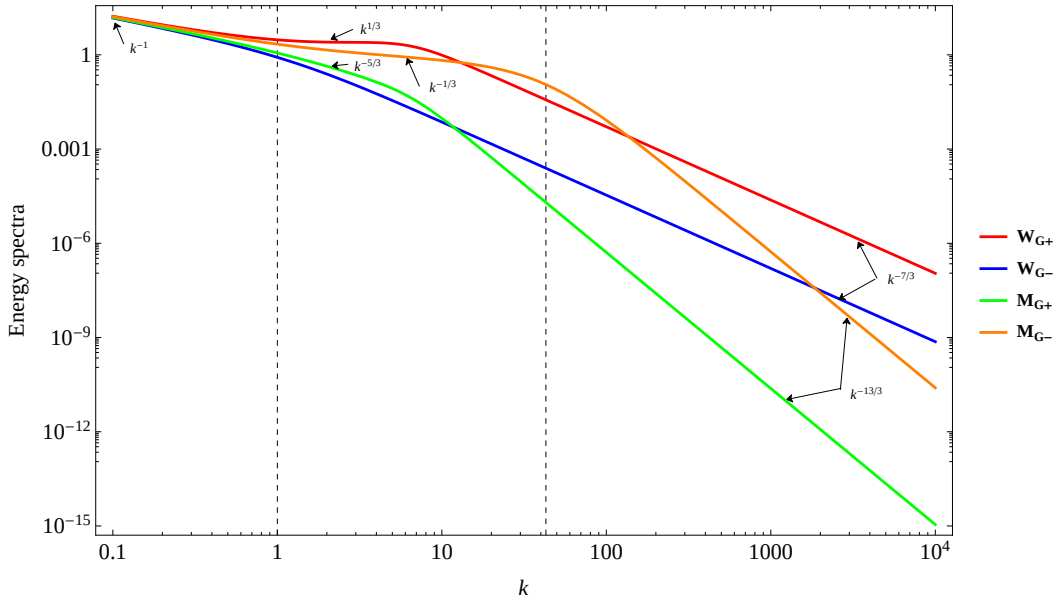

Figure 6.4: Here, W_{G_+} and W_{G_-} are the two values of (6.53) corresponding to μ_+ and μ_- respectively; the latter duo are given by (6.33). Recall that k has been normalized in units of $1/d_i$. The values of M_{G_+} and M_{G_-} are computed by means of (6.54). The two vertical dotted lines separate the ideal, Hall and electron inertia regimes respectively (when viewed from left to right).

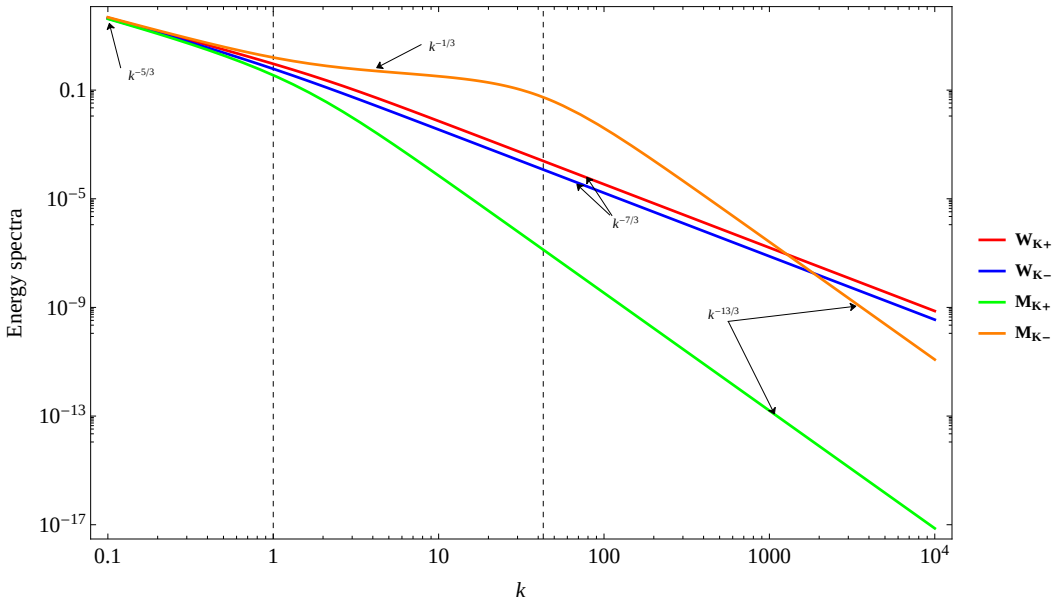

Figure 6.5: Here, W_{K_+} and W_{K_-} are the two values of (6.56) corresponding to μ_+ and μ_- respectively; the latter duo are given by (6.33). Recall that k has been normalized in units of $1/d_i$. The values of M_{K_+} and M_{K_-} are computed by means of (6.57). The two vertical dotted lines separate the ideal, Hall and electron inertia regimes respectively (when viewed from left to right).

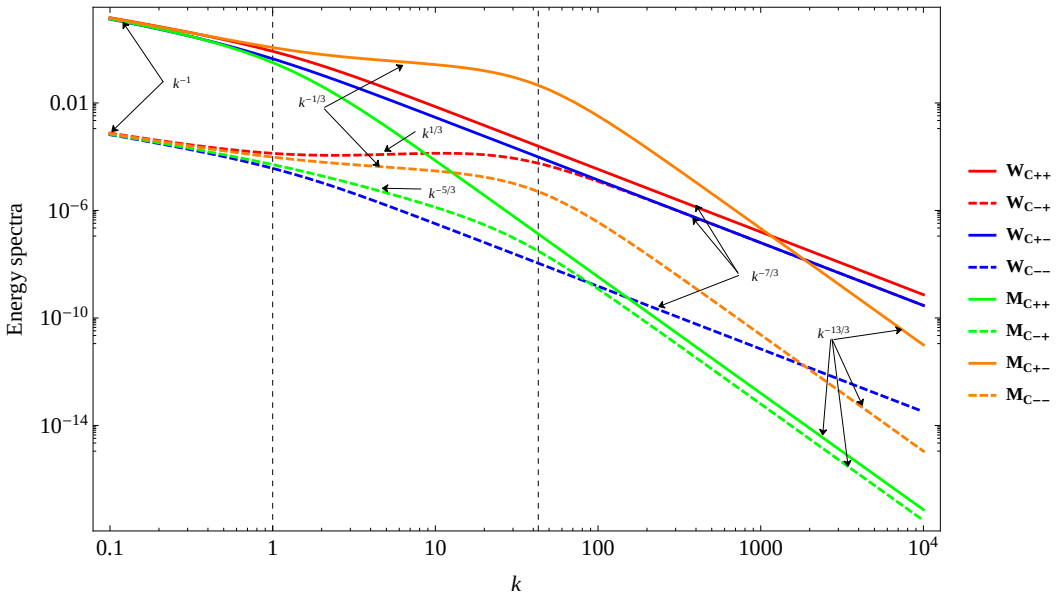

Figure 6.6: Here, the W_C's are the *four* values of (6.59) corresponding to μ_+ and μ_- respectively. The first sign denotes the choice of C (either C_+ and C_-) and the second denotes the choice of μ, whose expressions are given by (6.33). Recall that k has been normalized in units of $1/d_i$. The values of the M_C's are found by using (6.60), and they are also four in number. The two vertical dotted lines separate the ideal, Hall and electron inertia regimes respectively (when viewed from left to right).

6.5 The energy spectra of extended MHD in different regimes

In this Section, we shall draw upon the results of Secs. 4.3.3.2 and 6.4.2, and explicitly present the power-law scalings for the spectral energies in various regimes.

6.5.1 The ideal MHD regime

As noted in Sec. 4.3.3.2, the ideal MHD regime is obtained in the limit $k \ll 1$ in the normalized units. In this instance, it is known that $\mu_{\pm} \to \pm 1$. Thus, we end up with the following set of relations:

$$W_{E_1}(k) = (2\epsilon_E)^{2/3} k^{-5/3} = M_{E_1}(k), \tag{6.61}$$

$$W_{h_{e1}}(k) = (2\epsilon_{h_e})^{2/3} k^{-1} = M_{h_{e1}}(k), \tag{6.62}$$

$$W_{h_{i1}}(k) = (2\epsilon_{h_i})^{2/3} k^{-1} = M_{h_{i1}}(k), \tag{6.63}$$

$$W_{G_1}(k) = (2\epsilon_G)^{2/3} k^{-1} = M_{G_1}(k), \tag{6.64}$$

$$W_{K_1}(k) = (\epsilon_K)^{2/3} k^{-5/3} = M_{K_1}(k), \tag{6.65}$$

$$W_{C_{1_+}}(k) = \left(2\epsilon_{C_+}\right)^{2/3} k^{-1} = M_{C_{1_+}}(k), \tag{6.66}$$

$$W_{C_{1_-}}(k) = \left(2d_e^4\,\epsilon_{C_-}\right)^{2/3} k^{-1} = M_{C_{1_-}}(k). \tag{6.67}$$

The magnetic energy spectral are exactly equal to the kinetic energy spectral in each instance, since $\mu^2 = 1$. Note that in each of the above expressions, the label '1' denotes the ideal MHD (Alfvénic) limit.

6.5.2 The Hall regime

The regime where Hall effects are important (and dominant) is given by $k > 1$ and $d_e^2 k^2 \ll 1$. In the Hall regime, there are two values for $\mu_\pm$ that are very different, and thereby necessitate a different treatment.

By the subscript '2' we shall refer to the case with the above limits and where $\mu_+ \to k^{-1}$. In this instance, we find that

$$\begin{aligned} W_{E_2}(k) &= (2\epsilon_E)^{2/3} k^{-5/3}, \\ M_{E_2}(k) &= (2\epsilon_E)^{2/3} k^{-11/3}, \end{aligned} \tag{6.68}$$

$$\begin{aligned} W_{h_{e2}}(k) &= (2\epsilon_{h_e})^{2/3} k^{1/3}, \\ M_{h_{e2}}(k) &= (2\epsilon_{h_e})^{2/3} k^{-5/3}, \end{aligned} \tag{6.69}$$

$$\begin{aligned} W_{h_{i2}}(k) &= (2\epsilon_{h_i})^{2/3} k^{-7/3}, \\ M_{h_{i2}}(k) &= (2\epsilon_{h_i})^{2/3} k^{-13/3}, \end{aligned} \tag{6.70}$$

$$\begin{aligned} W_{G_2}(k) &= (2\epsilon_G)^{2/3} k^{1/3}, \\ M_{G_2}(k) &= (2\epsilon_G)^{2/3} k^{-5/3}, \end{aligned} \tag{6.71}$$

$$\begin{aligned} W_{K_2}(k) &= (2\epsilon_K)^{2/3} k^{-7/3}, \\ M_{K_2}(k) &= (2\epsilon_K)^{2/3} k^{-13/3}, \end{aligned} \tag{6.72}$$

$$\begin{aligned} W_{C_{2_+}}(k) &= \left(2\epsilon_{C_+}\right)^{2/3} k^{-7/3}, \\ M_{C_{2_+}}(k) &= \left(2\epsilon_{C_+}\right)^{2/3} k^{-13/3}, \end{aligned} \tag{6.73}$$

$$
\begin{aligned}
W_{C_{2_-}}(k) &= \left(2d_e^4\,\epsilon_{C_-}\right)^{2/3} k^{1/3}, \\
M_{C_{2_-}}(k) &= \left(2d_e^4\,\epsilon_{C_-}\right)^{2/3} k^{-5/3}.
\end{aligned} \tag{6.74}
$$

In the other limit, we are interested in the case where $\mu_- \to -k$, and this case is represented by the label '3' henceforth. In this instance, the spectra are given by

$$
\begin{aligned}
W_{E_3}(k) &= (2\epsilon_E)^{2/3} k^{-3}, \\
M_{E_3}(k) &= (2\epsilon_E)^{2/3} k^{-1},
\end{aligned} \tag{6.75}
$$

$$
\begin{aligned}
W_{h_{e3}}(k) &= (2\epsilon_{h_e})^{2/3} k^{-7/3}, \\
M_{h_{e3}}(k) &= (2\epsilon_{h_e})^{2/3} k^{-1/3},
\end{aligned} \tag{6.76}
$$

$$
\begin{aligned}
W_{h_{i3}}(k) &= \left(\frac{\epsilon_{h_i}}{2}\right)^{2/3} k^{-7/3}, \\
M_{h_{i3}}(k) &= \left(\frac{\epsilon_{h_i}}{2}\right)^{2/3} k^{-1/3},
\end{aligned} \tag{6.77}
$$

$$
\begin{aligned}
W_{G_3}(k) &= (2\epsilon_G)^{2/3} k^{-7/3}, \\
M_{G_3}(k) &= (2\epsilon_G)^{2/3} k^{-1/3},
\end{aligned} \tag{6.78}
$$

$$
\begin{aligned}
W_{K_3}(k) &= (2\epsilon_K)^{2/3} k^{-7/3}, \\
M_{K_3}(k) &= (2\epsilon_K)^{2/3} k^{-1/3},
\end{aligned} \tag{6.79}
$$

$$
\begin{aligned}
W_{C_{3_+}}(k) &= 2^{-4/3}\left(2\epsilon_{C_+}\right)^{2/3} k^{-7/3}, \\
M_{C_{3_+}}(k) &= 2^{-4/3}\left(2\epsilon_{C_+}\right)^{2/3} k^{-1/3},
\end{aligned} \tag{6.80}
$$

$$
\begin{aligned}
W_{C_{3_-}}(k) &= \left(2d_e^4\,\epsilon_{C_-}\right)^{2/3} k^{-7/3}, \\
M_{C_{3_-}}(k) &= \left(2d_e^4\,\epsilon_{C_-}\right)^{2/3} k^{-1/3}.
\end{aligned} \tag{6.81}
$$

6.5.3 The electron inertia regime

When the electron inertia effects become important, and dominate the landscape, the conditions $k \gg 1$ and $d_e^2 k^2 \gg 1$ must be met. In this regime, the two values of $\mu_\pm$ give rise to different spectra, as in Sec. 6.5.2.

In the first case, $\mu_+ \to 1/k$, and this is denoted by the subscript '4'. The various spectra exhibit the following scalings:

$$\begin{aligned} W_{E_4}(k) &= (2\epsilon_E)^{2/3} k^{-5/3}, \\ M_{E_4}(k) &= (2\epsilon_E)^{2/3} k^{-11/3}, \end{aligned} \tag{6.82}$$

$$\begin{aligned} W_{h_{e4}}(k) &= \left(2d_e^{-2}\epsilon_{h_e}\right)^{2/3} k^{-7/3}, \\ M_{h_{e4}}(k) &= \left(2d_e^{-2}\epsilon_{h_e}\right)^{2/3} k^{-13/3}, \end{aligned} \tag{6.83}$$

$$\begin{aligned} W_{h_{i4}}(k) &= (2\epsilon_{h_i})^{2/3} k^{-7/3}, \\ M_{h_{i4}}(k) &= (2\epsilon_{h_i})^{2/3} k^{-13/3}, \end{aligned} \tag{6.84}$$

$$\begin{aligned} W_{G_4}(k) &= \left(2d_e^{-4}\epsilon_G\right)^{2/3} k^{-7/3}, \\ M_{G_4}(k) &= \left(2d_e^{-4}\epsilon_G\right)^{2/3} k^{-13/3}, \end{aligned} \tag{6.85}$$

$$\begin{aligned} W_{K_4}(k) &= (2\epsilon_K)^{2/3} k^{-7/3}, \\ M_{K_4}(k) &= (2\epsilon_K)^{2/3} k^{-13/3}, \end{aligned} \tag{6.86}$$

$$\begin{aligned} W_{C_{4_+}}(k) &= \left(2\epsilon_{C_+}\right)^{2/3} k^{-7/3}, \\ M_{C_{4_+}}(k) &= \left(2\epsilon_{C_+}\right)^{2/3} k^{-13/3}, \end{aligned} \tag{6.87}$$

$$
\begin{aligned}
W_{C_{4_-}}(k) &= 2^{-4/3}\left(2\epsilon_{C_-}\right)^{2/3}k^{-7/3}, \\
M_{C_{4_-}}(k) &= 2^{-4/3}\left(2\epsilon_{C_-}\right)^{2/3}k^{-13/3}.
\end{aligned} \tag{6.88}
$$

When we consider the other limit, it corresponds to $\mu_- \to 1/\left(d_e^2 k\right)$ and we use the label '5' to identify this case. The spectral distributions for the magnetic and kinetic energies are

$$
\begin{aligned}
W_{E_5}(k) &= \left(2d_e^2\,\epsilon_E\right)^{2/3}k^{-5/3}, \\
M_{E_5}(k) &= \left(2d_e^{-4}\,\epsilon_E\right)^{2/3}k^{-11/3},
\end{aligned} \tag{6.89}
$$

$$
\begin{aligned}
W_{h_{e5}}(k) &= \left(2d_e^{-2}\,\epsilon_{h_e}\right)^{2/3}k^{-7/3}, \\
M_{h_{e5}}(k) &= \left(2d_e^{-8}\,\epsilon_{h_e}\right)^{2/3}k^{-13/3},
\end{aligned} \tag{6.90}
$$

$$
\begin{aligned}
W_{h_{i5}}(k) &= \left(\frac{\epsilon_{h_i}}{2}\right)^{2/3}k^{-7/3}, \\
M_{h_{i5}}(k) &= \left(\frac{\epsilon_{h_i}}{2}\right)^{2/3}d_e^{-4}k^{-13/3},
\end{aligned} \tag{6.91}
$$

$$
\begin{aligned}
W_{G_5}(k) &= \left(2\epsilon_G\right)^{2/3}k^{-7/3}, \\
M_{G_5}(k) &= \left(2\epsilon_G\right)^{2/3}d_e^{-4}k^{-13/3},
\end{aligned} \tag{6.92}
$$

$$
\begin{aligned}
W_{K_5}(k) &= \left(2\epsilon_K\right)^{2/3}k^{-7/3}, \\
M_{K_5}(k) &= \left(2\epsilon_K\right)^{2/3}d_e^{-4}k^{-13/3},
\end{aligned} \tag{6.93}
$$

$$
\begin{aligned}
W_{C_{5_+}}(k) &= 2^{-4/3}\left(2\epsilon_{C_+}\right)^{2/3}k^{-7/3}, \\
M_{C_{5_+}}(k) &= 2^{-4/3}\left(2\epsilon_{C_+}\right)^{2/3}d_e^{-4}k^{-13/3},
\end{aligned} \tag{6.94}
$$

$$
\begin{aligned}
W_{C_{5\_}}(k) &= \left(2d_e^4\,\epsilon_{C_-}\right)^{2/3} k^{-7/3}, \\
M_{C_{5\_}}(k) &= \left(2d_e^{-2}\,\epsilon_{C_-}\right)^{2/3} k^{-13/3}.
\end{aligned} \tag{6.95}
$$

This completes our analysis of the spectra in the different regimes, and for the various choices of the parameters. Our scalings are verified to be entirely consistent with the plots presented in Sec. 6.4.3.

We wish to observe that the primary difference between our model, and the results obtained in [82] is that the latter lacks electron inertia effects. Hence, the results of Secs. 6.5.1 and 6.5.2 are identical to that of [82], but our results in the regime where electron inertia effects are dominant, viz. the findings of Sec. 6.5.3, are altogether new.

6.6 Discussion and analysis

As the ideal MHD regime has been studied by many authors (see for e.g. the text by [18]), we shall not focus on it in detail. Instead, we focus primarily on the Hall and electron inertia regimes in our analysis. Let us commence our comparison by first studying the Hall regime, and comparing our results with the detailed analytical and numerical results of [54]; some of the chief conclusions obtained therein were also corroborated by [108]. The simulations undertaken by [54] demonstrated that the magnetic fluctuations can exhibit a wide range of power-law behaviour; see Fig. 6.7 which summarizes the magnetic energy spectra through different scales given in [54, 108, 136]. This conclusion matches our results in Sec. 6.5.2. Moreover, a careful inspection of Sec. 3.2 of [54] confirms that their findings are in exact agreement with our model:

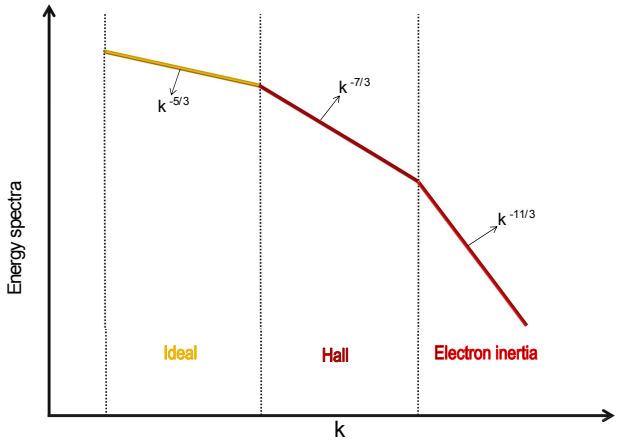

Figure 6.7: A schematic plot of the magnetic energy spectra in different scales.

1. As per [54], the kinetic energy exhibits a $-5/3$ slope, whilst the magnetic energy is characterized by a $-11/3$ spectrum in the Hall regime. This is precisely the scaling obtained in (6.68).

2. It was found in [54] that the magnetic energy displays a $-5/3$ scaling at large scales, and the $-11/3$ scaling at small scales. This is in contrast to the kinetic energy which displays the $-5/3$ behaviour at all scales. A careful inspection of (6.61) and (6.68) confirms that this is indeed the case.

3. The fact that the magnetic energy is slightly greater than the kinetic energy can be explained naturally via Hall MHD [54, 82, 144, 155], and is also consistent with observations [31, 61, 101]. The μ_- case in the Hall regime, that was studied in Secs. 4.3.3.2 and 6.5.2, is consistent

with these results.

One minor difference between our results and that of [54, 108] that the upper bound on the magnetic energy spectral index is $-11/3$ in the latter case, whereas our model suggests that $-13/3$ can be achieved, as seen from (6.73). The scaling of $-13/3$ is also supported by the previous Kolmogorov-like analysis of Hall MHD by [82] who also emphasized the important point that, in their model, the steepened spectra were very much a part of the inertial range, and were distinct from the dissipation range invoked in earlier studies.

In general, the fact that the Hall and electron inertia regimes predict slopes steeper than $-5/3$ is not a surprising fact, as this prediction has plenty of observational evidence in its favour [31, 135, 136, 156]. One of the remarkable features of the solar wind turbulence spectrum is the potential existence of three different magnetic spectra, with spectral 'breaks' separating them [23], of which two are well-documented: the Kolmogorov $-5/3$ spectrum at large scales, and an extended inertial range between the ion and electron gyroscales with an index of approximately -2.5 to -3 [6, 7, 10, 29, 50, 136, 151]. The last, on the other hand, is quite contested since it has been modelled as a power-law with an index of possibly around -4 by [136] (see also [151]), and as an exponential by [9, 10]. We will return to this aspect later and examine the reasons behind this ambiguity in greater detail. 3D anisotropic spectra have also suggested that such steep power laws do exist at sufficiently small scales [135]. This range is sometimes referred to as the dissipation range, and merits an extended discussion

of its features below.

If we suppose that such (steep) power laws do exist, one must search for potential candidates to explain this behaviour. At such scales, kinetic effects are likely to play an important role. For instance, it is expected that Landau damping plays a major role, in conjunction with the Kinetic Alfvén Wave (KAW) and (passive) ion entropy cascades, by transferring the energy to collisional scales and leading to ion and electron heating [140]. Collisionless damping also plays an important role in regulating the spectra in the dissipation range. For instance, it was shown in [73] by means of a local cascade model (with critical balance) that the spectrum could exhibit an exponential fall-off, quite similar to the results obtained in [9, 10]. On the other hand, when the critical balance conjecture was abandoned, it was shown in [74] that steep spectra that were nearly power-law in nature could be obtained, thus analogous to the analysis of solar wind observations undertaken by [136].

In addition, there are many other effects associated with Landau damping, as a result of which it has been identified as a major player in explaining the non-universal power law spectra of the solar wind [126]. In addition to Landau damping, we also wish to point out the major role played by other kinetic effects such as pressure anisotropy and its accompanying kinetic instabilities [84], phase mixing [141], intermittency and coherent structures [146]; a summary of some of these aspects can be found in [140].

Hence, there has been a great deal of work centred around (gyro)kinetic simulations of the solar wind [34, 73, 163, 166] and hybrid fluid-kinetic mod-

els [36, 165, 168]. Regardless of the physical model used, either kinetic Alfvénic waves or whistler waves are the primary candidates responsible for this turbulence [24, 39]. The analysis by [130] suggests that the former cannot serve as a viable candidate, as the whistlers subject to collisionless damping and do not reach the electron gyroscale (see also [56]), but this issue cannot be said to have been conclusively settled. This opens up the possibility of using Hall MHD, which serves as a natural model for whistler waves [52, 97]. Typically, Hall MHD and/or whistler turbulence yield spectra with the slope of $-7/3$ [6, 7, 54, 108, 147, 148, 155], which falls within the second, and *not* the third, range as per the observational evidence.

Furthermore, there are some inherent limitations to using Hall MHD as a universal model for solar wind turbulence, as discussed in [72]. From the perspective of two-fluid theory, the effects of electron inertia cannot be ignored at scales comparable to the electron skin depth [81], implying that Hall MHD cannot serve as our physical model.[1] It is at this juncture that we invoke the results from Sec. 6.5.3 that accurately capture the effects of electron inertia (as extended MHD was used in this work).

A careful scrutiny of Sec. 6.5.3 reveals that *all* of the magnetic energy spectral indices are either $-11/3$ or $-13/3$. We particularly emphasize the $-13/3$ slope as this does not appear to have been predicted before by any of the existent fluid models in the electron inertia regime, although [82] had discussed this scaling in the context of Hall MHD earlier. It is also

[1] It is known that $\beta \approx 1 - 2$ for the solar wind [118, 136], implying that the electron gyroradius and skin depth are approximately equal to each other.

very intriguing to note that the theoretically predicted slope of $-13/3$ is quite close to the value of -4.16 that was obtained from the solar wind observations at the smallest scales [136].

A cautionary statement is necessary: although the predictions of our model are quite similar to the solar wind data, the latter cannot be viewed as exact in this regime on account of instrumental inaccuracies [8, 137]. Instead, it has been shown that a spectrum of slopes peaked around approximately -4 is manifested [9, 137]. Hence, we can argue that our scalings are fairly close to the experimental evidence, as well as the 2D and 3D PIC simulation studies by [34] and [55] which have reported fairly similar results. We also wish to emphasize that a steep spectra, with a power-law index of -4.228, has also been observed for the interplanetary magnetic field, and this fact is evident upon inspection of Fig. 1 of [86]. This is conventionally attributed to the 'dissipation' range, but it is possible that this spectra could arise from the existence of an extended inertial range that gives rise to the aforementioned $-13/3$ spectrum in the electron inertia (and Hall) regime.

The $-11/3$ slope is interesting in its own right, as it exactly matches the results from the two-fluid simulations of [11]. The $-11/3$ spectrum also arises when electron MHD is used as the basic physical model [107]. As pointed out before, electron MHD is a limiting case of extended MHD, and it is founded on the narrow assumption that the ions are stationary. Thus, it is the complexity and broad scope of our model that is primarily reasonable for recovering a diverse spectrum of results in Sec. 6.5.

One of the other features that emerges from the wide-ranging nature of our model is that, in Sec. 6.5.3 and the first half of Sec. 6.5.2, we find that the magnetic energy spectra differs from the kinetic energy spectra by a factor that is proportional to $1/k^2$. This arises on account of the fact that there is a factor of μ^2 involved, and $\mu \propto k^{-1}$ in these instances. We observe that a somewhat similar result has been presented in [25], whose detailed analysis of MHD simulations and observations revealed that $W - M \propto k_{\perp}^{-2}$.

We end our analysis on a cautionary note, by summarizing some of the limitations of our treatment. Whilst it is true that extended MHD is a much better model than ideal (or Hall) MHD, it does not capture kinetic or dissipative effects. Moreover, we have not addressed the issue of parallel vs perpendicular (with respect to the mean magnetic field) magnetic fluctuations in our analysis, and this anisotropy is known to be an important feature of the solar wind [31] and other astrophysical plasmas [18]. However, we believe that the consistency of our results with all of the previous studies described above augurs well for this model. We also find that the spectra are not truly power laws (in the universal sense), as seen from Sec. 6.4.3. This agrees with the recent overview presented in [31]; see also the arguments put forth in [129].

Chapter 7

Conclusions

We have investigated the theory of extended MHD, especially by establishing the Hamiltonian-mechanical framework of the governing equations. The formulation of extended MHD has exact conservation of energy. By putting the extended MHD phenomena into the perspective of Hamiltonian mechanics, a variety of nonlinear structures has been elucidated by deriving fully nonlinear exact solutions. The theories provided us with a new understanding of different nonlinear dispersive waves in magnetized plasmas. The extended MHD model has been applied to derive nonlinear Alfvén, helicon and TG waves, as well as study turbulence in the solar wind. The Casimir invariants of the system, which are features of the noncanonicality of the Hamiltonian of the system, are the key of studying such plasma processes. Since the dynamics of plasma are restricted to stay on the surfaces of constant Casimir, thus all those phenomena appear as structures embodied on Casimir leaves.

In Chapter 2, we gave a brief review of the Hamiltonian theory of canonical and noncanonical dynamical systems in finite and infinite dimensional, with some emphasis on the Casimir invariants and the energy-Casimir method. As an example, we have presented the Hamiltonian structure of the ideal fluid. Casimir invariants of the system have been identified,

and the energy-Casimir functional has been employed to construct the Beltrami equilibrium solution.

In Chapter 3, we presented a rigorous and complete mathematical formulation of the Hamiltonian and Poisson bracket for the extended MHD model *for the first time*. In proving Jacobi's identity, we have unearthed an underlying algebraic relation that is represented by a generating bracket (3.26) satisfying an extended permutation law, which gives a unified frame for proving the Jacobi's identity for the hydrodynamics and magnetohydrodynamics models. The formulated Poisson algebra has a nontrivial center, i.e., the Hamiltonian system is noncanonical. Hence, there are Casimir invariants (helicities). We have studied the Casimir invariants of the extended MHD and the subsumed models, i.e., Hall MHD, inertial MHD and ideal MHD. We also have investigated the required boundary conditions for the extended MHD.

Chapter 4 is devoted to Alfvén waves as creations on Casimir leaves of extended MHD. We began by deriving the linear dispersion relation of extended MHD, and investigating its limits to Hall and ideal MHD. Moreover, we have considered the cases of an incompressible plasma ($C_s \to \infty$), a cold plasma ($C_s = 0$) and a warm plasma ($C_s \neq 0$), separately. Then, using the features of the Casimir invariants in determining the equilibrium of the system by extremizing the energy-Casimir functional, we have derived the exact Alfvén wave solutions of the fully nonlinear extended MHD system for the first time. The solutions consist of two Beltrami eigenfunctions, which incorporated different length scales. A remarkable feature of

inclusion of the small-scale effects is that the wave patterns are no longer arbitrary; the large-scale component of the wave cannot be independent of the small scale component, and the coexistence of them forbids the large-scale component to have a free wave form. This is in marked contrast to the ideal MHD picture that an Alfvén wave keeps an arbitrary shape constant when it propagates on a uniform ambient magnetic field. The solutions for ideal MHD and Hall MHD are also presented.

In Chapter 5, we have elucidated the multi-scale structure of electromagnetic waves in extended MHD. The derived analytical solution, satisfying the set of nonlinear equations, manifests the intrinsic coupling of the large scale and the electron skin depth small scale; the former is realized as a helicon and the latter as a TG mode. When the density is sufficiently high or the frequency is low, the TG mode chooses a different partner, which is the ion-cyclotron slow wave. It is remarkable that the coupling of such two modes imitates a linear combination. Moreover, the dispersion relations obtained by the linearized model do apply for fully nonlinear solutions with arbitrary amplitudes. This 'superficial linearity' is a manifestation of the beautiful algebraic structure underlying the extended MHD system. Such simplicity is because the Hamiltonian and the Casimir invariants are quadratic functionals of the wave fields. Moreover, we have studied the energy partition between these modes, which is determined by the helicities carried by the wave fields.

Chapter 6 is devoted entirely to study extended MHD turbulence and its applications to the solar wind. We have utilized the properties of

nonlinear Alfvén waves in extended MHD obtained in Chapter 4, which yielded an exact relation between the magnetic and kinetic fluctuations. Then, we have employed this result in conjunction with the Kolmogorov-like hypothesis, namely that the cascade rates of the energy and helicities (extended MHD invariants) were a product of the eddy turnover time and the corresponding energy and helicities. Based on this procedure, we have derived the magnetic and kinetic energy spectra in the ideal, Hall and electron inertia regimes. We demonstrate that our theoretical findings reproduced many previous results (experimental and theoretical) and showed a good agreement with the observational data in electron inertia regime. These theoretical predictions of our model emerge from the presence of an extended inertial range (electron inertia length scale), which is in contrast to the concept of the dissipation range in the Hall MHD based turbulent model. Hence, extended MHD constitutes a viable model for extracting the turbulent spectra across all scales, including those smaller than the electron gyroradius.

To conclude, the newly formulated Hamiltonian system of extended MHD is capable of analyzing various nonlinear phenomena on a wide range of scale hierarchy realized in plasma. While there are various formulations of 'generalized MHD' most of them fail to have proper structures to fulfill, for example, the energy conservation law. The underlying Poisson structure of the basic equations of motion has been obtained using a novel Lie algebra (generating bracket). Various variational principles have been applied for finding nontrivial interesting structures, which have an intrinsic multi-scale property, e.g., Alfvén, helicon and TG waves. The turbulent spectra for all

scales in extended MHD have been derived using the fully nonlinear waves solutions in conjunction with the Kolmogorov-like hypothesis.

Bibliography

[1] H. M. Abdelhamid, Y. Kawazura, and Z. Yoshida. Hamiltonian formalism of extended magnetohydrodynamics. *J. Phys. A Math. Theor.*, 48(23):235502, 2015.

[2] H. M. Abdelhamid, M. Lingam, and S. M. Mahajan. Extended MHD turbulence and its applications to the solar wind. *Astrophys. J.*, 829:87, 2016.

[3] H. M. Abdelhamid and Z. Yoshida. Nonlinear Alfvén waves in extended magnetohydrodynamics. *Phys. Plasmas*, 23(2):22105, 2016.

[4] E. Ahedo. Plasmas for space propulsion. *Plasma Phys. Control. Fusion*, 53(12):124037, 2011.

[5] P. Aigrain. Les' helicons' dans les semiconducteurs. In *Proceedings of the International Conference on Semiconductor Physics, Prague*, page 224, 1960.

[6] O. Alexandrova, V. Carbone, P. Veltri, and L. Sorriso-Valvo. Solar wind Cluster observations: Turbulent spectrum and role of Hall effect. *Planet. Space Sci.*, 55:2224–2227, 2007.

[7] O. Alexandrova, V. Carbone, P. Veltri, and L. Sorriso-Valvo. Small-scale energy cascade of the solar wind turbulence. *Astrophys. J.*, 674:1153–1157, 2008.

[8] O. Alexandrova, C. H. K. Chen, L. Sorriso-Valvo, T. S. Horbury, and S. D. Bale. Solar wind turbulence and the role of ion instabilities. *Space Sci. Rev.*, 178:101–139, 2013.

[9] O. Alexandrova, C. Lacombe, A. Mangeney, R. Grappin, and M. Maksimovic. Solar wind turbulent spectrum at plasma kinetic scales. *Astrophys. J.*, 760:121, 2012.

[10] O. Alexandrova, J. Saur, C. Lacombe, A. Mangeney, J. Mitchell, S. J. Schwartz, and P. Robert. Universality of solar-wind turbulent spectrum from MHD to electron scales. *Phys. Rev. Lett.*, 103(16):165003, 2009.

[11] N. Andrés, C. Gonzalez, L. Martin, P. Dmitruk, and D. Gómez. Two-fluid turbulence including electron inertia. *Phys. Plasmas*, 21(12):122305, 2014.

[12] V. I. Arnold. *Mathematical methods of classical mechanics*, volume 60 of *Graduate Texts in Mathematics*. Springer New York, New York, NY, 1989.

[13] V. I. Arnold and B. A. Khesin. *Topological methods in hydrodynamics*, volume 125 of *Applied Mathematical Sciences*. Springer New York, New York, NY, 1998.

[14] M. Asgari-Targhi, A. A. van Ballegooijen, S. R. Cranmer, and E. E. DeLuca. The spatial and temporal dependence of coronal heating by Alfvén wave turbulence. *Astrophys. J.*, 773:111, 2013.

[15] S. A. Balbus and J. F. Hawley. Instability, turbulence, and enhanced transport in accretion disks. *Rev. Mod. Phys.*, 70(1):1–53, 1998.

[16] M. A. Berger and G. B. Field. The topological properties of magnetic helicity. *J. Fluid Mech.*, 147(-1):133, 1984.

[17] D. Biskamp. *Magnetic reconnection in plasmas*. Cambridge monographs on plasma physics. Cambridge Univ. Press, 2000.

[18] D. Biskamp. *Magnetohydrodynamic turbulence*. Cambridge Univ. Press, 2003.

[19] D. Biskamp, E. Schwarz, and J. F. Drake. Two-dimensional electron magnetohydrodynamic turbulence. *Phys. Rev. Lett.*, 76:1264–1267, 1996.

[20] D. Biskamp, E. Schwarz, and J. F. Drake. Two-fluid theory of collisionless magnetic reconnection. *Phys. Plasmas*, 4(4):1002, 1997.

[21] D. Biskamp, E. Schwarz, A. Zeiler, A. Celani, and J. F. Drake. Electron magnetohydrodynamic turbulence. *Phys. Plasmas*, 6:751–758, 1999.

[22] S. Boldyrev. Spectrum of magnetohydrodynamic turbulence. *Phys. Rev. Lett.*, 96(11):115002, 2006.

[23] S. Boldyrev, C. H. K. Chen, Q. Xia, and V. Zhdankin. Spectral breaks of Alfvénic turbulence in a collisionless plasma. *Astrophys. J.*, 806:238, 2015.

[24] S. Boldyrev, K. Horaites, Q. Xia, and J. C. Perez. Toward a theory of astrophysical plasma turbulence at subproton scales. *Astrophys. J.*, 777:41, 2013.

[25] S. Boldyrev, J. C. Perez, J. E. Borovsky, and J. J. Podesta. Spectral scaling laws in magnetohydrodynamic turbulence simulations and in the solar wind. *Astrophys. J.*, 741:L19, 2011.

[26] R. W. Boswell. Dependence of helicon wave radial structure on electron inertia. *Aust. J. Phys.*, 25(4):403, 1972.

[27] R. W. Boswell. Effect of boundary conditions on radial mode structure of whistlers. *J. Plasma Phys.*, 31(02):197, 1984.

[28] R. W. Boswell and F. F. Chen. Helicons-the early years. *IEEE Trans. Plasma Sci.*, 25(6):1229–1244, 1997.

[29] S. Bourouaine, O. Alexandrova, E. Marsch, and M. Maksimovic. On spectral breaks in the power spectra of magnetic fluctuations in fast solar wind between 0.3 and 0.9 AU. *Astrophys. J.*, 749:102, 2012.

[30] S. I. Braginskii. Transport processes in a plasma. *Reviews of Plasma Physics*, 1:205, 1965.

[31] R. Bruno and V. Carbone. The solar wind as a turbulence laboratory. *Living Rev. Sol. Phys.*, 10, 2013.

[32] J. L. Burch, T. E. Moore, R. B. Torbert, and B. L. Giles. Magnetospheric multiscale overview and science objectives. *Space Sci. Rev.*, 199:5–21, 2016.

[33] E. Cafaro, D. Grasso, F. Pegoraro, F. Porcelli, and A. Saluzzi. Invariants and geometric structures in nonlinear Hamiltonian magnetic reconnection. *Phys. Rev. Lett.*, 80(20):4430–4433, 1998.

[34] E. Camporeale and D. Burgess. The dissipation of solar wind turbulent fluctuations at electron scales. *Astrophys. J.*, 730:114, 2011.

[35] S. S. Cerri, F. Califano, F. Jenko, D. Told, and F. Rincon. Subproton-scale cascades in solar wind turbulence: Driven hybrid-kinetic simulations. *Astrophys. J.*, 822:L12, 2016.

[36] B. D. G. Chandran, T. J. Dennis, E. Quataert, and S. D. Bale. Incorporating kinetic physics into a two-fluid solar-wind model with temperature anisotropy and low-frequency Alfvén-wave turbulence. *Astrophys. J.*, 743:197, 2011.

[37] S. Chandrasekhar and P. C. Kendall. On force-free magnetic fields. *Astrophys. J.*, 126:457, 1957.

[38] F. R. Chang-Díaz. Plasma propulsion for interplanetary flight. *Thin Solid Films*, 506-507:449–453, 2006.

[39] C. H. K. Chen, S. Boldyrev, Q. Xia, and J. C. Perez. Nature of subproton scale turbulence in the solar wind. *Phys. Rev. Lett.*, 110(22):225002, 2013.

[40] F. F. Chen. Industrial applications of low-temperature plasma physics. *Phys. Plasmas*, 2(6):2164, 1995.

[41] F. F. Chen. Physics of helicon discharges. *Phys. Plasmas*, 3(5):1783, 1996.

[42] F. F. Chen and D. Arnush. Generalized theory of helicon waves. I. Normal modes. *Phys. Plasmas*, 4(9):3411, 1997.

[43] F. F. Chen and R. W. Boswell. Helicons-the past decade. *IEEE Trans. Plasma Sci.*, 25(6):1245–1257, 1997.

[44] N. F. Cramer. *The physics of Alfvén waves*. Wiley-VCH Verlag GmbH & Co. KGaA, Weinheim, FRG, 2001.

[45] A. Cumming, P. Arras, and E. Zweibel. Magnetic field evolution in neutron star crusts due to the hall effect and Ohmic decay. *Astrophys. J.*, 609:999–1017, 2004.

[46] S. Dastgeer, A. Das, P. Kaw, and P. H. Diamond. Whistlerization and anisotropy in two-dimensional electron magnetohydrodynamic turbulence. *Phys. Plasmas*, 7:571–579, 2000.

[47] B. Davies. Helicon wave propagation: effect of electron inertia. *J. Plasma Phys.*, 4(01):43, 1970.

[48] B. Davies and P. J. Christiansen. Helicon waves in a gaseous plasma. *Plasma Phys.*, 11, 1969.

[49] E. Dubinin, K. Saure, and J. F. McKenzie. Nonlinear stationary whistler waves and whistler solitons (oscillitons). Exact solutions. *J. Plasma Phys.*, 69(4):S0022377803002319, 2003.

[50] L. Franci, S. Landi, L. Matteini, A. Verdini, and P. Hellinger. High-resolution hybrid simulations of kinetic plasma turbulence at proton scales. *Astrophys. J.*, 812:21, 2015.

[51] Freidberg, J. P. *Ideal magnetohydrodynamics.* Publisher: Plenum Press, New York, NY, 1987.

[52] S. Galtier. Wave turbulence in incompressible Hall magnetohydrodynamics. *J. Plasma Phys.*, 72:721–769, 2006.

[53] S. Galtier. Exact scaling laws for 3D electron MHD turbulence. *J. Geophys. Res.*, 113:A01102, 2008.

[54] S. Galtier and E. Buchlin. Multiscale Hall-magnetohydrodynamic turbulence in the solar wind. *Astrophys. J.*, 656:560–566, 2007.

[55] S. P. Gary, O. Chang, and J. Wang. Forward cascade of whistler turbulence: Three-dimensional particle-in-cell simulations. *Astrophys. J.*, 755:142, 2012.

[56] S. P. Gary and C. W. Smith. Short-wavelength turbulence in the solar wind: Linear theory of whistler and kinetic Alfvén fluctuations. *J. Geophys. Res.*, 114(A13):A12105, 2009.

[57] P. Goldreich and S. Sridhar. Toward a theory of interstellar turbulence. 2: Strong alfvenic turbulence. *Astrophys. J.*, 438:763, 1995.

[58] M. L. Goldstein. Major unsolved problems in space plasma physics. *Astrophys. Space Sci.*, 277:349–369, 2001.

[59] M. L. Goldstein, R. T. Wicks, S. Perri, and F. Sahraoui. Kinetic scale turbulence and dissipation in the solar wind: key observational results and future outlook. *Phil. Trans. Royal Soc. Lon. Ser. A*, 373:20140147–20140147, 2015.

[60] A. V. Gordeev, A. S. Kingsep, and L. I. Rudakov. Electron magnetohydrodynamics. *Phys. Rep.*, 243:215–315, 1994.

[61] R. Grappin, M. Velli, and A. Mangeney. 'Alfvenic' versus 'standard' turbulence in the solar wind. *Annales Geophysicae*, 9:416–426, 1991.

[62] D. Grasso, E. Tassi, H. M. Abdelhamid, and P. J. Morrison. Structure and computation of two-dimensional incompressible extended MHD. *arXiv 1611.00955*, 2016.

[63] E. Hameiri. The complete set of Casimir constants of the motion in magnetohydrodynamics. *Phys. Plasmas*, 11(7):3423, 2004.

[64] W. W. Hansen. A New type of expansion in radiation problems. *Phys. Rev.*, 47(2):139–143, 1935.

[65] A. Hasegawa and L. Chen. Plasma heating by Alfvén-wave phase mixing. *Phys. Rev. Lett.*, 32(9):454–456, 1974.

[66] C. Hasegawa, A. and Uberoi. *The Alfvén wave*. Technical, National Information Service, Springfield, VA, 1982.

[67] R. D. Hazeltine, D. D. Holm, J. E. Marsden, and P. J. Morrison. Generalized Poisson brackets and nonlinear Liapunov stability: Application to reduced MHD. *Plasma Physics*, 1984.

[68] M. Hirota, Y. Hattori, and P. J. Morrison. Explosive magnetic reconnection caused by an X-shaped current-vortex layer in a collisionless plasma. *Phys. Plasmas*, 22(5):052114, 2015.

[69] D. D. Holm. Hall magnetohydrodynamics: Conservation laws and Lyapunov stability. *Phys. Fluids*, 30(5):1310, 1987.

[70] D. D. Holm and B. A. Kupershmidt. Poisson brackets and clebsch representations for magnetohydrodynamics, multifluid plasmas, and elasticity. *Phys. D Nonlinear Phenom.*, 6(3):347–363, 1983.

[71] D. Hori, M. Furukawa, S. Ohsaki, and Z. Yoshida. A shell model for the Hall MHD system. *J. Plasma Fusion Res.*, 81:141–142, 2005.

[72] G. G. Howes. Limitations of Hall MHD as a model for turbulence in weakly collisional plasmas. *Nonlinear Processes in Geophys.*, 16:219–232, 2009.

[73] G. G. Howes, S. C. Cowley, W. Dorland, G. W. Hammett, E. Quataert, and A. A. Schekochihin. A model of turbulence in magnetized plasmas: Implications for the dissipation range in the solar wind. *J. Geophys. Res.*, 113:A05103, 2008.

[74] G. G. Howes, J. M. Tenbarge, and W. Dorland. A weakened cascade model for turbulence in astrophysical plasmas. *Phys. Plasmas*, 18(10):102305–102305, 2011.

[75] G. G. Howes, J. M. Tenbarge, W. Dorland, E. Quataert, A. A. Schekochihin, R. Numata, and T. Tatsuno. Gyrokinetic simulations of so-

lar wind turbulence from ion to electron scales. *Phys. Rev. Lett.*, 107(3):035004, 2011.

[76] J. D. Huba. Hall magnetohydrodynamics in space and laboratory plasmas. *Phys. Plasmas*, 2:2504–2513, 1995.

[77] Y. Kawazura and E. Hameiri. The complete set of Casimirs in Hall-magnetohydrodynamics. *Phys. Plasmas*, 19(8):082513, 2012.

[78] I. Keramidas Charidakos, M. Lingam, P. J. Morrison, R. L. White, and A. Wurm. Action principles for extended magnetohydrodynamic models. *Phys. Plasmas*, 21(9):092118, 2014.

[79] K. Kimura and P. J. Morrison. On energy conservation in extended magnetohydrodynamics. *Phys. Plasmas*, 21(8):082101, 2014.

[80] J. P. Klozenberg, B. McNamara, and P. C. Thonemann. The dispersion and attenuation of helicon waves in a uniform cylindrical plasma. *J. Fluid Mech.*, 21(03):545, 1965.

[81] N. A. Krall and A. W. Trivelpiece. *Principles of plasma physics*. International Series in Pure and Applied Physics. McGraw-Hill, 1973.

[82] V. Krishan and S. M. Mahajan. Magnetic fluctuations and Hall magnetohydrodynamic turbulence in the solar wind. *J. Geophys. Res.*, 109(A18):A11105, 2004.

[83] M. D. Kruskal and C. R. Oberman. On the stability of plasma in static equilibrium. *Phys. Fluids*, 1(4):275, 1958.

[84] M. W. Kunz, A. A. Schekochihin, C. H. K. Chen, I. G. Abel, and S. C. Cowley. Inertial-range kinetic turbulence in pressure-anisotropic astrophysical plasmas. *J. Plasma Phys.*, 81(5):325810501, 2015.

[85] L. D. Landau and E. M. Lifshits. *Mechanics*. Butterworth-Heinemann, 3 edition edition, 1976.

[86] R. J. Leamon, C. W. Smith, N. F. Ness, W. H. Matthaeus, and H. K. Wong. Observational constraints on the dynamics of the interplanetary magnetic field dissipation range. *J. Geophys. Res.*, 103:4775, 1998.

[87] G. Lesur, M. W. Kunz, and S. Fromang. Thanatology in protoplanetary discs. The combined influence of Ohmic, Hall, and ambipolar diffusion on dead zones. *Astron. Astrophys.*, 566:A56, 2014.

[88] W. Li, Y. Ruan, B. Luther-Davies, A. Rode, and R. Boswell. Dry-etch of As_2 S_3 thin films for optical waveguide fabrication. *J. Vac. Sci. Technol. A Vacuum, Surfaces, Film.*, 23(6):1626, 2005.

[89] A. E. Lifschitz. *Magnetohydrodynamics and spectral theory*. Springer Netherlands, Dordrecht, 1989.

[90] M. Lingam and A. Bhattacharjee. A heuristic model for MRI turbulent stresses in Hall MHD. *Mon. Not. R. Astron. Soc.*, 460:478–488, 2016.

[91] M. Lingam and A. Bhattacharjee. Hall current effects in mean-field dynamo theory. *Astrophys. J.*, 829(1):51, 2016.

[92] M. Lingam, G. Miloshevich, and P. J. Morrison. Concomitant Hamiltonian and topological structures of extended magnetohydrodynamics. *Phys. Lett. A*, 380:2400–2406, 2016.

[93] M. Lingam, P. J. Morrison, and G. Miloshevich. Remarkable connections between extended magnetohydrodynamics models. *Phys. Plasmas*, 22(7):072111, 2015.

[94] M. Lingam, P. J. Morrison, and E. Tassi. Inertial magnetohydrodynamics. *Phys. Lett. A*, 379(6):570–576, 2015.

[95] R. G. Littlejohn. Singular Poisson tensors. In *AIP Conf. Proc. Vol. 88*, pages 47–66. AIP, 1982.

[96] S. Mahajan and H. Miura. Linear superposition of nonlinear waves. *J. Plasma Phys.*, 75:145–152, 2009.

[97] S. M. Mahajan and V. Krishan. Exact solution of the incompressible Hall magnetohydrodynamics. *Mon. Not. R. Astron. Soc. Lett.*, 359:L27–L29, 2005.

[98] S. M. Mahajan and M. Lingam. Multi-fluid systems–Multi-Beltrami relaxed states and their implications. *Phys. Plasmas*, 22(9):092123, 2015.

[99] S. M. Mahajan, N. L. Shatashvili, S. V. Mikeladze, and K. I. Sigua. Acceleration of plasma flows due to reverse dynamo mechanism. *Astrophys. J.*, 634:419–425, 2005.

[100] S. M. Mahajan and Z. Yoshida. Double curl Beltrami flow: Diamagnetic structures. *Phys. Rev. Lett.*, 81(22):4863–4866, 1998.

[101] E. Marsch. Kinetic physics of the solar corona and solar wind. *Living Rev. Sol. Phys.*, 3, 2006.

[102] J. E. Marsden, T. Raiu, and A. Weinstein. Semidirect products and reduction in mechanics. *Trans. Am. Math. Soc.*, 281(1):147–147, 1984.

[103] J. E. Marsden and A. Weinstein. The Hamiltonian structure of the Maxwell-Vlasov equations. *Phys. D Nonlinear Phenom.*, 4(3):394–406, 1982.

[104] J. E. Marsden and A. Weinstein. Coadjoint orbits, vortices, and Clebsch variables for incompressible fluids. *Phys. D Nonlinear Phenom.*, 7(1-3):305–323, 1983.

[105] S. W. McIntosh, B. De Pontieu, M. Carlsson, V. Hansteen, P. Boerner, and M. Goossens. Alfvénic waves with sufficient energy to power the quiet solar corona and fast solar wind. *Nature*, 475(7357):477–480, 2011.

[106] J. F. McKenzie, E. Dubinin, K. Sauer, and T. B. Doyle. The application of the constants of motion to nonlinear stationary waves in complex plasmas: a unified fluid dynamic viewpoint. *J. Plasma Phys.*, 70(4):431–462, 2004.

[107] R. Meyrand and S. Galtier. A universal law for solar-wind turbulence at electron scales. *Astrophys. J.*, 721:1421–1424, 2010.

[108] R. Meyrand and S. Galtier. Spontaneous chiral symmetry breaking of Hall magnetohydrodynamic turbulence. *Phys. Rev. Lett.*, 109(19):194501, 2012.

[109] P. D. Mininni, D. O. Gómez, and S. M. Mahajan. Dynamo action in Hall magnetohydrodynamics. *Astrophys. J.*, 567:L81–L83, 2002.

[110] P. D. Mininni, D. O. Gomez, and S. M. Mahajan. Dynamo action in magnetohydrodynamics and Hall–magnetohydrodynamics. *Astrophys. J.*, 587(1):472–481, 2003.

[111] P. D. Mininni, D. O. Gómez, and S. M. Mahajan. Role of the Hall current in magnetohydrodynamic dynamos. *Astrophys. J.*, 584:1120–1126, 2003.

[112] H. Miura and K. Araki. Structure transitions induced by the Hall term in homogeneous and isotropic magnetohydrodynamic turbulence. *Phys. Plasmas*, 21(7):072313, 2014.

[113] H. K. Moffatt. The degree of knottedness of tangled vortex lines. *J. Fluid Mech.*, 35(01):117, 1969.

[114] H. K. Moffatt. The energy spectrum of knots and links. *Nature*, 347(6291):367–369, 1990.

[115] P. J. Morrison. Poisson brackets for fluids and plasmas. In M. Tabor and Y. M. Treve, editors, *American Institute of Physics Conference*

Series, volume 88 of *American Institute of Physics Conference Series*, pages 13–46, 1982.

[116] P. J. Morrison. Hamiltonian description of the ideal fluid. *Rev. Mod. Phys.*, 70(2):467–521, 1998.

[117] P. J. Morrison and J. M. Greene. Noncanonical Hamiltonian density formulation of hydrodynamics and ideal magnetohydrodynamics. *Phys. Rev. Lett.*, 45(10):790–794, 1980.

[118] D. J. Mullan and C. W. Smith. Solar wind statistics at 1 AU: Alfvén speed and plasma beta. *Sol. Phys.*, 234:325–338, 2006.

[119] S. Nazarenko. *Wave turbulence*, volume 825 of *Lecture notes in physics*. Springer Berlin Heidelberg, Berlin, Heidelberg, 2011.

[120] C. S. Ng, A. Bhattacharjee, K. Germaschewski, and S. Galtier. Anisotropic fluid turbulence in the interstellar medium and solar wind. *Phys. Plasmas*, 10:1954–1962, 2003.

[121] N. Nishizuka, M. Shimizu, T. Nakamura, K. Otsuji, T. J. Okamoto, Y. Katsukawa, and K. Shibata. Giant chromospheric anemone jet observed with Hinode and comparison with magnetohydrodynamic simulations: Evidence of propagating Alfvén waves and magnetic reconnection. *Astrophys. J.*, 683(1):L83–L86, 2008.

[122] S. Ohsaki and S. M. Mahajan. Hall current and Alfvén wave. *Phys. Plasmas*, 11(3):898, 2004.

[123] S. Ohsaki, N. L. Shatashvili, Z. Yoshida, and S. M. Mahajan. Magnetofluid coupling: eruptive events in the solar corona. *Astrophys. J.*, 559(1):L61–L65, 2001.

[124] Shuichi Ohsaki, Nana L. Shatashvili, Zensho Yoshida, and Swadesh M. Mahajan. Energy transformation mechanism in the solar atmosphere associated with magnetofluid coupling: explosive and eruptive events. *Astrophys. J.*, 570(1):395–407, 2002.

[125] M. Ottaviani and F. Porcelli. Nonlinear collisionless magnetic reconnection. *Phys. Rev. Lett.*, 71(23):3802–3805, 1993.

[126] T. Passot and P. L. Sulem. A model for the non-universal power law of the solar wind sub-ion-scale magnetic spectrum. *Astrophys. J.*, 812:L37, 2015.

[127] S. Perri, M. L. Goldstein, J. C. Dorelli, and F. Sahraoui. Detection of small-scale structures in the dissipation regime of solar-wind turbulence. *Phys. Rev. Lett.*, 109(19):191101, 2012.

[128] D. Perrone, F. Valentini, S. Servidio, S. Dalena, and P. Veltri. Vlasov simulations of multi-ion plasma turbulence in the solar wind. *Astrophys. J.*, 762:99, 2013.

[129] J. J. Podesta. Spectra that behave like power-laws are not necessarily power-laws. *Adv. Space Res.*, 57:1127–1132, 2016.

[130] J. J. Podesta, J. E. Borovsky, and S. P. Gary. A kinetic Alfvén wave cascade subject to collisionless damping cannot reach electron scales

in the solar wind at 1 AU. *Astrophys. J.*, 712:685–691, 2010.

[131] B. N. Rogers, R. E. Denton, J. F. Drake, and M. A. Shay. Role of dispersive waves in collisionless magnetic reconnection. *Phys. Rev. Lett.*, 87(19):195004, 2001.

[132] F. Sahraoui, G. Belmont, and M. L. Goldstein. New Insight into Short-wavelength Solar Wind Fluctuations from Vlasov Theory. *Astrophys. J.*, 748:100, 2012.

[133] F. Sahraoui, G. Belmont, and L. Rezeau. Hamiltonian canonical formulation of Hall-magnetohydrodynamics: Toward an application to weak turbulence theory. *Phys. Plasmas*, 10(5):1325, 2003.

[134] F. Sahraoui, M. L. Goldstein, K. Abdul-Kader, G. Belmont, L. Rezeau, P. Robert, and P. Canu. Observation and theoretical modeling of electron scale solar wind turbulence. *Comptes Rendus Physique*, 12:132–140, 2011.

[135] F. Sahraoui, M. L. Goldstein, G. Belmont, P. Canu, and L. Rezeau. Three dimensional anisotropic k spectra of turbulence at subproton scales in the solar wind. *Phys. Rev. Lett.*, 105(13):131101, 2010.

[136] F. Sahraoui, M. L. Goldstein, P. Robert, and Y. V. Khotyaintsev. Evidence of a cascade and dissipation of solar-wind turbulence at the electron gyroscale. *Phys. Rev. Lett.*, 102(23):231102, 2009.

[137] F. Sahraoui, S. Y. Huang, G. Belmont, M. L. Goldstein, A. Rétino, P. Robert, and J. De Patoul. Scaling of the electron dissipation range

of solar wind turbulence. *Astrophys. J.*, 777:15, 2013.

[138] R. Salmon. Hamiltonian fluid mechanics. *Annual Review of Fluid Mechanics*, 20:225–256, 1988.

[139] K. Sauer, E. Dubinin, and J. F. McKenzie. Wave emission by whistler oscillitons: Application to coherent lion roars. *Geophys. Res. Lett.*, 29(24):XXX–XXX, 2002.

[140] A. A. Schekochihin, S. C. Cowley, W. Dorland, G. W. Hammett, G. G. Howes, E. Quataert, and T. Tatsuno. Astrophysical gyrokinetics: Kinetic and fluid turbulent cascades in magnetized weakly collisional plasmas. *Astrophys. J. Suppl. Ser.*, 182:310–377, 2009.

[141] A. A. Schekochihin, J. T. Parker, E. G. Highcock, P. J. Dellar, W. Dorland, and G. W. Hammett. Phase mixing versus nonlinear advection in drift-kinetic plasma turbulence. *J. Plasma Phys.*, 82(2):905820212, 2016.

[142] T. J. Schep, F. Pegoraro, and B. N. Kuvshinov. Generalized two-fluid theory of nonlinear magnetic structures. *Phys. Plasmas*, 1(9):2843, 1994.

[143] D. D. Schnack. *Lectures in magnetohydrodynamics*, volume 780 of *Lecture Notes in Physics*. Springer Berlin Heidelberg, Berlin, Heidelberg, 2009.

[144] S. Servidio, W. H. Matthaeus, and V. Carbone. Statistical properties of ideal three-dimensional Hall magnetohydrodynamics: The spectral

structure of the equilibrium ensemble. *Phys. Plasmas*, 15(4):042314, 2008.

[145] S. Servidio, F. Valentini, F. Califano, and P. Veltri. Local kinetic effects in two-Dimensional plasma turbulence. *Phys. Rev. Lett.*, 108(4):045001, 2012.

[146] S. Servidio, F. Valentini, D. Perrone, A. Greco, F. Califano, W. H. Matthaeus, and P. Veltri. A kinetic model of plasma turbulence. *J. Plasma Phys.*, 81(1):325810107, 2015.

[147] D. Shaikh and P. K. Shukla. 3D simulations of fluctuation spectra in the Hall-MHD plasma. *Phys. Rev. Lett.*, 102(4):045004, 2009.

[148] D. Shaikh and G. P. Zank. Driven dissipative whistler wave turbulence. *Phys. Plasmas*, 12(12):122310, 2005.

[149] M. A. Shay, J. F. Drake, M. Swisdak, and B. N. Rogers. The scaling of embedded collisionless reconnection. *Phys. Plasmas*, 11(5):2199, 2004.

[150] S. Shinohara, T. Hada, T. Motomura, K. Tanaka, T. Tanikawa, K. Toki, Y. Tanaka, and K. P. Shamrai. Development of high-density helicon plasma sources and their applications. *Phys. Plasmas*, 16(5):57104, 2009.

[151] C. W. Smith, K. Hamilton, B. J. Vasquez, and R. J. Leamon. Dependence of the dissipation range spectrum of interplanetary magnetic

fluctuations on the rate of energy cascade. *Astrophys. J.*, 645:L85–L88, 2006.

[152] R. G. Spencer and A. N. Kaufman. Hamiltonian structure of two-fluid plasma dynamics. *Phys. Rev. A*, 25(4):2437–2439, 1982.

[153] J. P. Squire, F. R. Chang-Díaz, T. W. Glover, V. T. Jacobson, G. E. McCaskill, D. S. Winter, F. W. Baity, M. D. Carter, and R. H. Goulding. High power light gas helicon plasma source for VASIMR. *Thin Solid Films*, 506-507:579–582, 2006.

[154] S. Sridhar and P. Goldreich. Toward a theory of interstellar turbulence. 1: Weak Alfvenic turbulence. *Astrophys. J.*, 432:612, 1994.

[155] J. E. Stawarz and A. Pouquet. Small-scale behavior of Hall magnetohydrodynamic turbulence. *Phys. Rev. E*, 92(6):063102, 2015.

[156] O. Stawicki, S. P. Gary, and H. Li. Solar wind magnetic fluctuation spectra: Dispersion versus damping. *J.Geophys. Res.*, 106:8273–8282, 2001.

[157] R. L. Stenzel and J. M. Urrutia. Helicons in unbounded plasmas. *Phys. Rev. Lett.*, 114(20):205005, 2015.

[158] K. Takahashi, S. Takayama, A. Komuro, and A. Ando. Standing helicon wave induced by a rapidly bent magnetic field in plasmas. *Phys. Rev. Lett.*, 116(13):1–5, 2016.

[159] E. Tassi, P. J. Morrison, D. Grasso, and F. Pegoraro. Hamiltonian four-field model for magnetic reconnection: nonlinear dynamics and

extension to three dimensions with externally applied fields. *Nucl. Fusion*, 50(3):034007, 2010.

[160] E. Tassi, P. J. Morrison, F. L. Waelbroeck, and D. Grasso. Hamiltonian formulation and analysis of a collisionless fluid reconnection model. *Plasma Phys. Control. Fusion*, 50(8):085014, 2008.

[161] J. B. Taylor. Relaxation of toroidal plasma and generation of reverse magnetic fields. *Phys. Rev. Lett.*, 33(19):1139–1141, 1974.

[162] J. B. Taylor. Relaxation and magnetic reconnection in plasmas. *Rev. Mod. Phys.*, 58(3):741–763, 1986.

[163] J. M. TenBarge, G. G. Howes, and W. Dorland. Collisionless damping at electron scales in solar wind turbulence. *Astrophys. J.*, 774:139, 2013.

[164] K. Toki, S. Shinohara, T. Tanikawa, and K. P. Shamrai. Small helicon plasma source for electric propulsion. *Thin Solid Films*, 506:597–600, 2006.

[165] D. Told, J. Cookmeyer, F. Muller, P. Astfalk, and F. Jenko. Comparative study of gyrokinetic, hybrid-kinetic and fully kinetic wave physics for space plasmas. *New J. Phys.*, 18(6):065011, 2016.

[166] D. Told, F. Jenko, J. M. TenBarge, G. G. Howes, and G. W. Hammett. Multiscale nature of the dissipation range in gyrokinetic simulations of Alfvénic turbulence. *Phys. Rev. Lett.*, 115(2):025003, 2015.

[167] A. W. Trivelpiece and R. W. Gould. Space charge waves in cylindrical plasma columns. *J. Appl. Phys.*, 30(11):1784–1793, 1959.

[168] F. Valentini, P. Trávnívcek, F. Califano, P. Hellinger, and A. Mangeney. A hybrid-Vlasov model based on the current advance method for the simulation of collisionless magnetized plasma. *J. Comp. Phys.*, 225:753–770, 2007.

[169] F. Verheest, T. Cattaert, E. Dubinin, K. Sauer, and J. F. McKenzie. Whistler oscillitons revisited: the role of charge neutrality? *Nonlinear Process. Geophys.*, 11(4):447–452, 2004.

[170] D. Verscharen, E. Marsch, U. Motschmann, and J. Müller. Kinetic cascade beyond magnetohydrodynamics of solar wind turbulence in two-dimensional hybrid simulations. *Phys. Plasmas*, 19(2):022305–022305, 2012.

[171] M. Wardle. Magnetic fields in protoplanetary disks. *Astrophys. Space Sci.*, 311:35–45, 2007.

[172] G. M. Webb, C. M. Ko, R. L. Mace, J. F. McKenzie, and G. P. Zank. Integrable, oblique travelling waves in quasi-charge-neutral two-fluid plasmas. *Nonlinear Process. Geophys.*, 15(1):179–208, 2008.

[173] G. B. Whitham. *Linear and Nonlinear Waves*. John Wiley & Sons, 1974.

[174] L. Woltjer. A theorem on force-free magnetic fields. *Proc. Natl. Acad. Sci.*, 44:489–491, 1958.

[175] Z. Yoshida. Eigenfunction expansions associated with the curl derivatives in cylindrical geometries: Completeness of ChandrasekharKendall eigenfunctions. *J. Math. Phys.*, 33(4):1252, 1992.

[176] Z. Yoshida. Nonlinear Alfvén/Beltrami waves–An integrable structure built around the Casimir. *Commun. Nonlinear Sci. Numer. Simul.*, 17(5):2223–2232, 2012.

[177] Z. Yoshida. Self-organization by topological constraints: hierarchy of foliated phase space. *Adv. Phys. X*, 1(1):2–19, 2016.

[178] Z. Yoshida and E. Hameiri. Canonical Hamiltonian mechanics of Hall magnetohydrodynamics and its limit to ideal magnetohydrodynamics. *J. Phys. A Math. Theor.*, 46(33):335502, 2013.

[179] Z. Yoshida and S. M. Mahajan. Simultaneous Beltrami conditions in coupled vortex dynamics. *J. Math. Phys.*, 40(10):5080, 1999.

[180] Z. Yoshida and S. M. Mahajan. Variational principles and self-organization in two-fluid plasmas. *Phys. Rev. Lett.*, 88(9):095001, 2002.

[181] Z. Yoshida, S. M. Mahajan, and S. Ohsaki. Scale hierarchy created in plasma flow. *Phys. Plasmas*, 11(7):3660, 2004.

[182] Z. Yoshida and J. P. Morrison. A hierarchy of noncanonical Hamiltonian systems: circulation laws in an extended phase space. *Fluid Dyn. Res.*, 46(3):031412, 2014.

[183] V. E. Zakharov and E. A. Kuznetsov. Hamiltonian formalism for nonlinear waves. *Physics-Uspekhi*, 40(11):1087–1116, 1997.

[184] V. E. Zakharov, V. S. L'vov, and G. Falkovich. *Kolmogorov spectra of turbulence I.* Springer Series in Nonlinear Dynamics. Springer Berlin Heidelberg, Berlin, Heidelberg, 1992.

Publications

I include here only the publications during the doctoral course.

Publications relevant to the thesis

1. H. M. Abdelhamid, Y. Kawazura and Z. Yoshida, "Hamiltonian Formalism of Extended Magnetohydrodynamics," *J. Phys. A: Math. Theor.* 48, 235502 (2015).

2. H. M. Abdelhamid and Z. Yoshida, "Nonlinear Alfvén waves in extended magnetohydrodynamics," *Phys. Plasmas*, 23, 022105 (2016).

3. H. M. Abdelhamid, M. Lingam and S. Mahajan, "Extended MHD turbulence and its applications to the solar wind," *Astrophys. J*, 829:87(12pp), (2016).

4. H. M. Abdelhamid and Z. Yoshida," Nonlinear helicons bearing multiscale structures," *Phys. Plasmas*,24, 022107 (2017).

Other Publications

1. M. Lingam, H. M. Abdelhamid and S. R. Hudson, "Multi-region relaxed Hall magnetohydrodynamics with flow," *Phys. Plasmas*, 23, 082103 (2016).

2. D. Grasso, E. Tassi, H. M. Abdelhamid and P. J. Morrison, "Structure

and computation of two-dimensional incompressible extended MHD," *Phys. Plasmas*, 24, 012110 (2017).